Complementary α-arrestin - Rsp5 ubiquitin ligase complexes control selective nutrient transporter endocytosis in response to amino acid availability

Vasyl Ivashov[1]*, Johannes Zimmer[1]*, Sinead Schwabl[1], Jennifer Kahlhofer[1], Sabine Weys[1], Ronald Gstir[2], Thomas Jakschitz[2], Leopold Kremser[3], Günther K. Bonn[2], Herbert Lindner[3], Lukas A. Huber[1,2] Sébastien Léon[4], Oliver Schmidt[§1], David Teis[1]

*equal contributions

[1] Institute for Cell Biology, Biocenter, Medical University of Innsbruck, Austria
[2] ADSI – Austrian Drug Screening Institute GmbH, Innsbruck, Austria
[3] Division of Clinical Biochemistry, ProteinMicroAnalysis Facility, Biocenter, Medical University of Innsbruck, Austria
[4] Université de Paris, CNRS, Institut Jacques Monod, Paris, France.

§ Corresponding author:
Dr. Oliver Schmidt
Institute for Cell Biology, Biocenter, Medical University of Innsbruck
Innrain 80/82, CCB Building
A-6020, Innsbruck, Austria

oliver.schmidt@i-med.ac.at
fax: +43 512 9003 73100

Running title: Control of amino acid transporter endocytosis

Abstract

How cells adjust transport across their membranes is incompletely understood. Previously, we have shown that *S.cerevisiae* broadly re-configures the nutrient transporters at the plasma membrane in response to amino acid availability, through selective endocytosis of sugar- and amino acid transporters (AATs) (Müller et al., 2015). A genome-wide screen now revealed that Art2/Ecm21, a member of the α-arrestin family of Rsp5 ubiquitin ligase adaptors, is required for the simultaneous endocytosis of four AATs and induced during starvation by the general amino acid control pathway. Art2 uses a basic patch to recognize C-terminal acidic sorting motifs in these AATs and instructs Rsp5 to ubiquitinate proximal lysine residues. In response to amino acid excess, Rsp5 instead uses TORC1-activated Art1 to detect N-terminal acidic sorting motifs within the same AATs, which initiates exclusive substrate-induced endocytosis of individual AATs. Thus, amino acid availability activates complementary α-arrestin-Rsp5-complexes to control selective endocytosis for nutrient acquisition.

Introduction

Cells regulate the import of amino acids, glucose, and other nutrients to fuel metabolism, sustain growth or maintain homeostasis. For the selective transport of amino acids across the plasma membrane (PM) and other cellular membranes, the human genome encodes more than 60 known amino acid transporters (AATs). Mutations in AATs cause severe defects of amino acid metabolism, and the deregulation of AATs is linked to a range of human pathologies, including neurodegenerative diseases, diabetes and cancer (Kandasamy et al., 2018, Smith, 1990, McCracken and Edinger, 2013, Zhang et al., 2017).

AATs belong to the family of solute carriers (SLCs) and form selective pores that change from an outward- to an inward-facing conformation and thereby transport their amino acid substrates across membranes. Hence, the addition of AATs to the PM or their selective removal by endocytosis determines quantity and quality of amino acid transport. In human cells the molecular mechanism leading to the selective endocytosis of AATs are largely unclear.

The mechanisms for the endocytic down-regulation of AATs are beginning to emerge in the budding yeast, *S. cerevisiae*. Yeast cells frequently experience acute fluctuations in amino acid availability (Broach, 2012) and can rapidly remodel their 24-26 AATs to optimize the import of amino acids with regard to the quantity and quality of the nitrogen source available (Grenson et al., 1966, Grenson, 1966, Andre, 2018, Van Belle and Andre, 2001). The selective, ubiquitin-dependent endocytosis of AATs and other integral PM proteins frequently requires the HECT-type ubiquitin ligase Rsp5, the orthologue of Nedd4 in humans (Hein et al., 1995, Dupré et al., 2004, Belgareh-Touze et al., 2008). To specifically recognize and ubiquitinate PM proteins, Rsp5 interacts with a family of ubiquitin ligase adaptors, the α-arrestin proteins (Nikko et al., 2008, Lin et al., 2008). The yeast genome encodes 14 α-arrestin proteins (arrestin-related trafficking adaptors, ARTs; Art1-10, Bul1-3 and Spo23), which function in a partially redundant manner (reviewed in (Becuwe et al., 2012a, MacGurn et al., 2012, Babst, 2020, O'Donnell and Schmidt, 2019). Six α-arrestins have been identified in humans (Alvarez, 2008). α-Arrestin proteins use PPxY (PY) motifs to interact directly with the three WW domains of Rsp5/Nedd4 (Becuwe et al., 2012a, Rauch and Martin-Serrano, 2011). How α-arrestins recognize their cargoes in general, and more specifically AATs, is only partially understood, but appears to involve their arrestin domains. These domains have large, disordered loop- and tail-like insertions that contribute to the function of ARTs (Baile et al., 2019).

The activity of α–arrestins is controlled by complex post-translational modifications (PTMs) involving (de-)ubiquitination and (de-)phosphorylation. In several cases the binding of α–arrestins to Rsp5 results in their own ubiquitination, which is required for function (Lin et al., 2008, Becuwe et al., 2012b, Hovsepian et al., 2017). In case of Art1 ubiquitination determines its localization (Lin et al., 2008). Additional ubiquitination of ARTs can target them for proteasomal degradation, which is counteracted

by deubiquitinating enzymes (Ho et al., 2017). Several α–arrestins are activated by dephosphorylation events in response to nutrient availability or cellular stress (Becuwe et al., 2012a, O'Donnell et al., 2013, Alvaro et al., 2014, Becuwe et al., 2012b, Becuwe and Leon, 2014, Merhi and André, 2012). One example are high levels of amino acids, which activate the target of rapamycin complex 1 (TORC1). This leads to inhibition of the kinase Npr1 and thereby promotes the activity of Art1 (MacGurn et al., 2011). At the PM, Ppz phosphatases activate Art1 by dephosphorylation of its Npr1-dependent phosphorylation sites (Lee et al., 2019) and thereby stimulate ubiquitination and endocytosis of the Art1 cargoes Mup1 (methionine transporter), Can1 (arginine transporter), Tat2 (tyrosine and tryptophan transporter) and Lyp1 (lysine transporter) in response to substrate excess. Similarly, TORC1 signaling also promotes endocytosis of the general amino acid permease (Gap1) via the ARTs Bul1/2 (Merhi and Andre, 2012). It seems that nutrient-dependent TORC1 activation controls α–arrestin-mediated ubiquitin-dependent AAT endocytosis to adjust amino acid influx to metabolic needs.

Activated Art1 recognizes specific sorting signals in AATs. The flux of methionine through Mup1 or arginine through Can1 requires a conformational change into the inward-facing conformation. This conformational change probably dislodges a C-terminal plug, that otherwise 'seals' the pore and at the same time exposes an N-terminal acidic patch that is recognized by activated Art1. Art1 interacts with this acidic patch and then orients Rsp5 to ubiquitinate nearby lysine residues (Guiney et al., 2016, Gournas et al., 2018, Busto et al., 2018, Ghaddar et al., 2014). Similar results have been obtained for the uracil transporter Fur4 (Keener and Babst, 2013). A further layer of complexity may be added by stimulus-induced phosphorylation of nutrient transporters (Marchal et al., 1998, Paiva et al., 2009), akin to the recognition of G-protein-coupled receptors (GPCRs) by β–arrestins in mammalian cells (Nikko et al., 2008, Nobles et al., 2011). Hence, a molecular basis of α–arrestin-dependent nutrient transporter endocytosis in response to excess nutrients is emerging. We refer to this process as substrate-induced endocytosis.

Yet, not only substrate transport can induce nutrient transporter endocytosis, but also nutrient limitation, acute starvation or rapamycin treatment (Crapeau et al., 2014; Hovsepian et al., 2017; Jones et al., 2012; Laidlaw et al., 2020; Lang et al., 2014; Müller et al., 2015; Schmidt et al., 1998; Yang et al., 2020). Starvation-induced endocytosis is part of a coordinated catabolic cascade. Together with proteasomal degradation and with macro- and micro-autophagy it maintains amino acid homeostasis to allow entry into quiescence for cell survival during nutrient limitation. This catabolic cascade at the onset of starvation appears to be conserved in metazoans (Mejlvang et al., 2018, Edinger and Thompson, 2002a, Edinger and Thompson, 2002b, Vabulas and Hartl, 2005, Suraweera et al., 2012).

The molecular mechanisms of starvation-induced endocytosis are not clear. Hence, there is a significant knowledge gap in understanding how cells control nutrient transporter abundance upon amino acid and

115 nitrogen scarcity. Here, we have characterized systematically how amino acid abundance alters the
116 nutrient transporter repertoire at the PM of the budding yeast *S. cerevisiae*. We find that TORC1
117 signaling and the general amino acid control (GAAC) pathway toggle Art1- or Art2-Rsp5 complex
118 activities to induce endocytosis of the same set of four different AAT depending on amino acid
119 availability. In these AATs, activated Art1- or Art2-Rsp5 complexes recognize distinct acidic sorting
120 signals in the N-terminal (Art1 sorting signal) or C-terminal (Art2 sorting signal) regions to initiate
121 Rsp5-dependent ubiquitination and subsequent endocytic down-regulation. Using such complementary
122 α–arrestins switches in combination with distinct acidic sorting motifs in a single nutrient transporter
123 could be a more general mechanism to adjust transport across cellular membranes and thereby to meet
124 metabolic demands.
125
126

127 **Results**

128

129 **Amino acid availability induces selective endocytosis of nutrient transporters**

130 We employed *S. cerevisiae* as a model system to address how eukaryotic cells adjust their nutrient
131 transporters at the plasma membrane (PM) to nutrient availability. First, we used live cell fluorescence
132 microscopy to analyze in yeast cells the localization of 147 putative PM proteins that were C-terminally
133 GFP-tagged at their native chromosomal locus (Saier et al., 2016, Babu et al., 2012, Breker et al., 2014).
134 In cells growing exponentially under defined (rich) conditions we detected 49 GFP-tagged proteins at
135 the PM, including seven different amino acid transporters (AATs) and six different carbohydrate
136 transporters (Fig. 1A, S1A, Table S1). A fraction of these proteins was additionally detected inside the
137 vacuole (Fig. 1B, S1A), suggesting continuous turnover.

138

139 Next, we examined how amino acid availability affected this repertoire of PM proteins and used initially
140 the high affinity methionine transporter Mup1 as a model cargo because its regulation in response to
141 nutrient excess is well characterized (Busto et al., 2018, Lee et al., 2019, Gournas et al., 2018, Guiney
142 et al., 2016, Baile et al., 2019). Moreover, Mup1 is one of the most abundant PM proteins and it is easy
143 to follow its endocytosis and subsequent transport into the vacuole (Busto et al., 2018). In absence of
144 methionine in the growth medium Mup1-GFP localized to the PM (Fig. S1B). Low levels of methionine
145 in the growth medium did not efficiently trigger its endocytosis (Fig. S1B). Yet, once a critical
146 methionine concentration in the growth medium was reached, the vast majority of Mup1-GFP was
147 removed from the PM by endocytosis and was subsequently transported to the vacuole via the
148 multivesicular body (MVB) pathway (Fig. S1B). Substrate-induced endocytosis was rapid and efficient:
149 within 60-90 minutes after methionine addition Mup1 was almost quantitatively delivered to the
150 vacuole. Excess methionine appeared to exclusively induce endocytosis of Mup1 since all other tested
151 PM proteins remained at the cell surface (Fig. 1A, Table S1). This exclusive substrate-induced
152 endocytosis of Mup1 was also dependent on its methionine transport activity as shown by using the
153 Mup1-G78N mutant, which cannot transition to the open-inward conformation (Busto et al., 2018) (Fig.
154 S1C). These results are consistent with earlier reports showing that the high-affinity AATs Mup1, Can1,
155 Tat2 and Lyp1 undergo exclusive endocytic down-regulation in response to excess of their respective
156 substrates but remained stable at the PM when the substrate of another permease was present in excess
157 (Gournas et al., 2017, Busto et al., 2018, Nikko and Pelham, 2009).

158

159 Others and we had shown earlier that amino acid and nitrogen starvation (hereafter starvation) induced
160 the degradation of membrane proteins via the MVB pathway (Müller et al., 2015, Jones et al., 2012).
161 Consistently, in response to starvation 14 (out of 49) different PM proteins were selectively removed
162 from the PM and transported into the vacuole, including four AATs (Mup1, Can1, Lyp1, Tat2) and four
163 carbohydrate transporters (Hxt1, Hxt2, Hxt3, Itr1) (Fig. 1B, Table S1). PM localization of the general

164 amino acid permease Gap1 and the ammonium permease Mep2 was up-regulated, and the localization
165 of 35 GFP-tagged proteins to the PM remained largely unchanged, although in some instances the
166 vacuolar GFP fluorescence was increased (Fig. 1A, B, S1A, Table S1). The starvation-induced
167 endocytosis of Mup1 was independent of its capability to transport its substrate (Fig. S1C), and was also
168 observed upon starvation for individual essential amino acids (Fig. S1D). We re-evaluated the
169 starvation-induced endocytosis of Mup1, Can1, Lyp1, Tat2, Fur4, Hxt1, Hxt2 and Hxt3 in a different
170 genetic background (SEY6210; Fig. S1B, 3C, S3B, S6D). The overall response was similar.
171
172 Hence, in response to starvation, a broad range of nutrient transporters was selectively removed from
173 the PM by endocytosis and transported into the vacuole within 3-6 hours. In contrast, substrate-induced
174 endocytosis of AATs was quick and exclusive (Fig. 1A). Earlier work showed that substrate-induced
175 endocytosis of the AATs Mup1, Can1 and Lyp1 required TORC1 signaling to allow ubiquitination of
176 the transporters by the HECT-type ubiquitin ligase Rsp5 in complex with the α-arrestin Art1 (Lin et al.,
177 2008, Guiney et al., 2016, Busto et al., 2018, Gournas et al., 2018, MacGurn et al., 2011). Remarkably,
178 the same set of AATs underwent simultaneous starvation-induced endocytosis, but the molecular
179 mechanism was not clear.
180
181 **A genome-wide screen identifies regulators of starvation-induced endocytosis of AATs**
182 To identify the genes that are required for the starvation-induced endocytosis of Mup1, we conducted a
183 fluorescence-based genome-wide screen. We measured Mup1 sorting into the lumen of vacuoles via the
184 MVB pathway by fusing the pH-sensitive GFP variant pHluorin to the C-terminus of Mup1 (Mup1-
185 pHluorin) (Henne et al., 2015, Prosser et al., 2010). Fluorescence microscopy and fluorescence-activated
186 cell sorting (FACS) (Fig.2A, B) showed a strong signal of Mup1-pHluorin at the PM of cells growing
187 under defined rich conditions. In response to starvation the fluorescence of Mup1-pHluorin was
188 efficiently quenched in the acidic vacuoles of wild type (WT) cells, but not when the MVB pathway
189 was blocked (e.g. ESCRT-I mutant *vps23Δ*) (Fig. 2A, B). Hence Mup1-pHluorin is a suitable reporter
190 to identify mutants that block trafficking of Mup1 from the PM into the vacuole.
191
192 Next, Mup1-pHluorin was introduced into the yeast non-essential knock-out collection. 4745 mutants
193 expressing Mup1-pHluorin were grown in selection medium to exponential phase before they were
194 subjected to starvation for 18-22 hours (Fig. 2C). Automated FACS was used to measure Mup1-
195 pHluorin fluorescence intensity of at least 15000 cells before and after starvation. The vast majority of
196 mutants efficiently quenched the fluorescence of Mup1-pHluorin after starvation, but 128 mutants still
197 exhibited Mup1-pHluorin fluorescence after starvation (Fig. 2C, Table S2). To determine at which step
198 Mup1-pHluorin transport into vacuoles was blocked in these mutants, we used live cell fluorescence
199 microscopy. This allowed us to classify four phenotypes (Fig 2D, Table S2). Class 1 mutants retained
200 Mup1-pHluorin at the PM after starvation (105 mutants, e.g. *apm2Δ* mutants). In class 2 mutants Mup1-

201 pHluorin was detected on small intracellular objects (7 mutants, e.g. *vam3Δ* mutants). Class 3 mutants
202 accumulated Mup1-pHluorin in larger class E compartment-like objects (15 mutants, e.g. *vps4Δ*
203 mutants). One Class 4 mutant (*pep4Δ*) did not quench Mup1-pHluorin fluorescence inside the vacuole,
204 as it is deficient in the main lysosomal protease. Gene ontology (GO) analysis confirmed that our screen
205 identified major general regulators of endosomal transport (e.g. the ESCRT complexes) and was
206 enriched for proteins that are annotated as components of the PM, endosomes and vacuoles (Fig. S2,
207 Table S3) suggesting that is was successful. In addition, we identified many genes and components of
208 protein complexes that would not be predicted to be involved in the regulation of endocytosis (Fig. S2,
209 Table S2, S3).
210
211 Next, we aimed to narrow down genes that function specifically during starvation-induced endocytosis
212 and to distinguish them from general endocytic regulators (i.e. core components of endocytic trafficking
213 machineries). Therefore, most mutants (124) were exposed to methionine excess for 90 minutes and
214 then subjected to live cell fluorescence microscopy. Of the mutants falling into classes 2 - 4, the majority
215 was required for Mup1 sorting into the vacuole in response to both starvation and methionine excess.
216 Among them were many mutants in subunits of well-characterized protein complexes that constituted
217 the core machinery of endo-lysosomal trafficking (Fig. S2, Table S2, S3). However, the majority (100)
218 of the class 1 mutants (Mup1-pHluorin retained at the PM) was specifically required for starvation-
219 induced endocytosis but not for methionine-induced endocytosis (Fig. 2D, Table S2).
220
221 **The α–arrestin Art2 is specifically required for amino acid transporter endocytosis in response to**
222 **starvation**
223 A key step for the endocytic down-regulation of PM proteins is their selective ubiquitination. This
224 selectivity is mediated by α–arrestin molecules that direct the HECT-type ubiquitin ligase Rsp5 to
225 ubiquitinate specific PM proteins (Babst, 2020). Among the 14 α–arrestins encoded by the yeast
226 genome, our screen identified only Ecm21/Art2 to be specifically required for starvation-induced
227 endocytosis of Mup1.
228
229 We compared Art2-dependent starvation-induced endocytosis to Art1-dependent substrate-induced
230 endocytosis of Mup1-GFP. Efficient methionine-induced endocytosis of Mup1 required Art1 but not
231 Art2 (Fig. 3A), consistent with earlier observations (Guiney et al., 2016, MacGurn et al., 2011, Busto et
232 al., 2018). Starvation-induced endocytosis of Mup1 was slower than methionine-induced endocytosis.
233 In WT cells, 240 – 360 minutes after onset of starvation the majority of Mup1-GFP was removed from
234 the PM and sorted into vacuoles for degradation (Fig. 3A, B). In *art2Δ* mutants, but not in *art1Δ* mutants,
235 the vast majority of Mup1-GFP remained at the PM and was no longer delivered to vacuoles (Fig. 3A).
236 This was confirmed by Western blot (WB) analysis from total cell lysates. In WT cells, the proteolytic
237 degradation of Mup1-GFP inside vacuoles released free GFP, which remained stable and thus could be

238 monitored by Western blotting (Fig. 3B, lane 2-4). In *art2Δ* mutants only little free GFP could be
239 detected (Fig. 3B lane 7-8). Re-expression of Art1 or Art2 in the corresponding mutants restored
240 methionine- or starvation-induced Mup1 endocytosis, respectively (Fig. S3A). Importantly, Art2 was
241 required for the efficient starvation-induced endocytosis of all four AATs, Mup1, Can1, Lyp1, and Tat2
242 (Fig. 3A, C). Interestingly, the same four AATs (Mup1, Can1, Lyp1 and Tat2) also depend on Art1 for
243 efficient substrate-induced endocytosis (Gournas et al., 2017, MacGurn et al., 2011, Lin et al., 2008).
244 Starvation-induced endocytosis of other PM proteins (e.g. the uracil transporter Fur4 or the hexose
245 transporters Hxt1 and Hxt2) was largely independent of Art2 (Fig. S3B).
246
247 These results suggested a swap between the α–arrestins Art1 and Art2 by amino acid availability as a
248 rule for the regulation of four AATs. The starvation-induced endocytosis of Mup1, Can, Lyp1 and Tat2
249 required Art2. Substrate-induced endocytosis of Mup1, Can1 and Lyp1 required Art1, whereas in case
250 of Tat2 substrate-induced endocytosis was less stringent and could be mediated either by Art1 or Art2
251 (Nikko and Pelham, 2009).
252
253 **Up-regulation of Art2 by the GAAC pathway drives starvation-induced endocytosis of Mup1**
254 Our experiments so far demonstrated that Art1 and Art2 mediate the endocytic down-regulation of a set
255 of AATs in response to changes in amino acid availability in a mutually exclusive manner. Hence their
256 activity must be strictly regulated. α–arrestin proteins are subject to complex multi-level regulation and
257 their activation can require transcriptional regulation, (de-)phosphorylation and ubiquitination
258 (Hovsepian et al., 2017, Lin et al., 2008, Becuwe et al., 2012b). WB analysis of total cell lysates
259 indicated quantitative band shifts of Art1 in response to starvation (Fig. 4A, lanes 2,3) that most probably
260 represented Npr1-dependent phosphorylation and thus inhibition of Art1 activity upon TORC1
261 inactivation as previously described (MacGurn et al., 2011). The protein levels of the functional 6xHis-
262 TEV-3xFlag-tagged 170kD protein Art2-HTF (Fig. S4A) were comparably low under rich conditions
263 (Fig. 4A, lane 4, Fig. S4A), but were up-regulated in response to starvation (Fig. 4A, lanes 5,6).
264 Quantitative reverse transcription (RT) PCR analysis indicated that also the *ART2* mRNA levels
265 increased during starvation (Fig. 4B).
266
267 In search of the pathway responsible for induction of Art2, we queried the results of our screen and
268 identified the eIF2 kinase Gcn2 and several more *GCN* genes encoding key components of the general
269 amino acid control (GAAC) pathway (Table S2). Gcn2 is activated during amino acid starvation by
270 unloaded tRNAs and subsequently phosphorylates eIF2α to reduce protein synthesis in general, but
271 thereby stimulates specifically the translation of the transcription factor Gcn4. Gcn4 then activates the
272 transcription of genes, many of which are involved in amino acid metabolism (Hinnebusch, 2005).
273 *gcn4*Δ was not scored in our genome-wide screen because it failed the quality control due to its slow
274 growth phenotype. Interestingly, the promoter of *ART2* contained predicted Gcn4 binding sites (Venters

275 et al., 2011, Schuldiner et al., 1998). Disrupting the GAAC pathway (*gcn4*Δ) eliminated the induction
276 of Art2 in response to starvation at mRNA and protein levels (Fig. 4B,C). Consistently, the starvation-
277 induced endocytosis of Mup1-GFP was hampered in *gcn4*Δ cells and several other *gcn* mutants (Fig.
278 4D, S4B). Also, starvation-induced endocytosis of Can1 was dependent on the GAAC pathway (Fig.
279 S4C). When we introduced mutations in the predicted Gcn4 binding sites in the *ART2* promoter, Art2
280 protein levels no longer increased in response to starvation, and starvation-induced endocytosis of
281 Mup1-GFP was impaired (Fig. 4E).
282
283 The expression of a constitutively translated $Gcn4^{C}$ construct (Mueller and Hinnebusch, 1986) increased
284 Art2 protein levels already under rich conditions, as revealed by WB analysis (Fig. 4F, compare Art2
285 protein levels in lanes 1 and 3), and drove unscheduled Mup1-GFP endocytosis (Fig. 4F, lower panel).
286 Consistently, over-expression of Art2 in WT cells or in *gcn4*Δ mutants using the strong and
287 constitutively active *TDH3* promoter (Fig. S4D) initiated Mup1-GFP endocytosis already under nutrient
288 replete conditions (Fig. 4G) and bypassed the requirement of Gcn4 during starvation.
289
290 These results indicated that during amino acid starvation, Art2 transcription was induced via the GAAC
291 pathway, leading to the up-regulation of Art2 protein levels. Moreover, it seemed that the up-regulation
292 of Art2 protein levels was sufficient to drive Mup1 endocytosis. Hence, under amino acid replete
293 conditions Art2 must be tightly repressed to prevent AAT endocytosis.
294
295 **Art2 directs Rsp5-dependent ubiquitination of C-terminal lysine residues in Mup1**
296 To determine how Art2 contributed to Mup1 endocytosis, we examined its role in Mup1 ubiquitination.
297 WT cells were harvested and Mup1-GFP was immunoprecipitated in denaturing conditions before and
298 at different time points after starvation. Equal amounts of immunoprecipitated full-length Mup1-GFP
299 were subjected to SDS-PAGE and WB analysis to compare the extent of its ubiquitination at different
300 time points (Fig 5A). This analysis indicated that a pool of Mup1 was ubiquitinated prior to the onset of
301 starvation (Fig. 5A, lane 1). At the onset of starvation, ubiquitination of Mup1-GFP appeared to decrease
302 for some time (Fig. 5A lanes 2-4), until ubiquitination of Mup1-GFP began to increase again after 2-3
303 hours during starvation (Fig. 5A lanes 4-6), temporally coinciding with Art2 induction and starvation-
304 induced endocytosis. Mup1-GFP was still ubiquitinated in *art2Δ* cells growing under rich conditions
305 (Fig. 5B lane 4) and seemingly de-ubiquitinated at the onset of starvation, but the increase of
306 ubiquitination during starvation was no longer observed (Fig. 5B, lane 6). Hence, Art2 was essential for
307 the starvation-induced ubiquitination of Mup1.
308
309 α–Arrestins use PY motifs to bind to at least one of the three WW domains of Rsp5 (Lin et al., 2008).
310 Starvation-induced endocytosis of Mup1 (but not methionine-induced endocytosis) was particularly
311 dependent on the WW3 domain of Rsp5 (Fig. 5C, D, S5A). Art2 has four putative PY motifs (Fig. 5C)

312 and the PY motif within the predicted arrestin fold of Art2 (P748,P749,Y750) was required for
313 starvation-induced endocytosis (Fig. 5E). The Art2^{P748A,P749A,Y750A} mutant was expressed at similar levels
314 than the WT protein (Fig. S5B). We suggest that interaction between WW3 in Rsp5 and the PY motif
315 (748-750) of Art2 was required for the starvation-induced endocytosis of Mup1.
316
317 To identify lysine residues in Mup1 that were ubiquitinated in response to starvation, Mup1-GFP was
318 immunoprecipitated before and three hours after starvation, digested and subjected to liquid
319 chromatography-mass-spectrometry (LC-MS) (Fig S5C). Two N-terminal lysine residues (K16 and
320 K27) and two C-terminal lysine residues (K567 and K572) in Mup1 were found to be ubiquitinated (Fig.
321 5F. Fig S5C), consistent with available high-throughput proteomic datasets (Swaney et al., 2013,
322 Iesmantavicius et al., 2014). Earlier reports showed that two N-terminal lysine residues (K27, K28) in
323 Mup1 were ubiquitinated by Art1-Rsp5 and required for methionine-induced endocytosis (Guiney et al.,
324 2016, Busto et al., 2018, Ghaddar et al., 2014) (Fig. 5F). The role of ubiquitination at C-terminal lysine
325 residues was not clear.
326
327 To determine how these N- and C-terminal lysine residues contributed to Mup1 ubiquitination under
328 different growth conditions, we mutated the N-terminal (K27, K28) or C-terminal (K567, K572) lysine
329 residues to arginine and additionally generated a quadruple mutant (K27,28,567,572R). Equal amounts
330 of immunoprecipitated Mup1-GFP, Mup1^{K27,28R}-GFP, Mup1^{K567,572R}-GFP and Mup1^{K27,28,567,572R}-GFP
331 from exponentially growing cells or after starvation or methionine treatment were subjected to SDS-
332 PAGE and WB analysis to compare their ubiquitination (Fig. 5G, S5D). Preventing the ubiquitination
333 of the C-terminal lysine residues (K567,572R) abrogated starvation-induced ubiquitination of Mup1
334 (Fig. 5G, lanes 7-9), whereas Mup1^{K27,28R}-GFP was still ubiquitinated after starvation (Fig. 5G, lanes 4-
335 6). Upon methionine treatment, Mup1^{K567,572R}-GFP ubiquitination was comparable to WT Mup1 (Fig.
336 S5D, lanes 1-4), while the ubiquitination of Mup1^{K27,28R} was impaired as reported previously (Fig. S5D,
337 lanes 5,6) (Guiney et al., 2016, Busto et al., 2018, Ghaddar et al., 2014). The quadruple mutant Mup1^{K27,}
338 $^{28,\ 567,\ 572R}$-GFP always appeared to be devoid of ubiquitination (Fig. 5G, lanes 11,12; Fig. S5D, lanes
339 7,8), suggesting that the two N-terminal and the two C-terminal lysine residues are the major sites for
340 ubiquitination. Consistently, the quadruple lysine mutation rendered Mup1^{K27,28,567,572R}-GFP refractory
341 to methionine- and starvation-induced endocytosis (Fig. 5H). Mutations in the N-terminal lysine
342 residues (K27,28R) blocked methionine-induced endocytosis, but not starvation-induced endocytosis.
343 In contrast, starvation-induced endocytosis of Mup1^{K567,572R}-GFP was specifically blocked, but not its
344 methionine-induced endocytosis (Fig. 5H).
345
346 Collectively, these results suggested that Art2 directs Rsp5 to the ubiquitination of the C-terminal lysine
347 residues K567 and K572 during starvation, whereas Art1-Rsp5 complexes ubiquitinated Mup1 on the
348 two N-terminal lysine residues K27 and K28 in response to methionine excess (Fig. 5F).

349

350 **The C-terminus of Mup1 contains an acidic sorting signal for Art2**

351 In addition to ubiquitination, our mass-spectrometry analysis of immunoprecipitated Mup1-GFP from
352 starved cells identified potential phosphorylation sites at the N-terminus (S9,23,31,42 and T34) and at
353 the C-terminus of Mup1 (T552 and S568,573) (Fig. 6A, S5C). Additional phosphorylation on T560 was
354 reported in other studies (Swaney et al., 2013, Iesmantavicius et al., 2014). Of note, the C-terminal
355 phosphorylation sites were proximal (T552, T560) or directly adjacent (S568, S573) to lysine residues
356 K567 and K572 that were ubiquitinated in an Art2-dependent manner in response to starvation (Fig. 6A,
357 S5C).

358

359 Mutation of the C-terminal threonine residues to alanine (T552,560A) to prevent phosphorylation
360 specifically blocked starvation-induced endocytosis of Mup1^{T552,560A}-GFP, but not methionine-induced
361 endocytosis (Fig. S5E). Mutation of these phosphorylation sites also prevented ubiquitination of Mup1
362 during starvation (Fig. S5F). Blocking the phosphorylation of S568 and S573 also impaired starvation-
363 induced endocytosis of Mup1^{S568,573A}-GFP (Fig. S5E), yet starvation-induced ubiquitination could still
364 be detected (Fig. S5F). Mutation of most N-terminal serine and threonine residues, including all
365 experimentally determined phosphorylation sites, to alanine (T6,25,26,34A,S9,22,23,24,31,33,42A) did
366 not affect starvation-induced endocytosis of Mup1 (Fig. S5G). It seemed that the phosphorylation of C-
367 terminal threonine residues (T552, 560) contributed to the starvation-induced Art2-Rsp5 ubiquitination
368 of Mup1 and thus might add an additional layer of regulation, similar to the recognition of GPCRs by
369 β–arrestins in mammalian cells (Shukla et al., 2014, Nikko et al., 2008, Marchal et al., 2000, Hicke et
370 al., 1998).

371

372 An extended acidic Art1 sorting motif at the N-terminus of Mup1 is required for ubiquitination of
373 K27,28 and subsequent Mup1 endocytosis in response to methionine excess (Guiney et al., 2016, Busto
374 et al., 2018). Consistent with our model involving two distinct mechanisms for Mup1 endocytosis,
375 mutations in the acidic N-terminal Art1 sorting motif of Mup1 (D43A,G47A,Q49A,T52A,L54A)
376 blocked Art1-Rsp5-dependent methionine-induced endocytosis, but not Art2-Rsp5-dependent
377 starvation-induced endocytosis (Fig. S6A).

378

379 The C-terminus of Mup1 also contains an acidic patch (D549-D555), close to the ubiquitination sites
380 K567 and K572 and the C-terminal threonine phosphorylation sites (T552, 560) involved in starvation-
381 induced endocytosis (Fig. 6A, B). Mutation of the acidic residues in this region to basic amino acids (R)
382 demonstrated that this C-terminal acidic region was specifically required for starvation-induced
383 endocytosis. Live cell fluorescence microscopy revealed that Mup1^{D549R,D551R,E554R,D555R}-GFP remained
384 at the PM in response to starvation, whereas methionine-induced endocytosis was not impaired (Fig.
385 6B). Even Art2 overexpression failed to induce endocytosis during exponential growth or starvation

386 when the C-terminal acidic patch in Mup1 was mutated (Fig. S6B). Moreover, immunoprecipitation of
387 Mup1^{D549R,D551R,E554R,D555R}-GFP and subsequent SDS-PAGE and WB analysis revealed that it was no
388 longer efficiently ubiquitinated (Fig. 6C, lanes 4 - 6), suggesting that the C-terminal acidic patch was
389 essential for the Art2-Rsp5-dependent ubiquitination during starvation.
390
391 Comparing the amino acid sequences of the C-terminal tails of the four Art2-dependent cargoes, Mup1,
392 Can1, Tat2 and Lyp1, indicated similar acidic patches (Fig. 6D). To analyze if the acidic patch in Can1
393 also contributed to starvation-induced endocytosis, we mutated D567, E569, E574 and E575 to arginine.
394 Mutant Can1^{D567R,E569R,E574R,D575R}-GFP mostly localized to the PM under growing conditions.
395 Importantly, the Art2-dependent starvation-induced down-regulation of Can1^{D567R,E569R,E574R,D575R}-GFP
396 was impaired (Fig. S6C). These results imply that Mup1, Can1 and potentially also Lyp1 and Tat2 have
397 acidic amino acid sequences at their C-termini that could serve as sorting signal for Art2-mediated
398 starvation-induced endocytosis.
399
400 **The C-terminal acidic sorting signal of Mup1 is sufficient for Art2-dependent starvation-induced**
401 **endocytosis**
402 It seemed that the last 26 amino acid residues (aa 549–574) of Mup1 harbor three features that are
403 collectively required specifically for starvation-induced endocytosis: putative phosphorylation sites, the
404 acidic patch and the ubiquitination sites. Hence, we tested if the C-terminal region of Mup1 was
405 sufficient to convert an Art2-independent cargo into an Art2 cargo. We selected the low affinity glucose
406 transporter Hxt3, which was efficiently removed from the PM in response to starvation (Fig. S6D,
407 Fig.1B, Table S1). Live cell fluorescence microscopy and WB analysis showed that starvation-induced
408 endocytosis of Hxt3-GFP was independent of Art2, but instead required Art4 (Fig. S6D). In *art4*Δ
409 mutants, but not in *art2Δ* mutants, Hxt3-GFP remained mostly at the PM (Fig. S6D) in response to
410 starvation, and its vacuolar degradation was impaired (Fig. S6E, lane 4). However, when the C-terminal
411 30 amino acids of Mup1 (aa 545-574) were fused onto the C-terminus of Hxt3 (Fig. 6E), they restored
412 starvation-induced endocytosis in *art4*Δ mutants. This Hxt3-Mup1-C-GFP chimera was now efficiently
413 removed from the PM and transported to the vacuole in the vast majority of *art4*Δ cells (86%, n=76
414 cells) (Fig. 6E), most likely because it became an Art2 substrate. Indeed, the additional deletion of *ART2*
415 (*art2*Δ *art4*Δ*)* blocked starvation-induced endocytosis and demonstrated that Art2 now mediated the
416 degradation of Hxt3-Mup1-C-GFP in *art4*Δ mutants. The degradation of Hxt3-Mup1-C-GFP and the
417 concomitant accumulation of free GFP were further examined by SDS-PAGE and WB analysis from
418 total cell extracts (Fig. S6F). This analysis showed that the majority of the full length Hxt3-Mup1-C-
419 GFP chimera was degraded in WT cells, *art2*Δ and *art4*Δ mutants during starvation (Fig. S6F, lanes 2,
420 4, 8), but only poorly in *art2*Δ *art4*Δ double mutants (Fig. S6B, lane 6).
421
422 The Art2-dependent endocytosis of the Hxt3-Mup1-C-GFP chimera required two key features provided

423 by the C-terminus of Mup1 (the acidic patch and the two C-terminal lysine residues), since in *art4*Δ
424 cells starvation-induced endocytosis of Hxt3-Mup1-$C^{K567,572R}$-GFP and Hxt3-Mup1-
425 $C^{D549R,D551R,E554R,D555R}$-GFP was blocked (Fig. 6E).
426
427 Taken together, these results demonstrate that the C-terminus of Mup1 (aa 545–574) encodes a portable
428 acidic sorting signal that can be recognized by Art2 and directs Rsp5 to ubiquitinate specifically two
429 proximal lysine residues to promote starvation-induced endocytosis.
430
431 **A basic patch of Art2 is required for starvation-induced degradation of Mup1**
432 After having defined that the C-terminus of Mup1 (and possibly also the C-terminus of the AATs Can1,
433 Lyp1 and Tat2) provides a degron sequence for Art2-Rsp5 complexes, we addressed how it could be
434 specifically recognized. Upon inspection of the predicted arrestin domain in Art2, we noted a stretch of
435 positively charged residues within the arrestin-C domain (Fig. 7A). Converting these basic residues into
436 an acidic patch ($Art2^{K664D,R665D,R666D,K667D}$) abolished starvation-induced endocytosis of Mup1 (Fig. 7B).
437 Western blot analysis of total cell lysates showed that the Art2 basic patch mutant protein was expressed
438 at similar levels as WT Art2 and was also upregulated after 3 hours of starvation (Fig. S7A, lane 6). In
439 addition, the Art2 basic patch mutant also impaired, at least partially, starvation-induced endocytosis of
440 Can1 and Lyp1, while the endocytosis of Tat2 was independent of the basic patch (Fig. 7B, S7B).
441
442 Overall, it seemed that Art2 employed a positively charged region in its arrestin fold to recognize C-
443 terminal acidic patches in at least three different AATs (Mup1, Can1, Lyp1) and thus mediate their
444 endocytosis in starvation conditions.
445
446

447 **Discussion**

448

449 We have made progress towards understanding how yeast cells selectively re-configure their repertoire
450 of transporters at the PM in response to their nutritional status. The model in Fig. 7C provides the
451 conceptual framework for the mutually exclusive but complementary action of Art1-Rsp5 and Art2-
452 Rsp5 ubiquitin ligase complexes for mediating the selective endocytosis of the methionine transporter
453 Mup1 in response to changes in amino acid availability. Similar concepts may apply for the arginine
454 transporter Can1, the lysine transporter Lyp1 and the tryptophan and tyrosine transporter Tat2. Based
455 on our results and work from others, the endocytic down-regulation of these AATs can be described by
456 the following set of rules: (1) Reciprocal (de-)activation of the α–arrestins Art1 and Art2. (2) Art1 or
457 Art2 each recognize different acidic sorting signals on their client AATs that may require additional
458 phosphorylation. (3) To do so, they employ basic patches in their extended arrestin C-domains and
459 defined PY motifs to orient Rsp5 with high specificity towards proximal lysine residues. These rules
460 satisfy the plasticity required for different α–arrestin and AAT interactions that drive exclusive or
461 relatively broad substrate specificity depending on the metabolic context.

462

463 While both Art1 and Art2 lead to the degradation of AATs, they answer to distinct metabolic cues and
464 are thus wired into distinct signaling pathways. Activation of Art1 by amino acid influx requires the
465 coordinated interplay of TORC1 signaling to inactivate Npr1 (a kinase that negatively regulates Art1)
466 and the action of phosphatases (Gournas et al., 2017, Lee et al., 2019, MacGurn et al., 2011, Tumolo et
467 al., 2020). In response to amino acid limitation, TORC1 is no longer active. This will activate Npr1 to
468 phosphorylate Art1, thereby inactivating it. At the same time, the lack of amino acids will activate the
469 eIF2α kinase Gcn2. Gcn2 will phosphorylate eIF2α, which leads to the global down-regulation of
470 translation, but enables specific translation of the transcription factor Gcn4 (Hinnebusch, 2005). Gcn4
471 then induces transcription of genes required for amino acid biosynthesis and of *ART2*, which causes an
472 increase in Art2 protein levels and thus formation of Art2-Rsp5 complexes. This appears as primary
473 means to activate Art2, since unscheduled increase in Art2 protein levels was sufficient to drive Art2-
474 dependent nutrient transporter endocytosis already in cells growing under rich conditions. When amino
475 acids become available again, the system can efficiently reset. TORC1 is reactivated resulting in Art1
476 reactivation. Conversely, Gcn4 will become instable and rapidly degraded by the UPS (Kornitzer et al.,
477 1994, Meimoun et al., 2000, Irniger and Braus, 2003), and thus, the transcription of *ART2* will cease.
478 Interestingly, two de-ubiquitinating enzymes (Ubp2, Ubp15) de-ubiquitinate Art2 to influence its
479 protein stability (Ho et al., 2017, Kee et al., 2006). Inhibiting their activity could provide additional
480 control to repress Art2-dependent endocytosis in cells growing under rich conditions. Our screen
481 identified also two de-ubiquinating enzymes, Doa4 and Ubp6 to be specifically required for starvation-
482 induced endocytosis of Mup1. They could act directly on Art2 or Mup1 or help to maintain homeostasis
483 of the ubiquitin pool during starvation.

484

485 Art2 is subject to extensive post-translational modification, including ubiquitination and
486 phosphorylation. Database searches and our own proteomic experiments identified 68 phosphorylation
487 sites and 20 ubiquitination sites in Art2 (data not shown) (Swaney et al., 2013, Albuquerque et al., 2008,
488 Holt et al., 2009). How these modifications help to control the activity of Art2 remains a complex and
489 open questions. Several arrestins were found to be phospho-inhibited in specific conditions (MacGurn
490 et al., 2011, Becuwe et al., 2012b, O'Donnell et al., 2013, Hovsepian et al., 2017, Merhi and André,
491 2012, Llopis-Torregrosa et al., 2016), the common molecular basis of which is unknown. An exciting
492 hypothesis would be that α-arrestin hyper-phosphorylation would add negative charges, and thereby
493 prevent the recognition of acidic patches on transporters through electrostatic repulsion. Interestingly,
494 our screen identified the pleitropic type 2A-related serine-threonine phosphatase Sit4 as a class 1 hit.
495 Hence, Sit4 may be linked directly or indirectly to de-phosphorylation of Art2 and controlling its activity
496 as reported recently for the Art2-dependent regulation of vitamin B1 transporters (Savocco et al., 2019).
497

498 Through the complementary activation of Art1 and Art2 cells can coordinate amino acid uptake through
499 at least four high-affinity amino acid transporters with amino acid availability. The regulation of hexose
500 transporters by glucose availability appears to be conceptually related, with distinct α–arrestin-Rsp5
501 complexes in charge of down-regulating the same transporters at various glucose concentrations with
502 distinct mechanisms and kinetics (Hovsepian et al., 2017, Nikko and Pelham, 2009). In particular, the
503 endocytosis of high-affinity hexose transporters during glucose starvation involves Art8, the closest
504 paralogue of Art2, whose expression is also controlled by nutrient-regulated transcription (Hovsepian
505 et al., 2017). Altogether, a picture emerges in which the transcriptional control of α–arrestin expression
506 by nutrient-signaling pathways is critical to cope with nutrient depletion.
507

508 Our work also extends on previous findings regarding the determinants of α–arrestin/transporter
509 interaction, indicating communalities between starvation- and substrate-induced endocytosis. Art1-
510 Rsp5 and Art2-Rsp5 complexes both recognize specific acidic sequences on Mup1 (Fig. 7C). Activated
511 Art1-Rsp5 complexes recognize an acidic stretch in the N-terminus of Mup1 and Can1, close to the first
512 transmembrane domain. The exposure of these N-terminal acidic patches is linked to substrate transport
513 and conformational transitions in the transporters from the outward-open to the inward-open
514 conformation, which in Mup1 also includes the so-called 'C-plug' (aa 520–543) (Busto et al., 2018,
515 Guiney et al., 2016, Gournas et al., 2017). This conformational switch drives lateral re-localization of
516 Mup1 and Can1 into a disperse PM compartment, where they are ubiquitinated by Art1-Rsp5 (Gournas
517 et al., 2018, Busto et al., 2018). Art2 recognizes specifically an acidic patch in the C-terminal tail of
518 Mup1, and thereby directs Rsp5 to ubiquitinate two juxtaposed C-terminal lysine residues. The C-plug
519 is very close to the C-terminal acidic patch, but is not part of the C-terminal Mup1 degron. We speculate
520 that in the absence of nutrients AATs will spend more time in the outward open state with the C-Plug

521 in place. In this state, activated Art2-Rsp5 complexes can still engage the C-terminal acidic patches.
522 Hence, toggling Art1/Art2 activation in combination with accessibility of N- or C-terminal acidic sorting
523 signals in AATs, in part regulated by their conformational state, must fall together to allow selective
524 endocytosis.
525
526 An additional layer of regulation for endocytosis is provided by phosphorylation of AATs close to the
527 acidic sorting signal. At the moment we can only speculate about the kinase responsible for the
528 phosphorylation of the C-terminal serine or threonine sites of Mup1. Perhaps, constitutive PM-
529 associated kinases such as the yeast casein kinase 1 pair (Yck1/2) are involved, which are known to
530 recognize rather acidic target sequences and to regulate endocytosis (Hicke et al., 1998, Paiva et al.,
531 2009, Nikko et al., 2008, Marchal et al., 2002).
532
533 α-Arrestins lack the polar core in the arrestin domain that is used for cargo interactions in β-arrestins
534 (Aubry et al., 2009, Polekhina et al., 2013). Instead Art1-Rsp5 and Art2-Rsp5 complexes each use a
535 basic region in their arrestin C-domain to detect the acidic sorting signal in their client AATs. Studies
536 on the interaction between GPCRs and β-arrestins revealed a multimodal network of flexible
537 interactions: The N-domain of β-arrestin interacts with phosphorylated regions of the GPCR, their finger
538 loop inserts into the transmembrane domain bundle of the GPCR and loops at the C-terminal edge of β-
539 arrestin engage the membrane (Staus et al., 2020, Huang et al., 2020). Perhaps a similar concept also
540 holds true for α-arrestins. This is not unlikely given that their arrestin fold appears to be interspersed
541 with disordered loops and very long, probably unstructured N- and/or C-terminal tails, some of which
542 participate in cargo recognition or membrane interactions (Baile et al., 2019).
543
544 Despite the possible plasticity in substrate interactions, the selectivity of Art1-Rsp5 and Art2-Rsp5
545 complexes in ubiquitinating lysine residues proximal to the acidic patches of Mup1 is remarkable. Mup1
546 has 19 lysine residues at the cytoplasmic side: four at the N-terminal tail, six in the C-terminal tail and
547 9 in the intracellular loops of the pore domain. Yet, Art1-Rsp5 complexes only ubiquitinate K27 and
548 K28, whereas Art2-Rsp5 complexes only ubiquitinate K567 and K572. Also in the Hxt3-Mup1-C
549 chimeric protein, Art2-Rsp5 complexes ubiquitinated only the lysine residues close to the acidic patch,
550 despite 6 further lysine residues in the directly adjacent C-terminal tail of Hxt3. How is this possible?
551 We speculate that these two α-arrestin-Rsp5 complexes orient the HECT domain of Rsp5 with high
552 precision towards the lysine residues that are spatially close to the acidic patches. Once ubiquitinated,
553 the AAT can engage the endocytic machinery to be removed from the PM.
554
555 In conclusion, Art1-Rsp5 complexes act rapidly to prevent the accumulation of excess amino acids,
556 whereas the Art2-Rsp5 complexes help to degrade idle high affinity amino acid transporters over longer
557 periods of starvation to recycle their amino acid content. Starvation-induced endocytosis and the

558 subsequent degradation of membrane proteins is required to maintain intracellular amino acid
559 homeostasis (Müller et al., 2015, Jones et al., 2012). As such, it is well suited that Art2 activity and thus
560 starvation-induced endocytosis is co-regulated and coordinated with *de novo* amino acid biosynthesis
561 via the GAAC pathway. The down-regulation of AATs together with glucose transporters and further
562 PM proteins could also free up domains at the PM that are populated by selective nutrient transporters
563 (Spira et al., 2012, Grossmann et al., 2008) for transporters with broader substrate specificity such as
564 the general amino acid permease Gap1 and the ammonium transporter Mep2, which are strongly up-
565 regulated during starvation. Hence starvation-induced endocytosis could prepare cells – anticipatory –
566 for non-selective nutrient acquisition, as soon as nutrients become available again.
567
568 Altogether, our results provide a better understanding of the molecular mechanisms that couple
569 metabolic signaling and nutrient availability to nutrient transporter endocytosis in budding yeast. This
570 might provide basic insights and principles for the vastly more complex regulation of the nutrient
571 transporter repertoire in human cells under normal as well as pathophysiological conditions.
572
573
574

575 **Material and Methods**

576

577 **Yeast strains, media and growth conditions**

578 Yeast strains used for the microscopy screen for starvation-responsive endocytosis cargoes were mainly
579 derived from the Yeast C-terminal GFP Collection (Huh et al., 2003) with addition of further C-
580 terminally-tagged transporters in BY4741 (*MATa his3Δ1 leu2Δ0 met15Δ0 ura3Δ0*) and SEY6210
581 (*MATα leu2-3, 112 ura3-52 his3-200 trp1-901 lys2-801 suc2-9*) strain background (table S1). The FACS
582 screen for genes affecting the starvation-induced endocytosis of Mup1-pHluorin was performed using
583 the non-essential gene deletion strain collection purchased from Open Biosystems (*BY4742: MATα*
584 *his3Δ1 leu2Δ0 lys2Δ0 ura3Δ0*) transformed with pRS416 expressing Mup1-pHluorin. For all other
585 experiments the SEY6210 parental strain was used (table S4).

586 In all experiments except the genome-wide FACS screen cells were cultivated in rich medium
587 containing: 6,7g/L Yeast Nitrogen Base without amino acids (#HP26.1, Roth, Germany), 20mg/L
588 adenine hemisulfate (#A3159-25G, Sigma, Austria), 20mg/L arginine (#1655.1, Roth, Germany), 230
589 mg/L lysine monohydrate (#4207.1, Roth, Germany), 300 mg/L threonine (#T206.2, Roth, Germany),
590 30 mg/L tyrosine (#T207.1, Roth, Germany), 2% glucose (#X997.5, Roth, Germany). The rich medium
591 was supplemented when required for the auxotrophic strains with: 20 mg/L histidine (#3852.1, Roth,
592 Germany), 60 mg/L leucine (#3984.1, Roth, Germany), 20 mg/L tryptophan (#4858.2, Roth, Germany),
593 20 mg/L uracil (#7288.2, Roth, Germany), 20 mg/L methionine (#9359.1, Roth, Germany). Starvation
594 medium contained 1,7g/L Yeast Nitrogen Base without amino acids and ammonium sulfate (#J630-
595 100G, VWR, USA) and 2% glucose (#X997.5, Roth, Germany).

596 Yeast cells were cultivated in rich medium and kept for at least 24h in exponential growth phase by
597 dilution into fresh medium before onset of all experiments at mid-log phase. All cultivations were done
598 at 26°C. Substrate-induced endocytosis of Mup1 was triggered by the addition of 20 mg/L methionine
599 (#9359.1, Roth, Germany) and, unless otherwise stated, analyzed 1.5h after the treatment. For starvation
600 experiments, exponentially growing cells (0.4-0.6 OD_{600}/ml) were washed twice with and resuspended
601 in starvation medium (1 OD_{600nm}/ml) and incubated for the indicated times.

602

603 **Genetic modifications and cloning**

604 Genetic modifications were performed by PCR and/or homologous recombination using standard
605 techniques. All chromosomal tags were introduced at the C-terminus of the target ORFs to preserve the
606 endogenous 5 prime regulatory sequences. Chromosomally modified yeast strains were analyzed by
607 genotyping PCR and/or DNA-sequencing. Plasmid-expressed genes including their endogenous or
608 heterologous promoters were amplified from yeast genomic DNA and cloned into centromeric vectors
609 (pRS series). All plasmids were analyzed by DNA-sequencing. Standard techniques were used for yeast
610 transformation, mating and tetrad analysis or haploid selection. Plasmids and primers are listed in table
611 S4.

612

613 **Flow cytometry screen**

614 The yeast non-essential knock out collection (YSC1054; Open Biosystems) was transformed in 96-well
615 format using a standard lithium acetate/PEG-4000 yeast transformation protocol with a pRS416 plasmid
616 encoding Mup1-pHluorin. Transformants were selected on agar plates, inoculated into 160 µl of rich
617 medium (YNB medium lacking uracil as specified above containing 1.5x of all amino acids) and
618 incubated for 14h shaking (180 rpm) at 26° in 96-well plates (#83.3924, Sarstedt, Germany). Each plate
619 also contained the WT BY4742 parental strain and *art2*Δ as negative and positive controls. 60 µl of the
620 overnight cultures were transferred to 96-deep-well plates (#951033405, 96/2000µl, white border,
621 Eppendorf, Germany) containing 600 µl rich medium and further incubated for 5h. At this point 120 µl
622 of culture referred to as 'exponentially growing' were transferred to standard 96-well plates and
623 analyzed by flow cytometry. The remaining culture was harvested by centrifugation (1807 g; 3 min),
624 the medium was aspirated, cells were washed twice with 600 µl starvation medium and recovered by
625 centrifugation. Subsequently, cells were resuspended in 600 µl starvation medium and incubated
626 shaking (180 rpm) for 18-22h. 200 µl nitrogen-starved culture were transferred to standard 96-well
627 plates and analyzed by flow cytometry. All pipetting steps were performed using the MEA Robotic
628 System (PhyNexus, USA). Flow cytometry was performed in 96-well format using the Guava easyCyte
629 8HT-System (Sr.No. 6735128143), EMD Millipore, Merck, Germany) with the following settings:
630 Energy GRN: 72 plus (YEL=8; RED=8; NIR=8; RED2=8; NIR2=8), green channel, forward scatter
631 FSC= 14; sideward scatter SSC= 28; 15.000-20.000 counts/sample, acquire: 40sec, 3sec mix prior to
632 acquisition. GuavaSoft 2.7 software was used for data analysis. The positive/negative cut-off was set
633 for each plate empirically at the intercept of the log/starvation histograms of the WT and *art2*Δ controls
634 (*art2*Δ, which emerged as a well-reproducible hit early in the screen, was included as a negative control
635 in all further plates). All potential hits were re-examined by fluorescence microscopy. To this end, at
636 least 100 starved cells were analyzed by fluorescence microscopy after starvation and the percentage of
637 cells showing a degradation-deficient phenotype (Mup1-pHluorin at the plasma membrane, in small
638 cytosolic objects, class E-like objects or small objects within vacuoles) of the total number of cells
639 counted was calculated (table S2). Strains with more than 45% cells with retained fluorescence after at
640 least 18 hours of starvation were considered as hits. For a stringent final selection, we compared those
641 hits to the original FACS screen and finally only considered those in which at least once more the 30%
642 Mup1-pHluorin fluorescence was also retained after starvation in the FACS screen. In addition, most
643 hits were also scored for methionine-induced endocytosis of Mup1-pHluorin. Hits were considered
644 starvation-specific if the fluorescence was quenched in more than 67% of cells after 90 minutes of
645 methionine treatment (20µg/ml).

646

647 **Gene ontology analysis**

648 Gene Ontology (GO) enrichment analysis (Harris et al., 2004) was performed using 128 genes listed in

649 Appendix Table S2. They were mapped against the generic GO-Slim: process, generic GO-Slim:
650 component and macromolecular complex terms: component GO sets using the GoSLIM mapper of the
651 *Saccharomyces* genome database. We calculated the ratio of the observed (cluster frequency) vs. the
652 expected number of genes (genome frequency) associated with the GO term, referred to as enrichment
653 over genome (McClellan et al., 2007). Only GO terms with more than one associated gene were
654 reported. The full analysis is presented in Table S3.
655
656 **Fluorescence live cell wide-field microscopy**
657 For microscopy, cells were concentrated by centrifugation and directly mounted onto glass slides. Live
658 cell wide-field fluorescence microscopy was carried out using a Zeiss Axio Imager M1 equipped with
659 a sola light engine LED light source (Lumencore), a 100x oil immersion objective (NA 1.45) standard
660 GFP and mCherry fluorescent filters, a SPOT Xplorer CCD camera, and Visitron VisiView software
661 (version 2.1.4). The brightness and contrast of the images in the figures were linearly adjusted using
662 Photoshop CS5 (Adobe Version 12.0.4x64).
663
664 **Preparation of yeast whole cell protein extracts**
665 10 OD_{600nm} yeast cells were pelleted by centrifugation, resuspended in ice-cold water with 10%
666 trichloroacetic acid (#T0699, Sigma, Austria), incubated on ice for at least 30 min and washed twice
667 with ice cold acetone (#5025.5, Roth, Germany). The precipitate was resuspended in 200 µl extraction
668 buffer (150 mM Tris-HCl, pH 6,8 (#443866G, VWR, USA); 6% SDS (#CN30.3, Roth, Germany), 6M
669 urea (#51456-500G, Sigma, Austria), 6% glycerol (#3783.2, Roth, Germany), 3% β-mercaptoethanol
670 (#M6250, Sigma, Austria), 0,01% bromophenol blue (#44305, BDH Laboratory Supplies, England))
671 and solubilized with 0.75-1 mm glass beads (#A554.1, Roth Germany) for 15 min at RT and subsequent
672 heating at 42°C for 30 min and 60°C for 10 min.
673
674 **Western blot and immunodetection**
675 Protein extracts from total cells and eluates from immuno-precipitations were separated by standard
676 SDS-PAGE and transferred to PVDF membranes (#10600023, VWR, USA) for the detection of Mup1-
677 GFP, Art2-HTF and Pgk1 or to nitrocellulose membranes (#10600004, VWR, USA) for the detection
678 of ubiquitinated Mup1. PVDF membranes were stained with Coomassie Brilliant Blue R250 (#3862.2,
679 Roth, Germany) for assessment of transfer and loading. Antibodies used in this study include: α-FLAG
680 M2 (#F1804, Sigma, Austria), α-GFP IgG1K (#11814460001, Sigma, Austria), α-Pgk1 22C5D8
681 (#459250, Invitrogen, USA), α-ubiquitin P4D1 (#3936S, Santa Cruz Biotechnology, USA).
682
683 **Immunoprecipitation**
684 Mup1-GFP immunoprecipitation protocol was adapted from (Hovsepian et al., 2017). 50 OD_{600nm} yeast
685 cells were harvested by centrifugation and mechanically disrupted by glass bead lysis (0.75-1 mm) at

686 4°C in 500 µl ice-cold RIPA lysis buffer (50 mM Tris-HCl, pH 7.5, 150 mM NaCl (#3957.5, Roth,
687 Germany), 0.1% SDS, 2 mM EDTA (#ED-1KG, Sigma, Austria), 50 mM NaF (#SO0323, Scharlau,
688 Spain), 1% Nonidet P 40 (#74385, Fluka, Germany), 0.5% Na-deoxycholate (#D6750-25G, Sigma,
689 Austria), 1% glycerol) containing protease inhibitors (cOmplete Protease Inhibitor Cocktail
690 (#11697498001, Sigma, Austria), yeast protease inhibitor cocktail (yPIC, #P8215-5ML, Sigma,
691 Austria), 2 mM phenylmethylsulfonyl fluoride (PMSF, #P7626-5G, Sigma, Austria)) and 20 mM *N*-
692 ethylmaleimide (NEM, #E3876-5G, Sigma, Austria) using four cycles of lysis (2 min), each separated
693 by 2 min chilling on ice. The lysate was then rotated for 30 min at 4°C for solubilization. 500 µl wash
694 buffer (50 mM Tris-HCl, pH 7.5, 150 mM NaCl, 1% Nonidet P 40, 5% glycerol) containing 20 mM
695 NEM were added and the sample was mixed and further rotated for 1h at 4°C. After vortexing for 3
696 min, the lysate was centrifuged at 10000g for 10 min at 4°C. The cleared lysate was then added to 25 µl
697 of GFP-Trap_MA magnetic agarose beads (#gtma-20, ChromoTek, Germany) prewashed twice in 1 ml
698 wash buffer. The sample was rotated for 5h at 4°C. The beads were collected using a magnetic rack and
699 washed twice by rotating for 15 min at 4°C with 1.5 ml ice-cold wash buffer. The beads were further
700 washed for 30 min at RT with 1.5 ml saline buffer (50 mM Tris-HCl, pH 7.5, 150 mM NaCl), containing
701 0.1% Tween-20 (#9127.1, Roth, Germany), resuspended in 50 µl 2x urea sample buffer (150 mM Tris-
702 HCl, pH 6.8, 6M urea, 6% SDS, 0.01% bromophenol blue) and incubated for 30 min at 1400 rpm and
703 37°C in a thermomixer. Then, 50 µl boiling buffer (50 mM Tris-HCl, pH 7.5, 1 mM EDTA, 1%, 20%
704 glycerol) was added and the sample was further incubated for 30 min at 1400 rpm and 42°C in a
705 thermomixer. The resulting eluates were subjected to WB analysis. For mass spectrometry analysis of
706 Mup1-GFP 300 OD_{600} equivalents were used with the following modifications: Cells were lysed by with
707 glass beads (3x 1min) at 4°C in 3ml RIPA buffer (50 mM Tris/HCl, pH 7,5, 200 mM NaCl, 10%
708 glycerol, 1% NP-40, 1% Na-Deoxycholate, 0,1% SDS, 2 mM EDTA, 0,1% Tween-20, 25mM NaF, 1x
709 PhosStop (#PHOSS-RO, Sigma, Germany), 1x Complete EDTA-free protease inhibitors, 0.67 mM
710 DTT, 1x yPIC, 2mM PMSF, 20mM NEM. Subsequently another 3 ml of RIPA buffer were added and
711 the lysate was sonicated 5x 1min at 4°C in a water bath sonicator. Lysates were incubated 30 minutes
712 on ice and then centrifuged at 10000g for 10 minutes to remove debris. 80 ul of equilibrated GFP-trap
713 beads were added to the supernatant and incubated rolling for 16 hours at 4°C. Beads were washed at
714 4°C 3 x 15 min with RIPA buffer supplemented with 500 mM NaCl and then 3x 15 min with urea wash
715 buffer (50 mM Tris/HCl pH 7.5, 100 mM NaCl, 4M Urea). Mup1-GFP was eluated from beads using
716 urea sample buffer as described above. Eluates were separated via SDS-PAGE and Mup1-GFP was
717 visualized by Coomassie staining. Slices were cut from the gel (including the visible Mup1-GFP protein
718 bands and the region above containing ubiquitinated Mup1-GFP) and subjected for further mass
719 spectrometry sample preparation.
720
721 **Mass spectrometry sample preparation and analysis.**
722 Coomassie-stained gel bands were excised from SDS-PAGE gels, reduced with dithiothreitol, alkylated

723 with iodoacetamide and digested with trypsin (Promega) as previously described (Faserl et al., 2019).
724 Tryptic digest were analyzed using an UltiMate 3000 RSCLnano-HPLC system coupled to a Q Exactive
725 HF mass spectrometer (both Thermo Scientific, Bremen, Germany) equipped with a Nanospray Flex
726 ionization source. The peptides were separated on a homemade fritless fused-silica micro-capillary
727 column (75 µm i.d. x 280 µm o.d. x 10 cm length) packed with 3.0 µm reversed-phase C18 material.
728 Solvents for HPLC were 0.1% formic acid (solvent A) and 0.1% formic acid in 85% acetonitrile (solvent
729 B). The gradient profile was as follows: 0-4 min, 4% B; 4-57 min, 4-35% B; 57-62 min, 35-100% B,
730 and 62-67 min, 100 % B. The flow rate was 250 nL/min.
731 The Q Exactive HF mass spectrometer was operating in the data dependent mode selecting the top 20
732 most abundant isotope patterns with charge >1 from the survey scan with an isolation window of 1.6
733 mass-to-charge ratio (m/z). Survey full scan MS spectra were acquired from 300 to 1750 m/z at a
734 resolution of 60,000 with a maximum injection time (IT) of 120 ms, and automatic gain control (AGC)
735 target 1e6. The selected isotope patterns were fragmented by higher-energy collisional dissociation with
736 normalized collision energy of 28 at a resolution of 30,000 with a maximum IT of 120 ms, and AGC
737 target 5e5.
738 Data Analysis was performed using Proteome Discoverer 4.1 (Thermo Scientific) with search engine
739 Sequest. The raw files were searched against yeast database (orf_trans_all) with sequence of Mup1-GFP
740 added. Precursor and fragment mass tolerance was set to 10 ppm and 0.02 Da, respectively, and up to
741 two missed cleavages were allowed. Carbamidomethylation of cysteine was set as static modification.
742 Oxidation of methionine, ubiquitination of lysine, and phosphorylation of serine threonine, and tyrosine
743 were set as variable modifications. Peptide identifications were filtered at 1% false discovery rate.
744
745 **RNA isolation and quantitative PCR (RT-qPCR)**
746 Exponentially growing or starved cells (40 OD_{600nm}) were harvested by centrifugation and immediately
747 frozen in lq. N_2. Cell pellets were lysed with 1 mm glass beads in a FastPrep-24 homogenizer (MP
748 biosciences) in Qiagen RLT buffer, and RNA was extracted using the RNeasy Mini Kit (#74104,
749 Qiagen, Germany). Yield and purity were determined photometrically. cDNA was prepared from 5 µg
750 DNAse I-treated RNA using the RevertAid First Strand cDNA Synthesis Kit (#K1622, Thermo Fisher,
751 USA) with oligo-dT primer according to the standard protocol. qPCR was performed in 10µl scale with
752 4µl of cDNA, 5µl TaqMan Gene Expression Master Mix (#4369016, Thermo Fisher, USA) and 0.5 µl
753 TaqMan probe on a PikoReal 96 Real-Time PCR System (Thermo Fisher, USA) with 7 min initial
754 denaturation (95°C) and 40 cycles of 5 sec 95°C and 30 sec 60°C. TaqMan gene expression assays were
755 from Thermo Fisher (*PGK1*: Sc04104844_s1; *ECM21/ART2:* Sc04099967_s1). All probes and primer
756 anneal within coding sequences. Each RT-qPCR analysis was done from 2-3 independent biological
757 samples in 3-4 technical replicates. Data were analyzed with the PikoReal software (version 2.2; Thermo
758 Fisher) with manual threshold adjustment, and relative mRNA abundance was calculated in Microsoft
759 Excel using the $\Delta\Delta C_T$ method. Statistical comparisons were calculated using the Student t-test.

Acknowledgments:

We are greatful to Claudine Kraft and Scott Emr for reagents. This work was supported by EMBO/Marie Curie (ALTF 642-2012; EMBOCOFUND2010, GA-2010-267146) and 'Tiroler Wissenschaftsfond' to O.S., Austrian Science Fund (FWF-Y444-B12, P30263, P29583) and MCBO (W1101-B18) to D.T and Agence Nationale pour la Recherche ("P-Nut", ANR-16-CE13-0002-01) to S.L.

Competing interests :

The authors have no competing interests.

Author contributions:

V.I., J.Z., S.W., J.K, R.G., T.J., G.K.B and L.A.H. performed the screens. V.I. and J.Z. analyzed Mup1 ubiquitination and J.Z. characterized the contribution of the GAAC. V.I and S.S. analyzed Mup1 degrons and Art2 basic patches. V.I., L.K. and H.L performed and analyzed mass spectrometry experiments. V.I., J.Z., S.S., J.K., S.L. and O.S. constructed yeast strains and plasmids and conducted microscopy, biochemical and genetic experiments. O.S. and D.T. and analyzed data, conceptualized and guided the study; S.L., D.T. and O.S. wrote the manuscript.

774 **References**

ALBUQUERQUE, C. P., SMOLKA, M. B., PAYNE, S. H., BAFNA, V., ENG, J. & ZHOU, H. 2008. A multidimensional chromatography technology for in-depth phosphoproteome analysis. *Mol Cell Proteomics,* 7**,** 1389-96.

ALVAREZ, C. E. 2008. On the origins of arrestin and rhodopsin. *BMC Evol Biol,* 8**,** 222.

ALVARO, C. G., O'DONNELL, A. F., PROSSER, D. C., AUGUSTINE, A. A., GOLDMAN, A., BRODSKY, J. L., CYERT, M. S., WENDLAND, B. & THORNER, J. 2014. Specific alpha-arrestins negatively regulate Saccharomyces cerevisiae pheromone response by down-modulating the G-protein-coupled receptor Ste2. *Mol Cell Biol,* 34**,** 2660-81.

ANDRE, B. 2018. Tribute to Marcelle Grenson (1925-1996), A Pioneer in the Study of Amino Acid Transport in Yeast. *Int J Mol Sci,* 19.

AUBRY, L., GUETTA, D. & KLEIN, G. 2009. The arrestin fold: variations on a theme. *Curr Genomics,* 10**,** 133-42.

BABST, M. 2020. Regulation of nutrient transporters by metabolic and environmental stresses. *Curr Opin Cell Biol,* 65**,** 35-41.

BABU, M., VLASBLOM, J., PU, S., GUO, X., GRAHAM, C., BEAN, B. D., BURSTON, H. E., VIZEACOUMAR, F. J., SNIDER, J., PHANSE, S., FONG, V., TAM, Y. Y., DAVEY, M., HNATSHAK, O., BAJAJ, N., CHANDRAN, S., PUNNA, T., CHRISTOPOLOUS, C., WONG, V., YU, A., ZHONG, G., LI, J., STAGLJAR, I., CONIBEAR, E., WODAK, S. J., EMILI, A. & GREENBLATT, J. F. 2012. Interaction landscape of membrane-protein complexes in Saccharomyces cerevisiae. *Nature,* 489**,** 585-9.

BAILE, M. G., GUINEY, E. L., SANFORD, E. J., MACGURN, J. A., SMOLKA, M. B. & EMR, S. D. 2019. Activity of a ubiquitin ligase adaptor is regulated by disordered insertions in its arrestin domain. *Mol Biol Cell,* 30**,** 3057-3072.

BECUWE, M., HERRADOR, A., HAGUENAUER-TSAPIS, R., VINCENT, O. & LEON, S. 2012a. Ubiquitin-mediated regulation of endocytosis by proteins of the arrestin family. *Biochem Res Int,* 2012**,** 242764.

BECUWE, M. & LEON, S. 2014. Integrated control of transporter endocytosis and recycling by the arrestin-related protein Rod1 and the ubiquitin ligase Rsp5. *Elife,* 3.

BECUWE, M., VIEIRA, N., LARA, D., GOMES-REZENDE, J., SOARES-CUNHA, C., CASAL, M., HAGUENAUER-TSAPIS, R., VINCENT, O., PAIVA, S. & LEON, S. 2012b. A molecular switch on an arrestin-like protein relays glucose signaling to transporter endocytosis. *J Cell Biol,* 196**,** 247-59.

BELGAREH-TOUZE, N., LEON, S., ERPAPAZOGLOU, Z., STAWIECKA-MIROTA, M., URBAN-GRIMAL, D. & HAGUENAUER-TSAPIS, R. 2008. Versatile role of the yeast ubiquitin ligase Rsp5p in intracellular trafficking. *Biochem Soc Trans,* 36**,** 791-6.

BREKER, M., GYMREK, M., MOLDAVSKI, O. & SCHULDINER, M. 2014. LoQAtE--Localization and Quantitation ATlas of the yeast proteomE. A new tool for multiparametric dissection of single-protein behavior in response to biological perturbations in yeast. *Nucleic Acids Res,* 42**,** D726-30.

BROACH, J. R. 2012. Nutritional control of growth and development in yeast. *Genetics,* 192**,** 73-105.

BUSTO, J. V., ELTING, A., HAASE, D., SPIRA, F., KUHLMAN, J., SCHAFER-HERTE, M. & WEDLICH-SOLDNER, R. 2018. Lateral plasma membrane compartmentalization links protein function and turnover. *EMBO J,* 37.

DUPRÉ, S., URBAN-GRIMAL, D. & HAGUENAUER-TSAPIS, R. 2004. Ubiquitin and endocytic internalization in yeast and animal cells. *Biochim Biophys Acta,* 1695**,** 89-111.

EDINGER, A. L. & THOMPSON, C. B. 2002a. Akt maintains cell size and survival by increasing mTOR-dependent nutrient uptake. *Mol Biol Cell,* 13**,** 2276-88.

EDINGER, A. L. & THOMPSON, C. B. 2002b. Antigen-presenting cells control T cell proliferation by regulating amino acid availability. *Proc Natl Acad Sci U S A,* 99**,** 1107-9.

FASERL, K., CHETWYND, A. J., LYNCH, I., THORN, J. A. & LINDNER, H. H. 2019. Corona Isolation Method Matters: Capillary Electrophoresis Mass Spectrometry Based Comparison of Protein Corona Compositions Following On-Particle versus In-Solution or In-Gel Digestion. *Nanomaterials (Basel),* 9.

GHADDAR, K., MERHI, A., SALIBA, E., KRAMMER, E. M., PREVOST, M. & ANDRE, B. 2014. Substrate-induced ubiquitylation and endocytosis of yeast amino acid permeases. *Mol Cell Biol,* 34**,** 4447-63.

GOURNAS, C., GKIONIS, S., CARQUIN, M., TWYFFELS, L., TYTECA, D. & ANDRE, B. 2018. Conformation-dependent partitioning of yeast nutrient transporters into starvation-protective membrane domains. *Proc Natl Acad Sci U S A,* 115**,** E3145-E3154.

GOURNAS, C., SALIBA, E., KRAMMER, E. M., BARTHELEMY, C., PREVOST, M. & ANDRE, B. 2017. Transition of yeast Can1 transporter to the inward-facing state unveils an alpha-arrestin target sequence promoting its ubiquitylation and endocytosis. *Mol Biol Cell,* 28**,** 2819-2832.

GRENSON, M. 1966. Multiplicity of the amino acid permeases in Saccharomyces cerevisiae. II. Evidence for a specific lysine-transporting system. *Biochim Biophys Acta,* 127**,** 339-46.

GRENSON, M., MOUSSET, M., WIAME, J. M. & BECHET, J. 1966. Multiplicity of the amino acid permeases in Saccharomyces cerevisiae. I. Evidence for a specific arginine-transporting system. *Biochim Biophys Acta,* 127**,** 325-38.

GROSSMANN, G., MALINSKY, J., STAHLSCHMIDT, W., LOIBL, M., WEIG-MECKL, I., FROMMER, W. B., OPEKAROVA, M. & TANNER, W. 2008. Plasma membrane microdomains regulate turnover of transport proteins in yeast. *J Cell Biol,* 183**,** 1075-88.

GUINEY, E. L., KLECKER, T. & EMR, S. D. 2016. Identification of the endocytic sorting signal recognized by the Art1-Rsp5 ubiquitin ligase complex. *Mol Biol Cell,* 27**,** 4043-4054.

HARRIS, M. A., CLARK, J., IRELAND, A., LOMAX, J., ASHBURNER, M., FOULGER, R., EILBECK, K., LEWIS, S., MARSHALL, B., MUNGALL, C., RICHTER, J., RUBIN, G. M., BLAKE, J. A., BULT, C., DOLAN, M., DRABKIN, H., EPPIG, J. T., HILL, D. P., NI, L., RINGWALD, M., BALAKRISHNAN, R., CHERRY, J. M., CHRISTIE, K. R., COSTANZO, M. C., DWIGHT, S. S., ENGEL, S., FISK, D. G., HIRSCHMAN, J. E., HONG, E. L., NASH, R. S., SETHURAMAN, A., THEESFELD, C. L., BOTSTEIN, D., DOLINSKI, K., FEIERBACH, B., BERARDINI, T., MUNDODI, S., RHEE, S. Y., APWEILER, R., BARRELL, D., CAMON, E., DIMMER, E., LEE, V., CHISHOLM, R., GAUDET, P., KIBBE, W., KISHORE, R., SCHWARZ, E. M., STERNBERG, P., GWINN, M., HANNICK, L., WORTMAN, J., BERRIMAN, M., WOOD, V., DE LA CRUZ, N., TONELLATO, P., JAISWAL, P., SEIGFRIED, T. & WHITE, R. 2004. The Gene Ontology (GO) database and informatics resource. *Nucleic Acids Res,* 32**,** D258-61.

HEIN, C., SPRINGAEL, J. Y., VOLLAND, C., HAGUENAUER-TSAPIS, R. & ANDRE, B. 1995. NPl1, an essential yeast gene involved in induced degradation of Gap1 and Fur4 permeases, encodes the Rsp5 ubiquitin-protein ligase. *Mol Microbiol,* 18**,** 77-87.

HENNE, W. M., ZHU, L., BALOGI, Z., STEFAN, C., PLEISS, J. A. & EMR, S. D. 2015. Mdm1/Snx13 is a novel ER-endolysosomal interorganelle tethering protein. *J Cell Biol,* 210**,** 541-51.

HICKE, L., ZANOLARI, B. & RIEZMAN, H. 1998. Cytoplasmic tail phosphorylation of the alpha-factor receptor is required for its ubiquitination and internalization. *J Cell Biol,* 141**,** 349-58.

HINNEBUSCH, A. G. 2005. Translational regulation of GCN4 and the general amino acid control of yeast. *Annu Rev Microbiol,* 59**,** 407-50.

HO, H. C., MACGURN, J. A. & EMR, S. D. 2017. Deubiquitinating enzymes Ubp2 and Ubp15 regulate endocytosis by limiting ubiquitination and degradation of ARTs. *Mol Biol Cell,* 28**,** 1271-1283.

HOLT, L. J., TUCH, B. B., VILLEN, J., JOHNSON, A. D., GYGI, S. P. & MORGAN, D. O. 2009. Global analysis of Cdk1 substrate phosphorylation sites provides insights into evolution. *Science,* 325**,** 1682-6.

HOVSEPIAN, J., DEFENOUILLERE, Q., ALBANESE, V., VACHOVA, L., GARCIA, C., PALKOVA, Z. & LEON, S. 2017. Multilevel regulation of an alpha-arrestin by glucose depletion controls hexose transporter endocytosis. *J Cell Biol*.

HUANG, W., MASUREEL, M., QU, Q., JANETZKO, J., INOUE, A., KATO, H. E., ROBERTSON, M. J., NGUYEN, K. C., GLENN, J. S., SKINIOTIS, G. & KOBILKA, B. K. 2020. Structure of the neurotensin receptor 1 in complex with beta-arrestin 1. *Nature,* 579**,** 303-308.

HUH, W. K., FALVO, J. V., GERKE, L. C., CARROLL, A. S., HOWSON, R. W., WEISSMAN, J. S. & O'SHEA, E. K. 2003. Global analysis of protein localization in budding yeast. *Nature,* 425**,** 686-91.

IESMANTAVICIUS, V., WEINERT, B. T. & CHOUDHARY, C. 2014. Convergence of ubiquitylation and phosphorylation signaling in rapamycin-treated yeast cells. *Mol Cell Proteomics,* 13**,** 1979-92.

IRNIGER, S. & BRAUS, G. H. 2003. Controlling transcription by destruction: the regulation of yeast Gcn4p stability. *Curr Genet,* 44**,** 8-18.

JONES, C. B., OTT, E. M., KEENER, J. M., CURTISS, M., SANDRIN, V. & BABST, M. 2012. Regulation of membrane protein degradation by starvation-response pathways. *Traffic,* 13**,** 468-82.

KANDASAMY, P., GYIMESI, G., KANAI, Y. & HEDIGER, M. A. 2018. Amino acid transporters revisited: New views in health and disease. *Trends Biochem Sci,* 43**,** 752-789.

KEE, Y., MUNOZ, W., LYON, N. & HUIBREGTSE, J. M. 2006. The deubiquitinating enzyme Ubp2 modulates Rsp5-dependent Lys63-linked polyubiquitin conjugates in Saccharomyces cerevisiae. *J Biol Chem,* 281**,** 36724-31.

KEENER, J. M. & BABST, M. 2013. Quality control and substrate-dependent downregulation of the nutrient transporter Fur4. *Traffic,* 14**,** 412-27.

KORNITZER, D., RABOY, B., KULKA, R. G. & FINK, G. R. 1994. Regulated degradation of the transcription factor Gcn4. *EMBO J,* 13**,** 6021-30.

LEE, S., HO, H. C., TUMOLO, J. M., HSU, P. C. & MACGURN, J. A. 2019. Methionine triggers Ppz-mediated dephosphorylation of Art1 to promote cargo-specific endocytosis. *J Cell Biol,* 218**,** 977-992.

LIN, C. H., MACGURN, J. A., CHU, T., STEFAN, C. J. & EMR, S. D. 2008. Arrestin-related ubiquitin-ligase adaptors regulate endocytosis and protein turnover at the cell surface. *Cell,* 135**,** 714-25.

LLOPIS-TORREGROSA, V., FERRI-BLAZQUEZ, A., ADAM-ARTIGUES, A., DEFFONTAINES, E., VAN HEUSDEN, G. P. & YENUSH, L. 2016. Regulation of the Yeast Hxt6 Hexose Transporter by the Rod1 alpha-Arrestin, the Snf1 Protein Kinase, and the Bmh2 14-3-3 Protein. *J Biol Chem,* 291**,** 14973-85.

MACGURN, J. A., HSU, P.-C., SMOLKA, M. B. & EMR, S. D. 2011. TORC1 Regulates Endocytosis via Npr1-Mediated Phosphoinhibition of a Ubiquitin Ligase Adaptor. *Cell,* 147**,** 1104-1117.

MACGURN, J. A., HSU, P. C. & EMR, S. D. 2012. Ubiquitin and membrane protein turnover: from cradle to grave. *Annu Rev Biochem,* 81**,** 231-59.

MARCHAL, C., DUPRE, S. & URBAN-GRIMAL, D. 2002. Casein kinase I controls a late step in the endocytic trafficking of yeast uracil permease. *J Cell Sci,* 115**,** 217-26.

MARCHAL, C., HAGUENAUER-TSAPIS, R. & URBAN-GRIMAL, D. 1998. A PEST-like sequence mediates phosphorylation and efficient ubiquitination of yeast uracil permease. *Mol Cell Biol,* 18**,** 314-21.

MARCHAL, C., HAGUENAUER-TSAPIS, R. & URBAN-GRIMAL, D. 2000. Casein kinase I-dependent phosphorylation within a PEST sequence and ubiquitination at nearby lysines signal endocytosis of yeast uracil permease. *J Biol Chem,* 275**,** 23608-14.

MCCLELLAN, A. J., XIA, Y., DEUTSCHBAUER, A. M., DAVIS, R. W., GERSTEIN, M. & FRYDMAN, J. 2007. Diverse cellular functions of the Hsp90 molecular chaperone uncovered using systems approaches. *Cell,* 131**,** 121-35.

MCCRACKEN, A. N. & EDINGER, A. L. 2013. Nutrient transporters: the Achilles' heel of anabolism. *Trends Endocrinol Metab,* 24**,** 200-8.

MEIMOUN, A., HOLTZMAN, T., WEISSMAN, Z., MCBRIDE, H. J., STILLMAN, D. J., FINK, G. R. & KORNITZER, D. 2000. Degradation of the transcription factor Gcn4 requires the kinase Pho85 and the SCF(CDC4) ubiquitin-ligase complex. *Mol Biol Cell,* 11**,** 915-27.

MEJLVANG, J., OLSVIK, H., SVENNING, S., BRUUN, J. A., ABUDU, Y. P., LARSEN, K. B., BRECH, A., HANSEN, T. E., BRENNE, H., HANSEN, T., STENMARK, H. & JOHANSEN, T. 2018. Starvation induces rapid degradation of selective autophagy receptors by endosomal microautophagy. *J Cell Biol.*

MERHI, A. & ANDRE, B. 2012. Internal amino acids promote Gap1 permease ubiquitylation via TORC1/Npr1/14-3-3-dependent control of the Bul arrestin-like adaptors. *Mol Cell Biol,* 32**,** 4510-22.

MERHI, A. & ANDRÉ, B. 2012. Internal amino acids promote Gap1 permease ubiquitylation via TORC1/Npr1/14-3-3-dependent control of the Bul arrestin-like adaptors. *Mol Cell Biol,* 32**,** 4510-22.

MUELLER, P. P. & HINNEBUSCH, A. G. 1986. Multiple upstream AUG codons mediate translational control of GCN4. *Cell,* 45**,** 201-7.

MÜLLER, M., SCHMIDT, O., ANGELOVA, M., FASERL, K., WEYS, S., KREMSER, L., PFAFFENWIMMER, T., DALIK, T., KRAFT, C., TRAJANOSKI, Z., LINDNER, H., TEIS, D. & MIZUSHIMA, N. 2015. The coordinated action of the MVB pathway and autophagy ensures cell survival during starvation. *Elife,* 4**,** e07736.

NIKKO, E. & PELHAM, H. R. 2009. Arrestin-mediated endocytosis of yeast plasma membrane transporters. *Traffic,* 10**,** 1856-67.

NIKKO, E., SULLIVAN, J. A. & PELHAM, H. R. 2008. Arrestin-like proteins mediate ubiquitination and endocytosis of the yeast metal transporter Smf1. *EMBO Rep,* 9**,** 1216-21.

NOBLES, K. N., XIAO, K., AHN, S., SHUKLA, A. K., LAM, C. M., RAJAGOPAL, S., STRACHAN, R. T., HUANG, T. Y., BRESSLER, E. A., HARA, M. R., SHENOY, S. K., GYGI, S. P. & LEFKOWITZ, R. J. 2011. Distinct phosphorylation sites on the beta(2)-adrenergic receptor establish a barcode that encodes differential functions of beta-arrestin. *Sci Signal,* 4**,** ra51.

O'DONNELL, A. F., HUANG, L., THORNER, J. & CYERT, M. S. 2013. A calcineurin-dependent switch controls the trafficking function of alpha-arrestin Aly1/Art6. *J Biol Chem,* 288**,** 24063-80.

O'DONNELL, A. F. & SCHMIDT, M. C. 2019. AMPK-Mediated Regulation of Alpha-Arrestins and Protein Trafficking. *Int J Mol Sci,* 20.

PAIVA, S., VIEIRA, N., NONDIER, I., HAGUENAUER-TSAPIS, R., CASAL, M. & URBAN-GRIMAL, D. 2009. Glucose-induced ubiquitylation and endocytosis of the yeast Jen1 transporter: role of lysine 63-linked ubiquitin chains. *J Biol Chem,* 284**,** 19228-36.

POLEKHINA, G., ASCHER, D. B., KOK, S. F., BECKHAM, S., WILCE, M. & WALTHAM, M. 2013. Structure of the N-terminal domain of human thioredoxin-interacting protein. *Acta Crystallogr D Biol Crystallogr,* 69**,** 333-44.

PROSSER, D. C., WHITWORTH, K. & WENDLAND, B. 2010. Quantitative analysis of endocytosis with cytoplasmic pHluorin chimeras. *Traffic,* 11**,** 1141-50.

RAUCH, S. & MARTIN-SERRANO, J. 2011. Multiple interactions between the ESCRT machinery and arrestin-related proteins: implications for PPXY-dependent budding. *J Virol,* 85**,** 3546-56.

SAIER, M. H., JR., REDDY, V. S., TSU, B. V., AHMED, M. S., LI, C. & MORENO-HAGELSIEB, G. 2016. The Transporter Classification Database (TCDB): recent advances. *Nucleic Acids Res,* 44**,** D372-9.

SAVOCCO, J., NOOTENS, S., AFOKPA, W., BAUSART, M., CHEN, X., VILLERS, J., RENARD, H. F., PREVOST, M., WATTIEZ, R. & MORSOMME, P. 2019. Yeast alpha-arrestin Art2 is the key regulator of ubiquitylation-dependent endocytosis of plasma membrane vitamin B1 transporters. *PLoS Biol,* 17**,** e3000512.

SCHULDINER, O., YANOVER, C. & BENVENISTY, N. 1998. Computer analysis of the entire budding yeast genome for putative targets of the GCN4 transcription factor. *Curr Genet,* 33**,** 16-20.

SHUKLA, A. K., WESTFIELD, G. H., XIAO, K., REIS, R. I., HUANG, L. Y., TRIPATHI-SHUKLA, P., QIAN, J., LI, S., BLANC, A., OLESKIE, A. N., DOSEY, A. M., SU, M., LIANG, C. R., GU, L. L., SHAN, J. M., CHEN, X., HANNA, R., CHOI, M., YAO, X. J., KLINK, B. U., KAHSAI, A. W., SIDHU, S. S., KOIDE, S., PENCZEK, P. A., KOSSIAKOFF, A. A., WOODS, V. L., JR., KOBILKA, B. K., SKINIOTIS, G. & LEFKOWITZ, R. J. 2014. Visualization of arrestin recruitment by a G-protein-coupled receptor. *Nature,* 512**,** 218-22.

SMITH, R. J. 1990. Glutamine metabolism and its physiologic importance. *JPEN J Parenter Enteral Nutr,* 14**,** 40S-44S.

SPIRA, F., MUELLER, N. S., BECK, G., VON OLSHAUSEN, P., BEIG, J. & WEDLICH-SOLDNER, R. 2012. Patchwork organization of the yeast plasma membrane into numerous coexisting domains. *Nat Cell Biol,* 14**,** 640-8.

STAUS, D. P., HU, H., ROBERTSON, M. J., KLEINHENZ, A. L. W., WINGLER, L. M., CAPEL, W. D., LATORRACA, N. R., LEFKOWITZ, R. J. & SKINIOTIS, G. 2020. Structure of the M2 muscarinic receptor-beta-arrestin complex in a lipid nanodisc. *Nature,* 579**,** 297-302.

SURAWEERA, A., MUNCH, C., HANSSUM, A. & BERTOLOTTI, A. 2012. Failure of amino acid homeostasis causes cell death following proteasome inhibition. *Mol Cell,* 48**,** 242-53.

SWANEY, D. L., BELTRAO, P., STARITA, L., GUO, A., RUSH, J., FIELDS, S., KROGAN, N. J. & VILLEN, J. 2013. Global analysis of phosphorylation and ubiquitylation cross-talk in protein degradation. *Nat Methods,* 10**,** 676-82.

TUMOLO, J. M., HEPOWIT, N. L., JOSHI, S. S. & MACGURN, J. A. 2020. A Snf1-related nutrient-responsive kinase antagonizes endocytosis in yeast. *PLoS Genet,* 16**,** e1008677.

VABULAS, R. M. & HARTL, F. U. 2005. Protein synthesis upon acute nutrient restriction relies on proteasome function. *Science,* 310**,** 1960-3.

VAN BELLE, D. & ANDRE, B. 2001. A genomic view of yeast membrane transporters. *Curr Opin Cell Biol,* 13**,** 389-98.

VENTERS, B. J., WACHI, S., MAVRICH, T. N., ANDERSEN, B. E., JENA, P., SINNAMON, A. J., JAIN, P., ROLLERI, N. S., JIANG, C., HEMERYCK-WALSH, C. & PUGH, B. F. 2011. A comprehensive genomic binding map of gene and chromatin regulatory proteins in Saccharomyces. *Mol Cell,* 41**,** 480-92.

ZHANG, J., PAVLOVA, N. N. & THOMPSON, C. B. 2017. Cancer cell metabolism: the essential role of the nonessential amino acid, glutamine. *EMBO J,* 36**,** 1302-1315.

ZIMMERMANN, L., STEPHENS, A., NAM, S. Z., RAU, D., KUBLER, J., LOZAJIC, M., GABLER, F., SODING, J., LUPAS, A. N. & ALVA, V. 2018. A Completely Reimplemented MPI Bioinformatics Toolkit with a New HHpred Server at its Core. *J Mol Biol,* 430**,** 2237-2243.

775
776

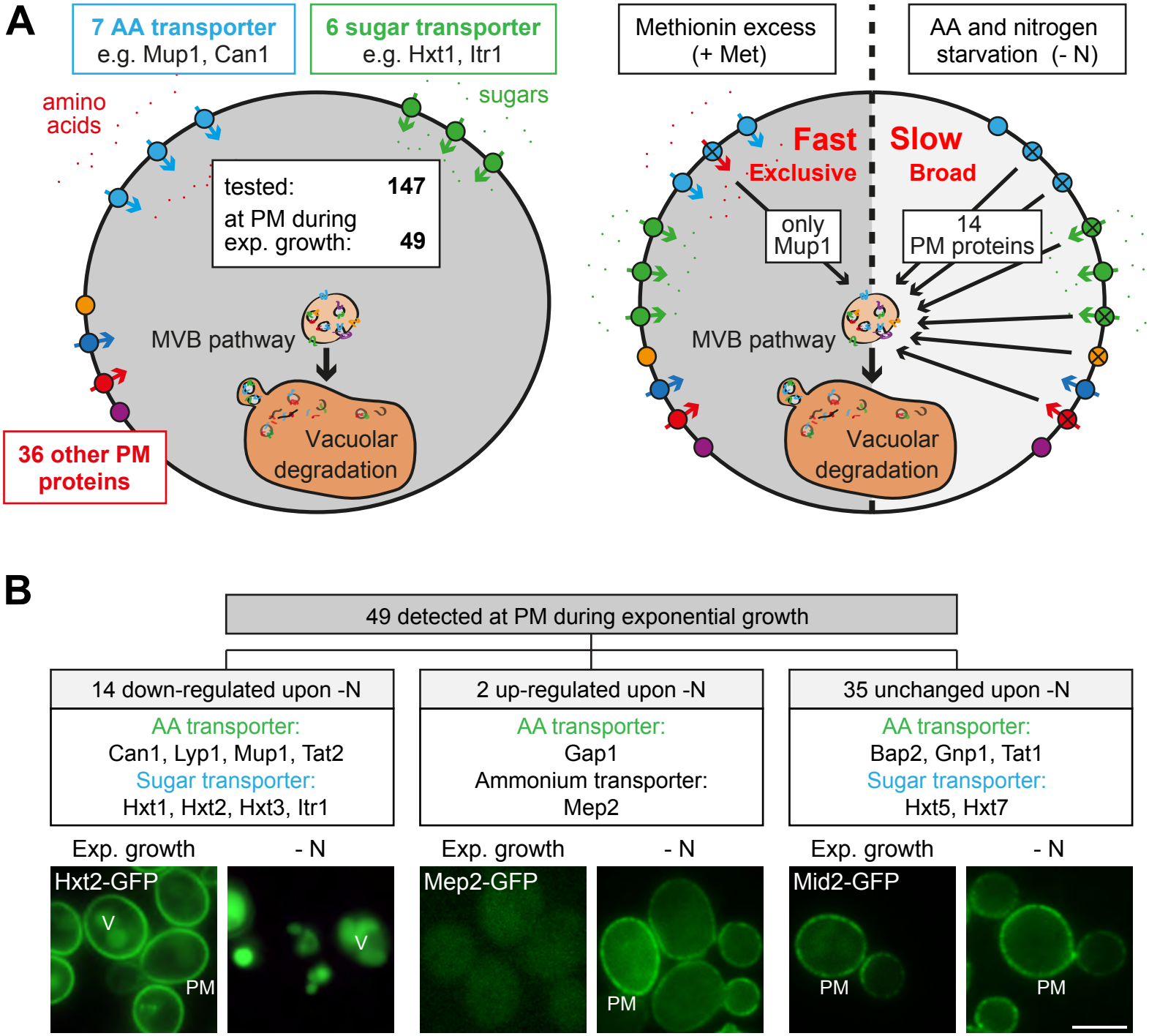
A
7 AA transporter
e.g. Mup1, Can1
6 sugar transporter
e.g. Hxt1, Itr1
amino acids
sugars
tested: 147
at PM during exp. growth: 49
MVB pathway
Vacuolar degradation
36 other PM proteins
Methionin excess (+ Met)
AA and nitrogen starvation (- N)
Fast
Exclusive
Slow
Broad
only Mup1
14 PM proteins
MVB pathway
Vacuolar degradation
B
49 detected at PM during exponential growth
14 down-regulated upon -N
AA transporter:
Can1, Lyp1, Mup1, Tat2
Sugar transporter:
Hxt1, Hxt2, Hxt3, Itr1
2 up-regulated upon -N
AA transporter:
Gap1
Ammonium transporter:
Mep2
35 unchanged upon -N
AA transporter:
Bap2, Gnp1, Tat1
Sugar transporter:
Hxt5, Hxt7
Exp. growth
- N
Hxt2-GFP
V
PM
V
Exp. growth
- N
Mep2-GFP
PM
Exp. growth
- N
Mid2-GFP
PM
PM

Figure 1

Figure 1: Amino acid and nitrogen starvation triggers broad but specific endocytosis and lysosomal degradation of plasma membrane proteins.

A) Left: a library of 147 yeast strains expressing chromosomally GFP-tagged membrane proteins was tested for plasma membrane (PM) localization during nutrient replete exponential growth. Right: verified PM proteins were starved for amino acids and nitrogen (- N) 6-8h or treated with 20 µg/ml L-methionine (+Met) after 24h of exponential growth. The localization of GFP was assayed by fluorescence microscopy. **B)** Summary of the phenotypes of GFP-tagged PM proteins during starvation. Indicated are numbers of PM proteins that are down-regulated, up-regulated or unchanged compared to the exponential growth phase, each exemplified by one representative strain. PM: plasma membrane; V: vacuole. Scale bars = 5 µm. See also Fig. S1 and Table S1.

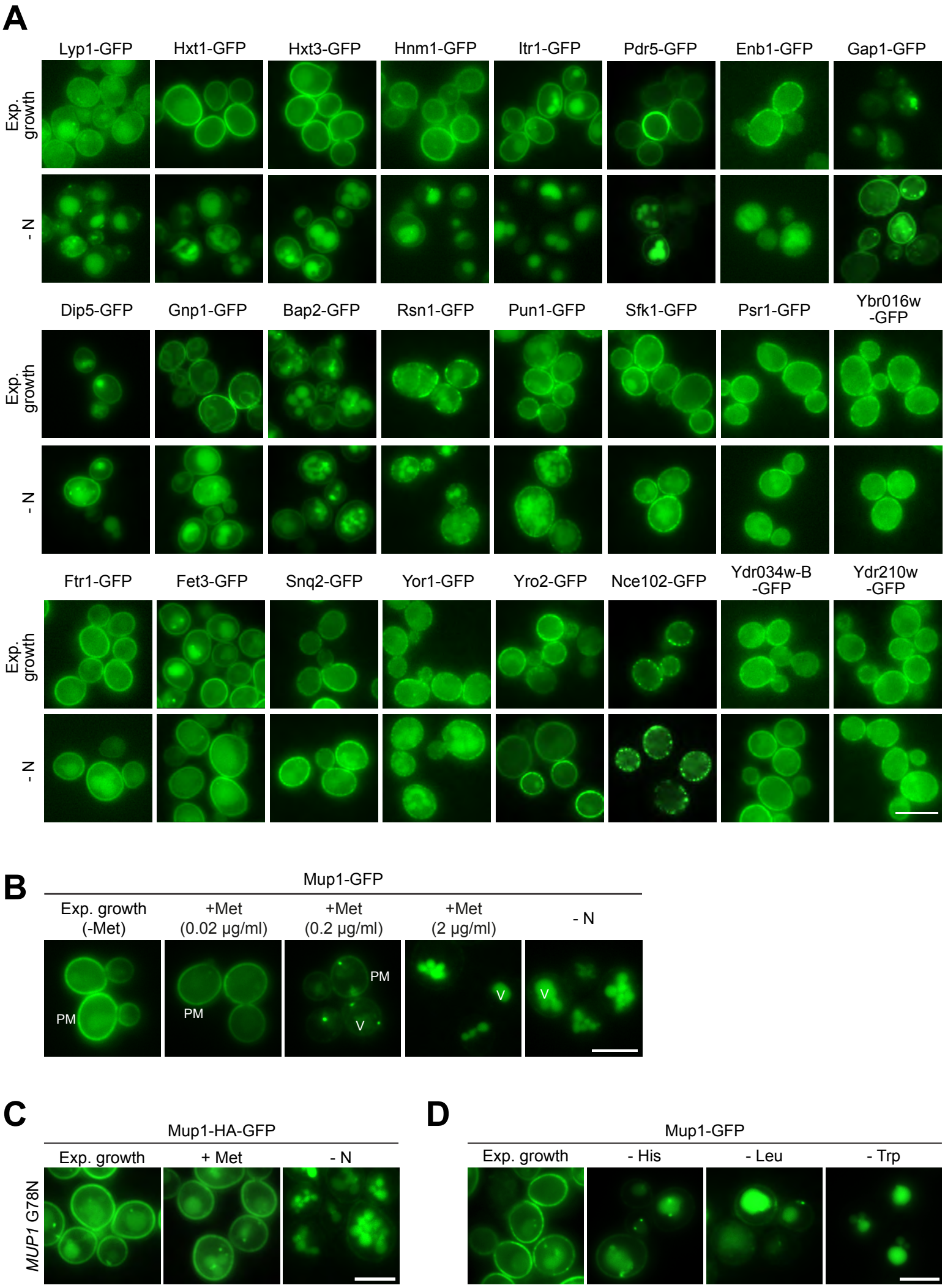

Figure S1 - related to Fig. 1

13 **Figure S1: Related to Fig. 1**

14 **A)** Live-cell fluorescence microscopy analysis of chromosomally GFP-tagged plasma membrane
15 proteins. Cells were starved (- N) for 6-8h after 24h exponential growth. **B)** Live-cell fluorescence
16 microscopy analysis of WT cells expressing *MUP1-GFP*. Cells were treated with the indicated
17 methionine concentrations (+ Met) for 1.5h or starved (- N) for 6h after 24h exponential growth. **C)**
18 Live-cell fluorescence microscopy analysis of *MUP1(G78N)-HA-GFP* cells. Cells were treated with 20
19 µg/ml L-methionine (+ Met) for 1.5h or starved (- N) for 6h after 24h exponential growth. PM: plasma
20 membrane; V: vacuole. Scale bars = 5 µm. **D)** Live-cell fluorescence microscopy analysis of WT cells
21 expressing *MUP1-GFP*. Cells were starved for histidine (- His), leucine (- Leu) or tryptophan (- Trp)
22 for 4.5h after in presence of all other amino acids required for growth after 24h nutrient replete
23 exponential growth.

24

25

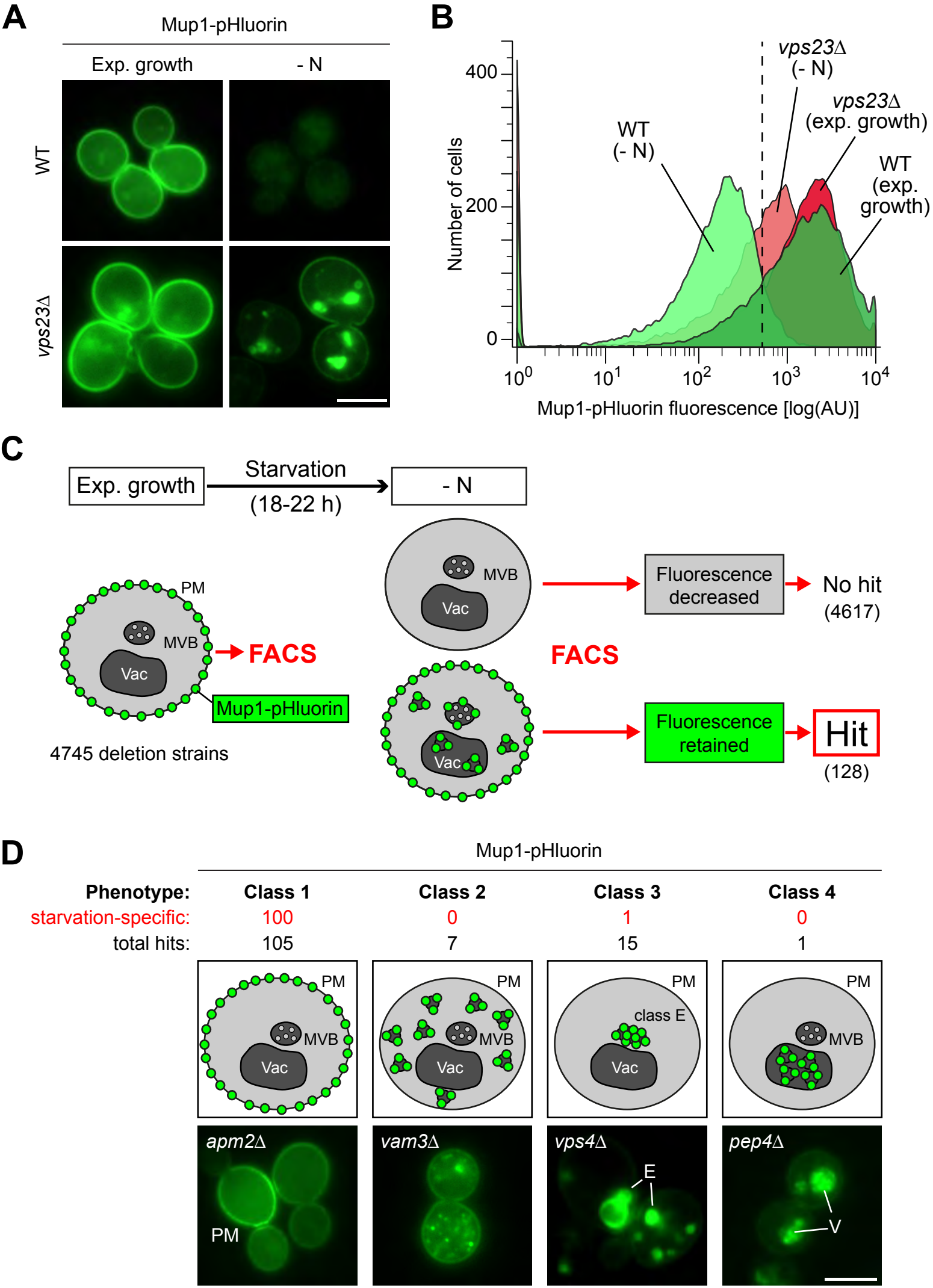
A
Mup1-pHluorin
Exp. growth
- N
WT
vps23Δ
B
Number of cells
400
200
0
vps23Δ
(- N)
vps23Δ
(exp. growth)
WT
(- N)
WT
(exp.
growth)
10^0
10^1
10^2
10^3
10^4
Mup1-pHluorin fluorescence [log(AU)]
C
Exp. growth
Starvation
(18-22 h)
- N
PM
MVB
Vac
FACS
Mup1-pHluorin
4745 deletion strains
MVB
Vac
Fluorescence
decreased
No hit
(4617)
FACS
Vac
Fluorescence
retained
Hit
(128)
D
Mup1-pHluorin
Phenotype:
Class 1
Class 2
Class 3
Class 4
starvation-specific:
100
0
1
0
total hits:
105
7
15
1
PM
MVB
Vac
PM
MVB
Vac
PM
class E
Vac
PM
MVB
apm2Δ
PM
vam3Δ
vps4Δ
E
pep4Δ
V

Figure 2

Figure 2: A genome wide screen revealed genes affecting Mup1-pHluorin endocytosis during starvation.

A) Live-cell fluorescence microscopy analysis of WT (BY4742) and *vps23*Δ cells expressing *MUP1-pHluorin* from plasmid and starved (- N) for 18-22h. The images exemplify quenched pHluorin fluorescence in vacuoles of wild type (WT)-like cells and retained fluorescence in mutants with defects in the starvation-induced endocytosis of Mup1-pHluorin. **B)** The strains from (A) were exponentially grown in 96-well plates for 5h and starved (- N) for 18-22h. At least 15000 cells from each strain and condition were analyzed by flow cytometry. The exemplified histograms display decrease of fluorescence in wild type (WT)-like strains and fluorescence retention in mutants with defects in the starvation-induced endocytosis of Mup1-pHluorin (e.g. *vps23*Δ). **C)** Workflow of the flow-cytometry-based genome-wide screen for mutants defective in starvation-induced endocytosis of Mup1-pHluorin. **D)** Summary of phenotypes of all mutants scored in the starvation-induced endocytosis screen (C) as determined by fluorescence microscopy. Class 1 mutants retain Mup1-pHluorin fluorescence at the plasma membrane (PM); class 2 mutants in small cytosolic objects; class 3 mutants in class E-like objects (E); class 4 mutants within vacuoles (V). Each phenotype is exemplified by one representative deletion mutant. Indicated are the numbers of strains that share a similar phenotype and the number of hits specific for starvation-induced endocytosis of Mup1-pHluorin (red). Scale bars = 5 µm. See also Fig. S2 and table S2.

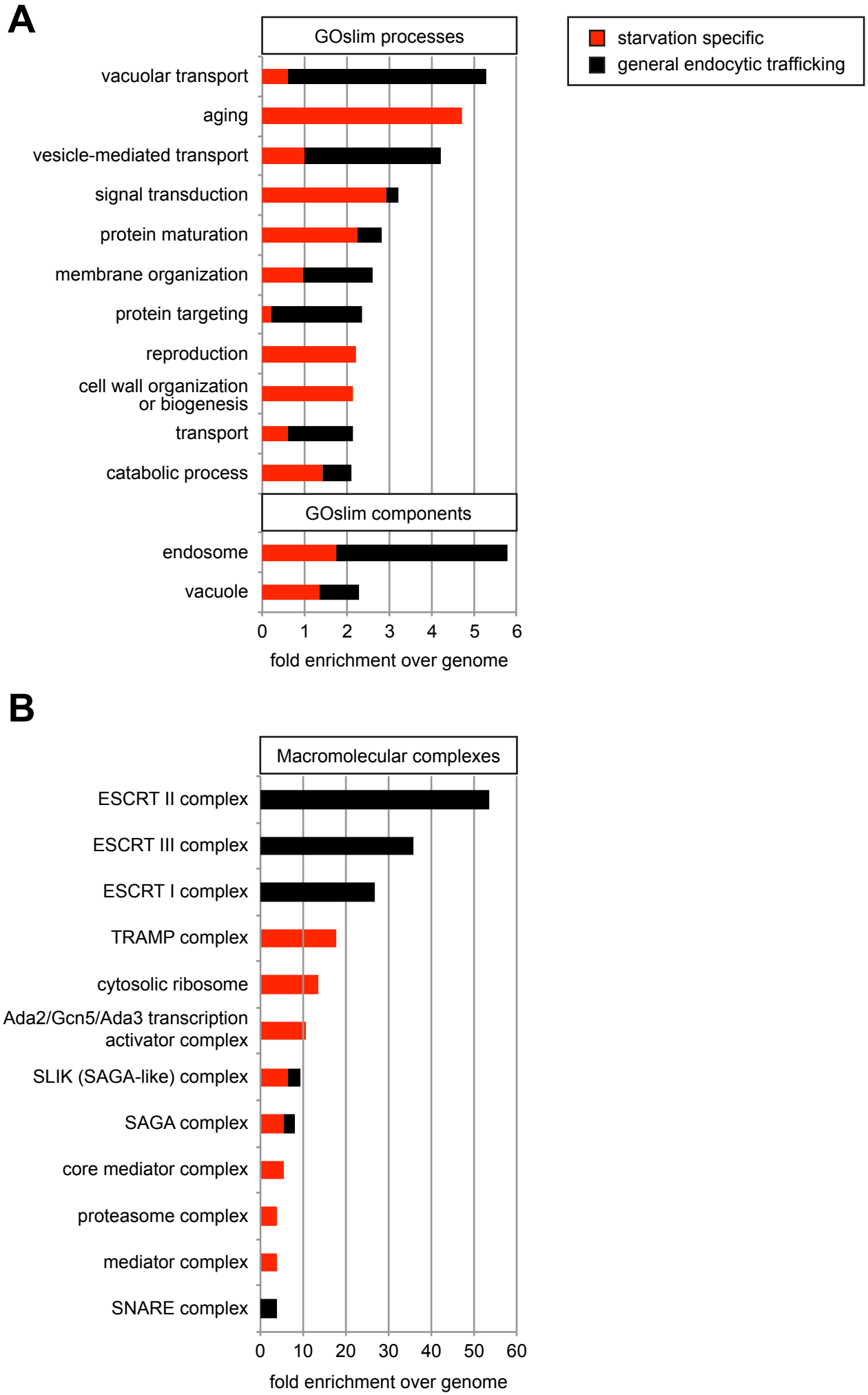

Figure S2 - related to Fig. 2

46 **Figure. S2: related to Fig. 2**

47 **A)** Enrichment of cellular processes and components GO terms in 128 hits from the genome-wide screen
48 for genes involved in the starvation-induced endocytosis of Mup1-pHluorin (table S2). Data are
49 represented as fold-enrichment over whole genome frequency, with the fraction of starvation-specific
50 genes in red and general endocytic trafficking regulators in black. Only GO terms with more than two-
51 fold enrichment over genome were included. (B) Enrichment of macromolecular complex GO terms in
52 128 hits from the genome-wide screen for genes involved in the starvation-induced endocytosis of
53 Mup1-pHluorin analyzed as in (A). See also table S3.

54

55

56

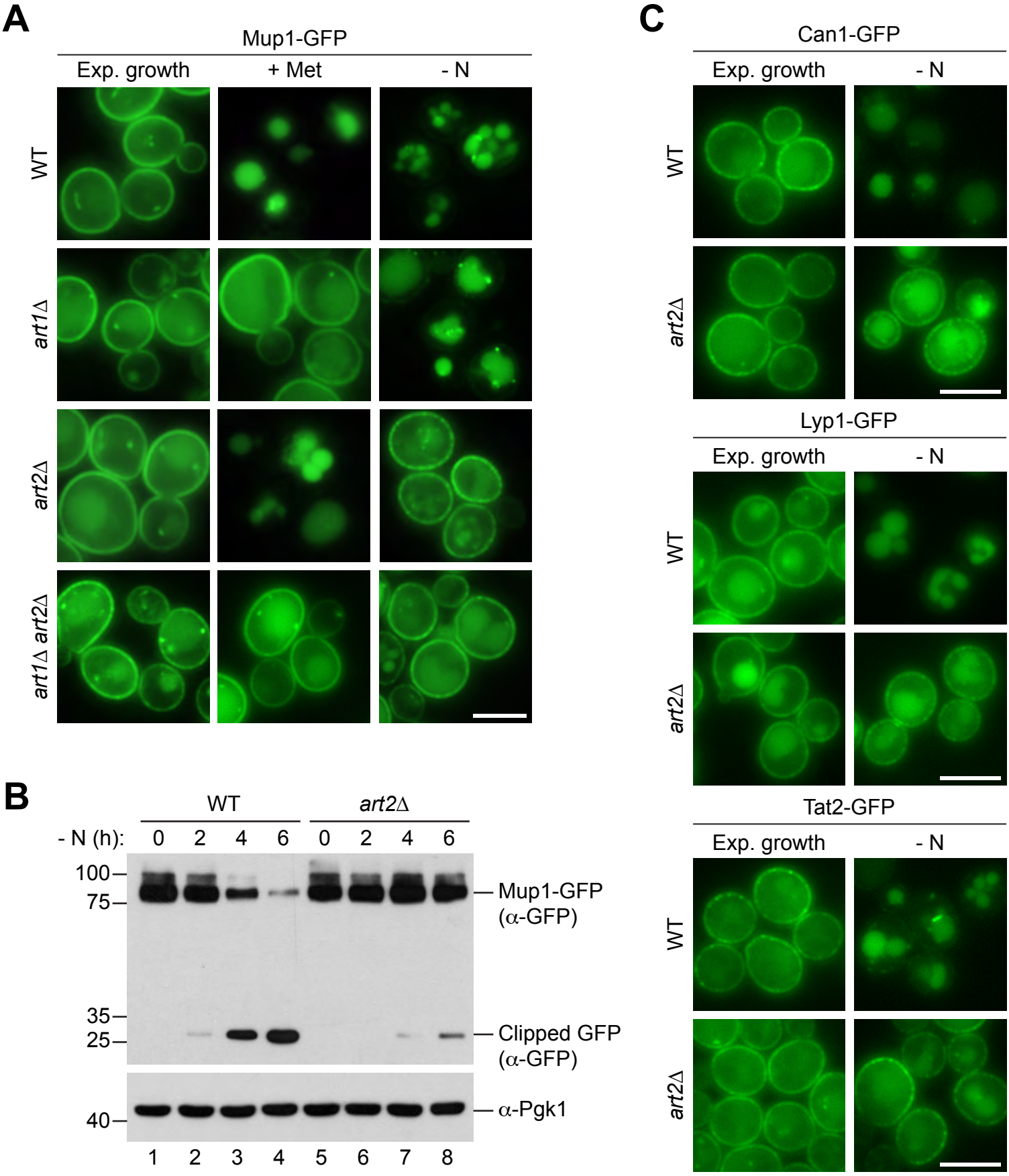
A
Mup1-GFP
Exp. growth
+ Met
- N
WT
art1Δ
art2Δ
art1Δ art2Δ
B
WT
art2Δ
- N (h):
0 2 4 6 0 2 4 6
100
75
35
25
40
Mup1-GFP
(α-GFP)
Clipped GFP
(α-GFP)
α-Pgk1
1 2 3 4 5 6 7 8
C
Can1-GFP
Exp. growth
- N
WT
art2Δ
Lyp1-GFP
Exp. growth
- N
WT
art2Δ
Tat2-GFP
Exp. growth
- N
WT
art2Δ

Figure 3

57 **Figure 3: Art1 and Art2 are non-redundant in promoting substrate- and starvation-induced**
58 **endocytosis of amino acid transporters.**
59 **A)** Live-cell fluorescence microscopy analysis of Mup1-GFP endocytosis in wild type (WT), *art1*Δ,
60 *art2*Δ and *art1*Δ *art2*Δ cells expressing *MUP1-GFP* from plasmid. Cells were treated with 20 µg/ml L-
61 methionine (+ Met) for 1.5h or starved (- N) for 6h after 24h exponential growth. **B)** SDS PAGE and
62 Western blot analysis with the indicated antibodies of whole cell protein extracts from wild type (WT)
63 and *art2*Δ cells expressing *MUP1-GFP* that were starved (- N) for the indicated times after 24h
64 exponential growth. **C)** Live-cell fluorescence microscopy analysis of wild type (WT) and *art2*Δ cells
65 expressing *CAN1-GFP*, *LYP1-GFP* or *TAT2-GFP*. Cells were starved (- N) for 6h after 24h exponential
66 growth. Scale bars = 5 µm. See also Fig. S3.
67
68

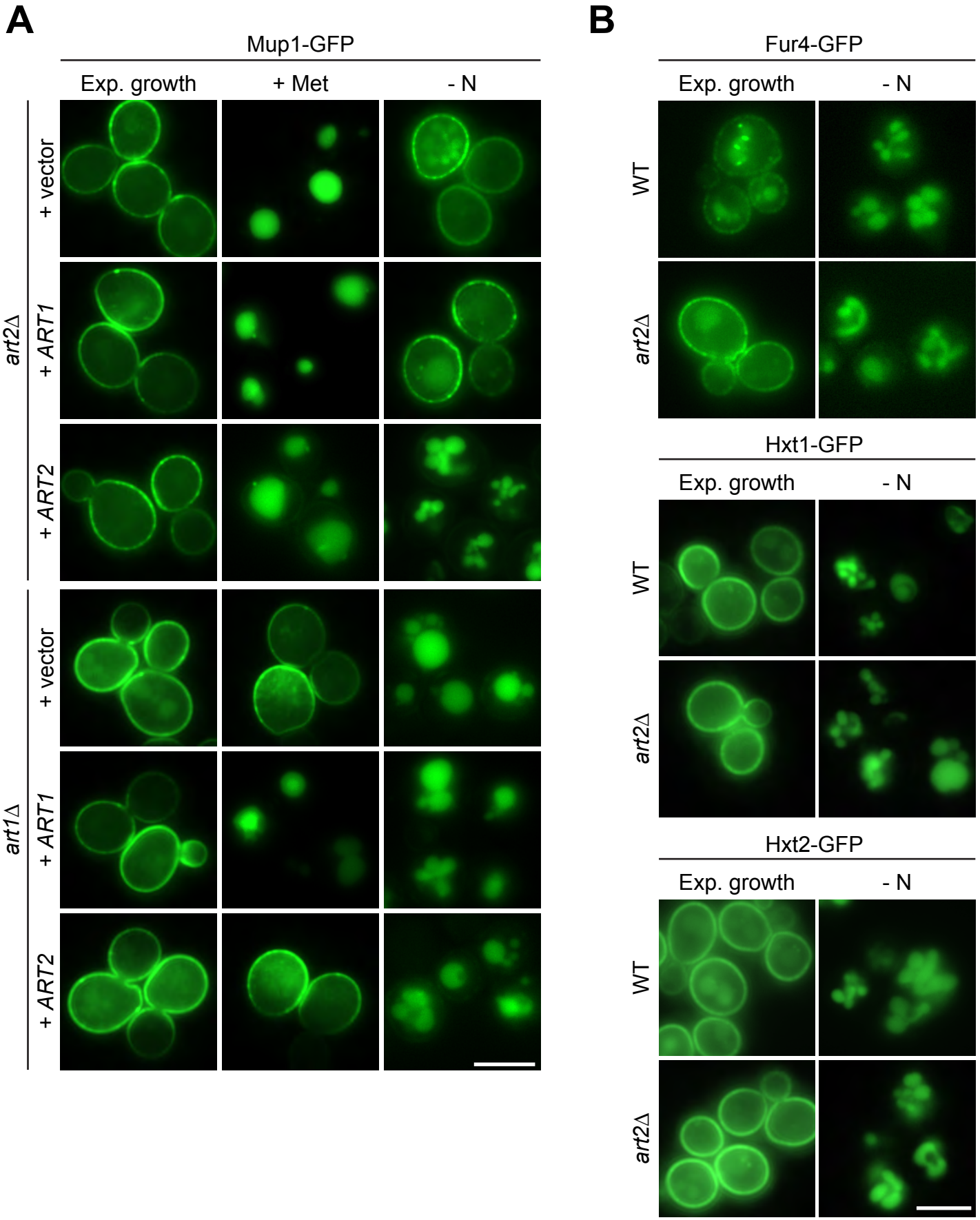

Figure S3 - related to Fig. 3

69 **Figure S3: Related to Fig. 3**

70 **A)** Live-cell fluorescence microscopy analysis of *art2*Δ and *art1Δ* cells expressing *MUP1-GFP* and
71 plasmids encoding *ART1*, *ART2* or empty vectors as indicated. Cells were treated with 20 µg/ml L-
72 methionine (+ Met) for 1.5h or starved (- N) for 6h after 24h exponential growth. **B)** Live-cell
73 fluorescence microscopy analysis of wild type (WT) and *art2*Δ cells expressing pRS416-*FUR4-GFP*,
74 *HXT1-GFP* or *HXT2-GFP*. Cells were starved (- N) for 6h after 24h exponential growth. Scale bars = 5
75 µm.

76

77

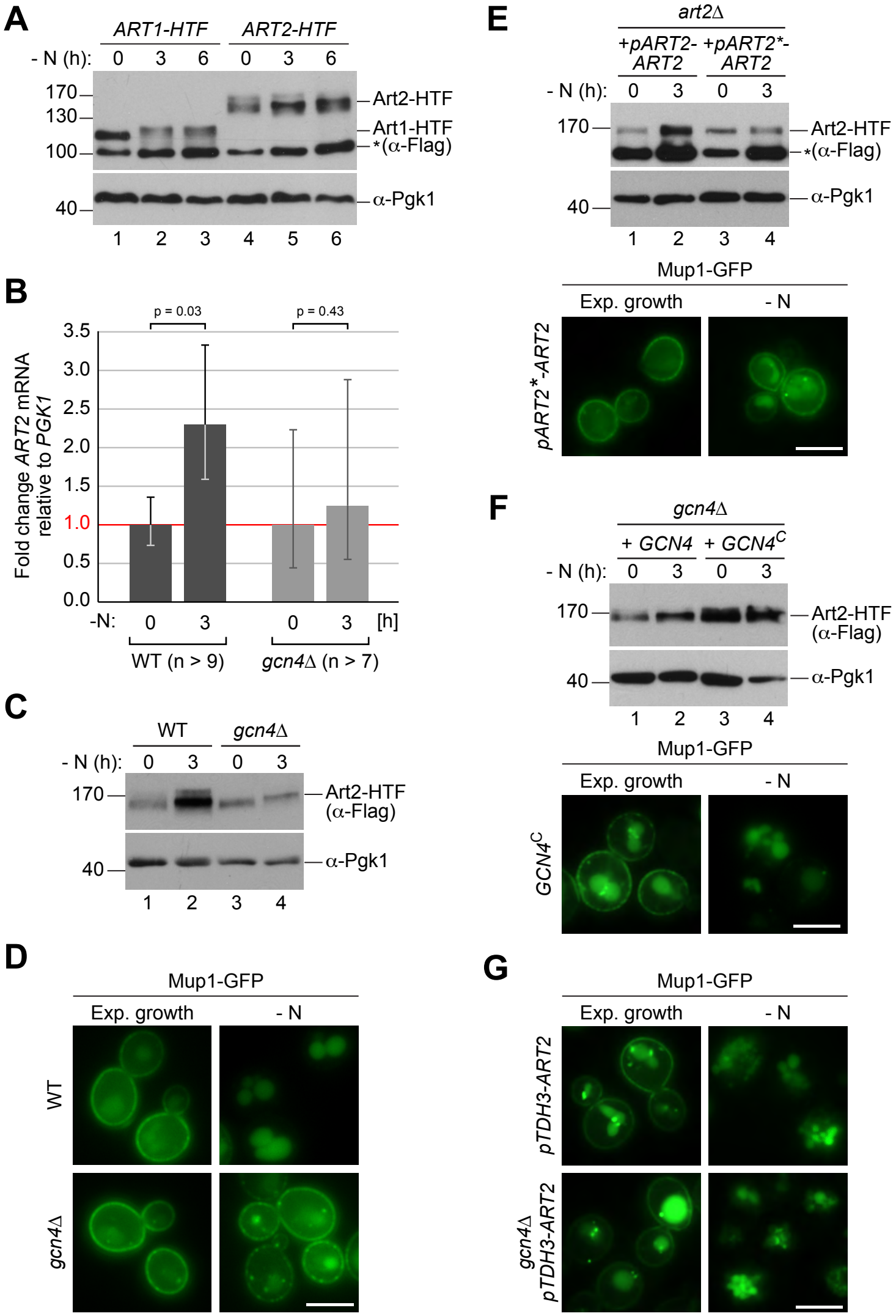
A
ART1-HTF
ART2-HTF
- N (h): 0 3 6 0 3 6
170
130
100
40
Art2-HTF
Art1-HTF
*(α-Flag)
α-Pgk1
1 2 3 4 5 6
B
p = 0.03
p = 0.43
Fold change ART2 mRNA relative to PGK1
3.5
3.0
2.5
2.0
1.5
1.0
0.5
0.0
-N: 0 3 0 3 [h]
WT (n > 9)
gcn4Δ (n > 7)
C
WT
gcn4Δ
- N (h): 0 3 0 3
170
40
Art2-HTF (α-Flag)
α-Pgk1
1 2 3 4
D
Mup1-GFP
Exp. growth
- N
WT
gcn4Δ
E
art2Δ
+pART2-ART2
+pART2*-ART2
- N (h): 0 3 0 3
170
40
Art2-HTF
*(α-Flag)
α-Pgk1
1 2 3 4
Mup1-GFP
Exp. growth
- N
pART2*-ART2
F
gcn4Δ
+ GCN4
+ GCN4C
- N (h): 0 3 0 3
170
40
Art2-HTF (α-Flag)
α-Pgk1
1 2 3 4
Mup1-GFP
Exp. growth
- N
GCN4C
G
Mup1-GFP
Exp. growth
- N
pTDH3-ART2
gcn4Δ pTDH3-ART2

Figure 4

78 **Figure 4: The general amino acid control pathway promotes starvation-induced endocytosis**
79 **Mup1 by up-regulating Art2.**
80 **A)** SDS PAGE and Western blot analysis with the indicated antibodies of whole cell protein extracts
81 from WT cells expressing *ART1-HTF* or *ART2-HTF*. Cells were starved (- N) for the indicated times
82 after 24h exponential growth. The asterisk indicates a non-specific background band of the FLAG
83 antibody. **B)** RT-qPCR analysis of *ART2* transcript levels (normalized to the stable *PGK1* transcript) in
84 wild type (WT) and *gcn4*Δ cells. Cells were starved (- N) for 3h after 24h exponential growth. Values
85 are presented as fold-change of the starting values (t = 0). Error bars represent the standard deviation.
86 Statistical significance was assessed by Student's t-test. **C)** SDS PAGE and Western blot analysis with
87 the indicated antibodies of whole cell protein extracts from the indicated strains expressing *ART2-HTF*.
88 Cells were starved (- N) for 3h after 24h exponential growth. **D)** Live-cell fluorescence microscopy
89 analysis of the indicated strains expressing *MUP1-GFP* from plasmid. Cells were starved (- N) for 6h
90 after 24h exponential growth. **E), F)** The indicated strains were analyzed as in C) (upper panels) and D)
91 (lower panels). **G)** Live-cell fluorescence microscopy analysis of *art2*Δ or *gcn4*Δ cells expressing
92 pRS415-*MUP1-GFP* and pRS416-*pTDH3-ART2* starved (- N) for 6h after 24h exponential growth.
93 Scale bars = 5 µm. See also Fig. S4.
94
95

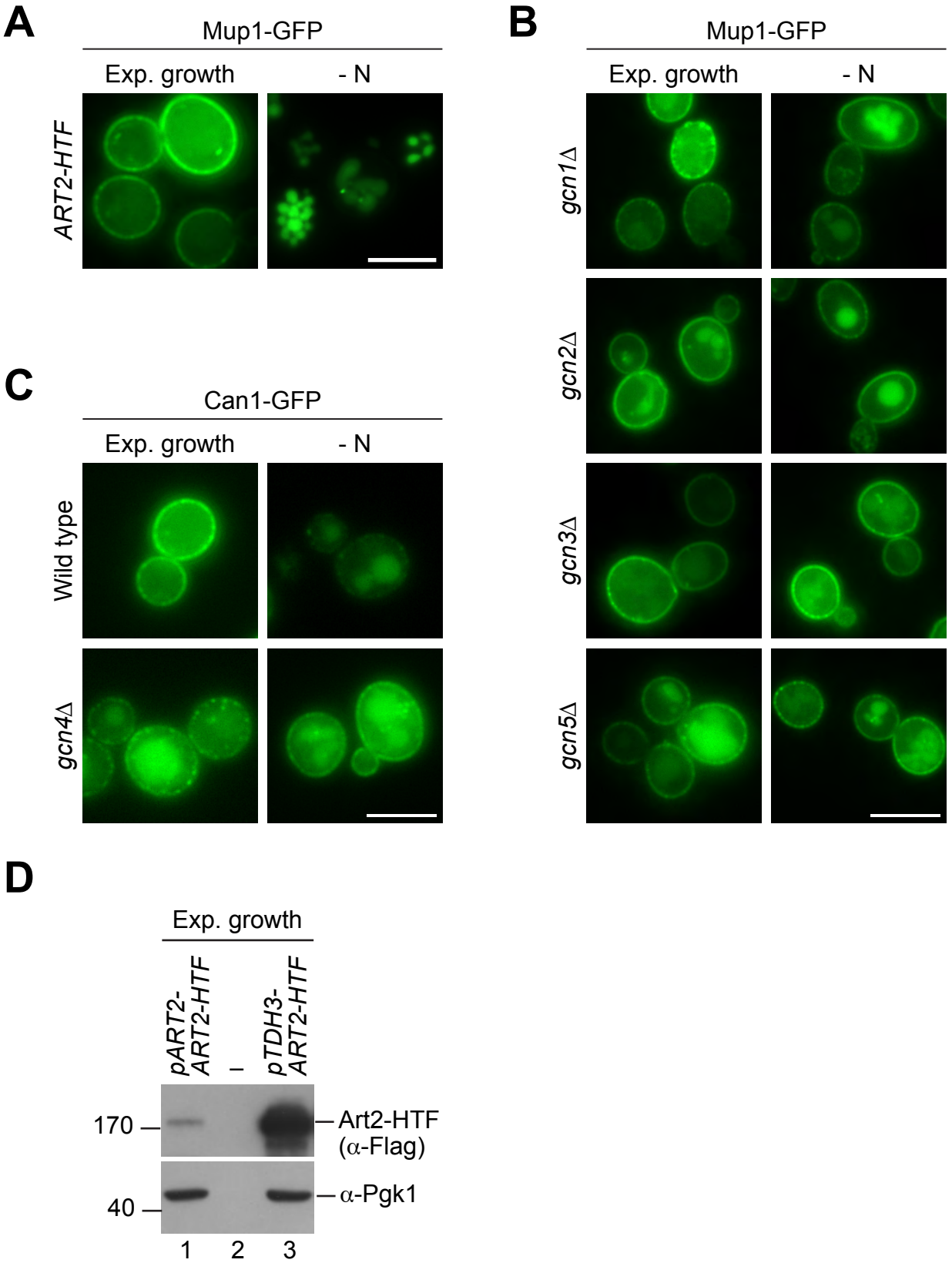

Figure S4 - related to Fig. 4

Figure S4: Related to Fig. 4.

A)-C) Live-cell fluorescence microscopy analysis of the indicated strains starved (- N) for 6h after 24h exponential growth. **D)** SDS PAGE and Western blot analysis with the indicated antibodies of whole cell protein extracts from WT cells expressing *pART2-ART2-HTF* or pRS416-*pTDH3-ART2-HTF* after 24h exponential growth. Scale bars = 5 µm.

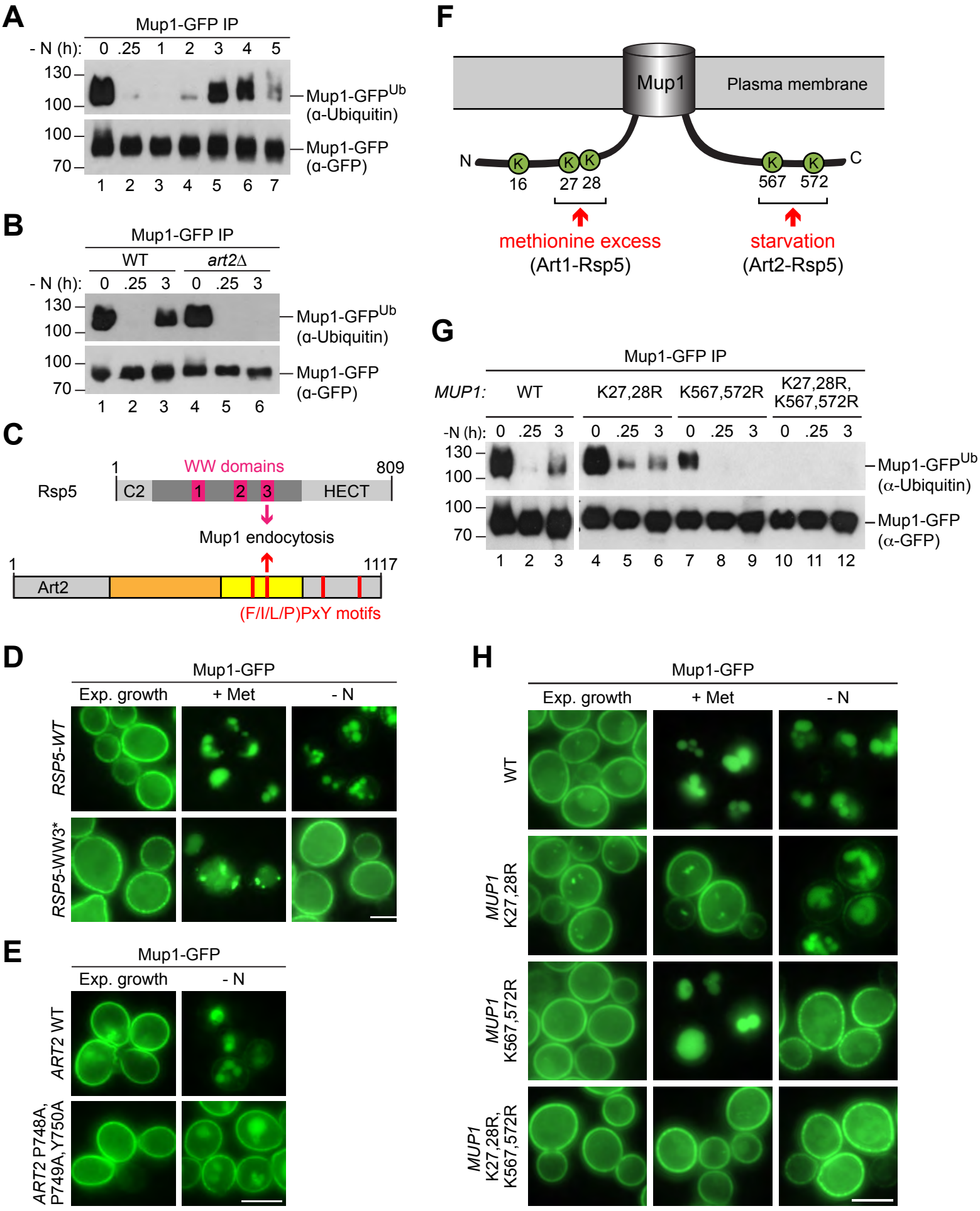
A
Mup1-GFP IP
- N (h): 0 .25 1 2 3 4 5
130
100
100
70
Mup1-GFPUb
(α-Ubiquitin)
Mup1-GFP
(α-GFP)
1 2 3 4 5 6 7
B
Mup1-GFP IP
WT
art2Δ
- N (h): 0 .25 3 0 .25 3
130
100
100
70
Mup1-GFPUb
(α-Ubiquitin)
Mup1-GFP
(α-GFP)
1 2 3 4 5 6
C
Rsp5
1
WW domains
809
C2
1
2
3
HECT
Mup1 endocytosis
1
1117
Art2
(F/I/L/P)PxY motifs
D
Mup1-GFP
Exp. growth
+ Met
- N
RSP5-WT
RSP5-WW3*
E
Mup1-GFP
Exp. growth
- N
ART2 WT
ART2 P748A, P749A, Y750A
F
Mup1
Plasma membrane
N
C
K
16
27 28
567
572
methionine excess
(Art1-Rsp5)
starvation
(Art2-Rsp5)
G
Mup1-GFP IP
MUP1:
WT
K27,28R
K567,572R
K27,28R, K567,572R
-N (h): 0 .25 3 0 .25 3 0 .25 3 0 .25 3
130
100
100
70
Mup1-GFPUb
(α-Ubiquitin)
Mup1-GFP
(α-GFP)
1 2 3 4 5 6 7 8 9 10 11 12
H
Mup1-GFP
Exp. growth
+ Met
- N
WT
MUP1 K27,28R
MUP1 K567,572R
MUP1 K27,28R, K567,572R

Figure 5

Figure 5: Art2-Rsp5 mediates the starvation-induced ubiquitination of Mup1-GFP at two specific C-terminal lysine residues.

A), B) SDS PAGE and Western blot analysis with the indicated antibodies of immunoprecipitated Mup1-GFP from WT cells or *art2*Δ cells starved for the indicated times after 24h of exponential growth. Equal amounts of immunoprecipitated Mup1-GFP were loaded to compare the extent of ubiquitination. **C)** Scheme depicting the domain arrangement of Rsp5 and Art2, indicating the localization of the WW domains and PY motifs required for starvation-induced endocytosis of Mup1. **D)** Live-cell fluorescence microscopy analysis of *rsp5*Δ cells expressing pRS416-*MUP1-GFP* and pRS415- *HTF-RSP5-WT* (wild type) or pRS415- *HTF-RSP5-WW3**. Cells were treated with 20 µg/ml L-methionine (+ Met) for 1.5h or starved (- N) for 6h after 24h exponential growth. **E)** Live-cell fluorescence microscopy analysis of *art2*Δ cells expressing *MUP1-GFP* and pRS416-*ART2* (WT) or pRS416-*ART2 P748A,P749A,Y750A*. Cells were starved (- N) for 6h after 24h exponential growth. **F)** Scheme of Mup1 topology with the N- and C-terminal ubiquitination sites targeted during substrate excess by Art1-Rsp5 and during starvation by Art2-Rsp5. Ubiquitinated lysines (K) shown in green with numbers corresponding to amino acid positions in the Mup1 sequence. **G)** WT cells expressing *MUP1-GFP* WT or the indicated *MUP1-GFP* mutants starved for the indicated times after 24h of exponential growth analyzed as in B). **H)** Live-cell fluorescence microscopy analysis of cells expressing *MUP1-GFP* (wild type (WT)), *MUP1 K27,28R, MUP1 K567,572R-GFP or MUP1 K27,28R,567,572R-GFP* as in D). Scale bars = 5 µm. See also Fig. S5.

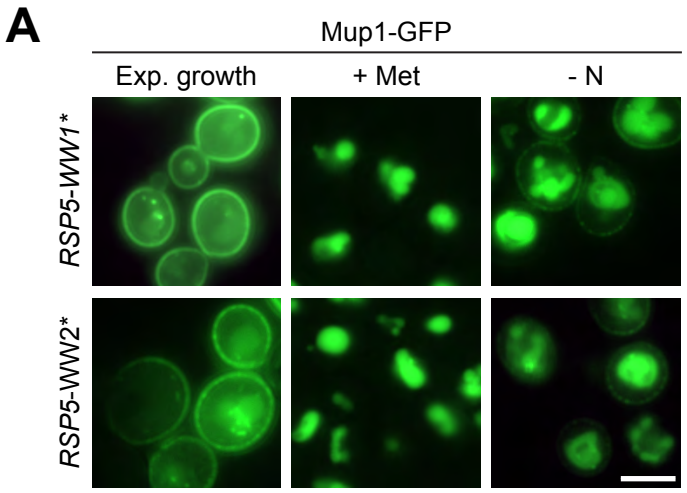

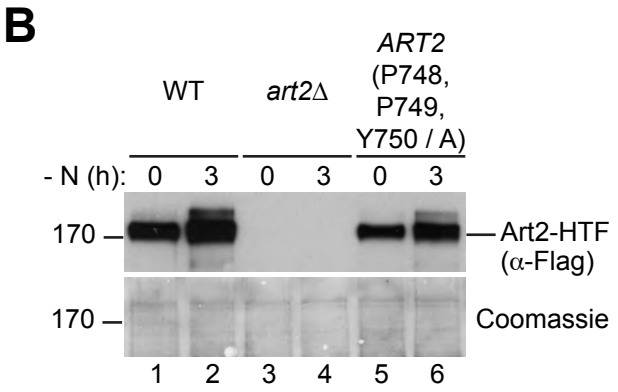

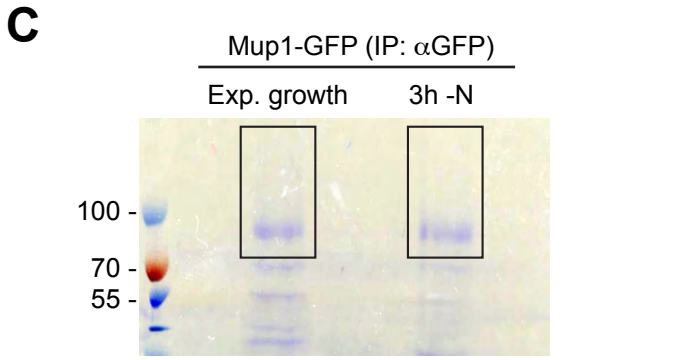

Ub. sites	Exp. / -N	Phospho sites	Exp. / -N
K16	both	S9	both
K27	both	S23	both
K567	both	S31	both
K572	both	T34	-N
		S42	both
		T552	both
		S568	both
		S573	-N

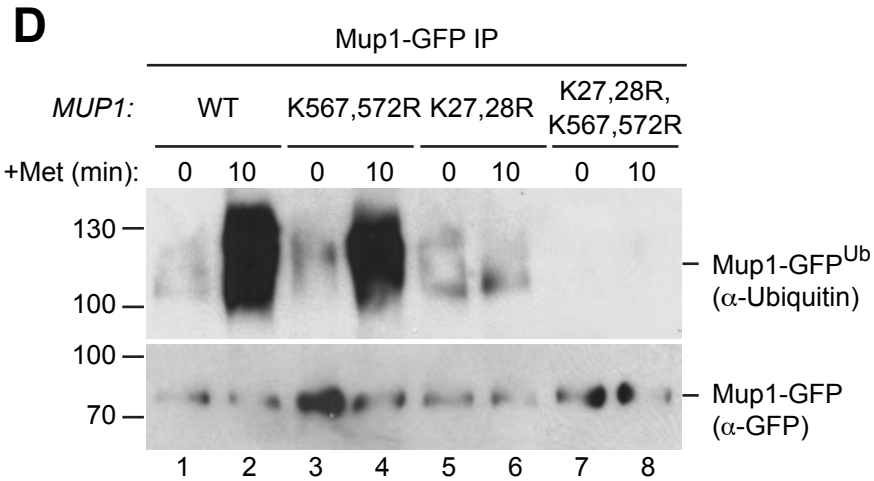

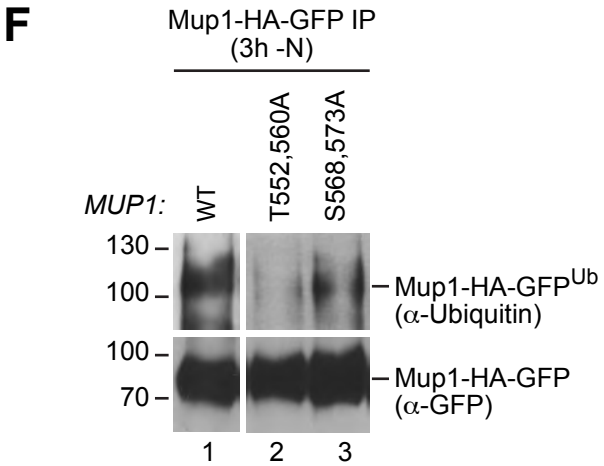

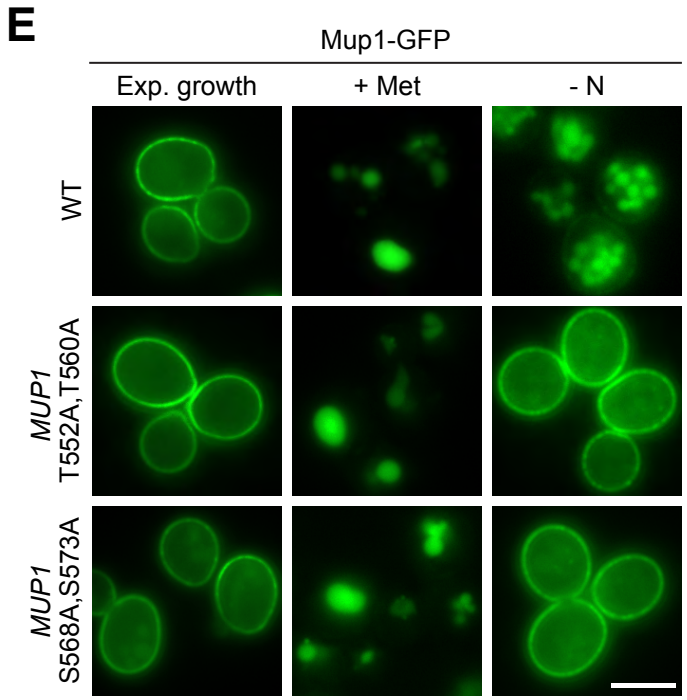

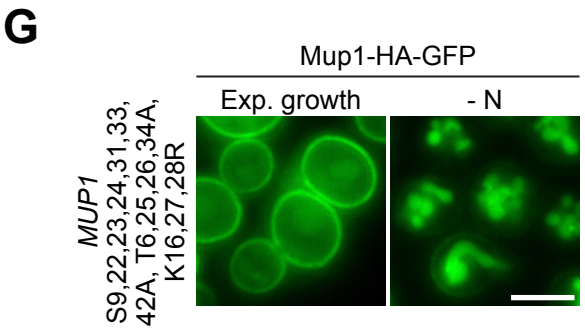

Figure S5 - related to Fig. 5

124 **Figure S5: Related to Fig. 5**

125 **A)** Live-cell fluorescence microscopy analysis of *rsp5*Δ cells expressing pRS416-*MUP1-GFP* and
126 pRS415-*HTF-RSP5-WW1** or pRS415-*HTF-RSP5-WW2**. Cells were treated with 20 µg/ml L-
127 methionine (+ Met) for 1.5h or starved (- N) for 6h after 24h exponential growth. **B)** SDS PAGE and
128 Western blot analysis with the indicated antibodies of whole cell protein extracts from *art2*Δ cells
129 expressing pRS416-*ART2-HTF* (WT), pRS416 or pRS416-*ART2 P748A,P749A,Y750A-HTF*. Cells
130 were starved (- N) for 3h after 24h exponential growth. **C)** Upper panel: Coomassie-stained SDS PAGE
131 of immunoprecipitated Mup1-GFP from WT cells after 24h exponential growth or subsequent 3h
132 starvation (-N). The black rectangles indicate the regions of the gel analyzed by mass spectrometry.
133 Lower panel: Ubiquitinated lysine (K) and phosphorylated serine (S) and threonine (T) residues of Mup1
134 identified by mass spectrometry during exponential growth and/or starvation with numbers
135 corresponding to amino acid positions in the Mup1 sequence. **D)** SDS PAGE and Western blot analysis
136 with the indicated antibodies of immunoprecipitated Mup1-GFP from WT cells or the indicated *MUP1*
137 mutants treated with 20 µg/ml L-methionine for 10 min after 24h of exponential growth. Equal amounts
138 of immunoprecipitated Mup1-GFP were loaded to compare the extent of ubiquitination. **E)** Live-cell
139 fluorescence microscopy analysis of cells expressing *MUP1-GFP* (wild type (WT)), *MUP1 T552,560A-*
140 *GFP* or *MUP1 S568,573A-GFP*. Cells were treated with 20 µg/ml L-methionine (+ Met) for 1.5h or
141 starved (- N) for 6h after 24h exponential growth. **F)** *MUP1-HA-GFP* (wild type (WT)), *MUP1*
142 *T552,560A-HA-GFP* or *MUP1 S568,573A-HA-GFP* cells were starved (- N) for 3h and analyzed as in
143 D). **G)** Live-cell fluorescence microscopy analysis of cells expressing *MUP1*
144 *T6,25,26,34A,S9,22,23,24,31,33,42A,K16,27,28R-HA-GFP*. Cells were starved (- N) for 3h after 24h
145 exponential growth. Scale bars = 5 µm.

146

147

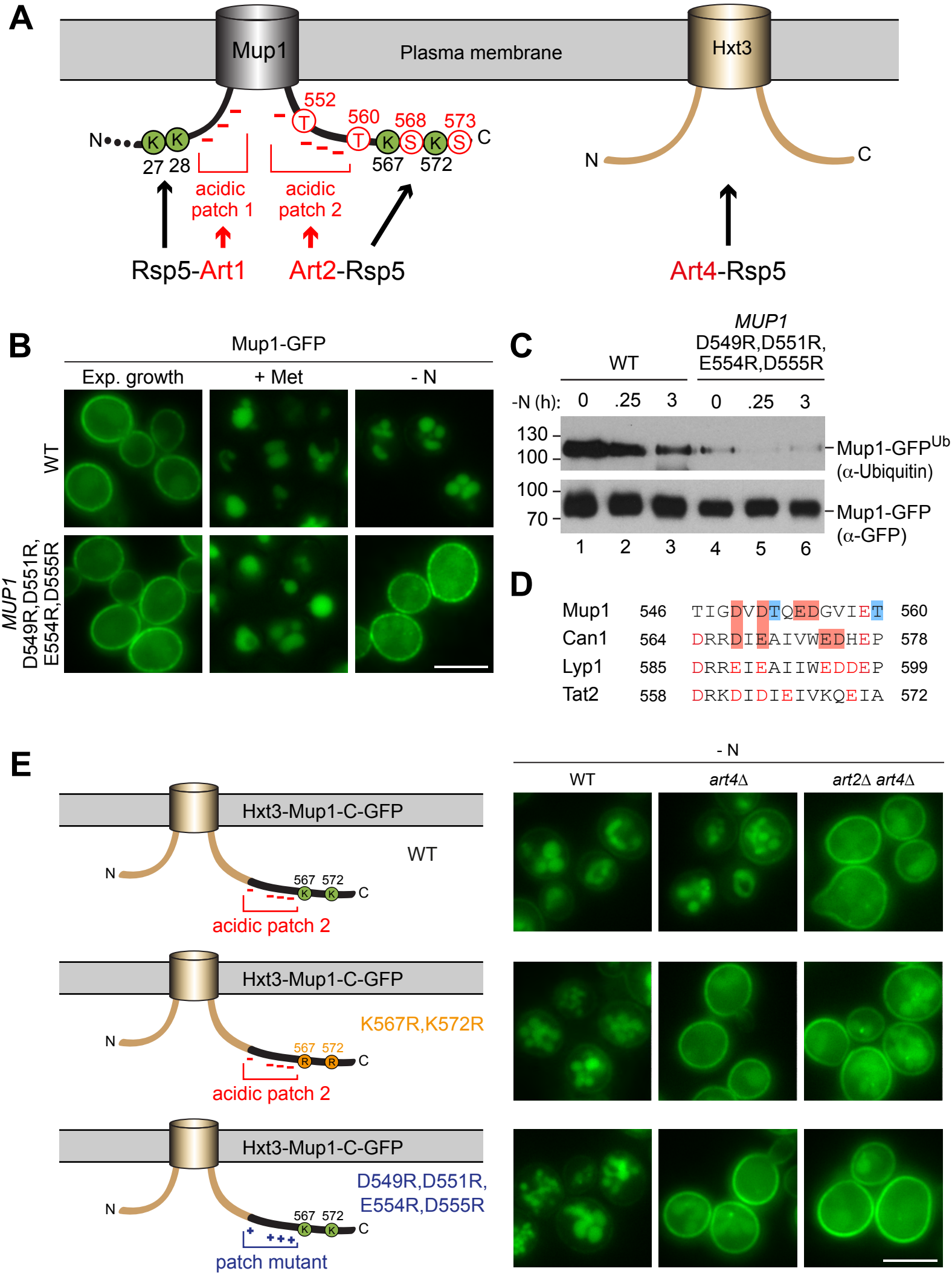
A
Mup1
Plasma membrane
Hxt3
552
560
568
573
N
C
27 28
567 572
acidic patch 1
acidic patch 2
Rsp5-Art1
Art2-Rsp5
Art4-Rsp5
B
Mup1-GFP
Exp. growth
+ Met
- N
WT
MUP1 D549R,D551R, E554R,D555R
C
WT
MUP1 D549R,D551R, E554R,D555R
-N (h): 0 .25 3 0 .25 3
130
100
100
70
Mup1-GFP^Ub (α-Ubiquitin)
Mup1-GFP (α-GFP)
1 2 3 4 5 6
D
Mup1 546 TIGDVDTQEDGVIET 560
Can1 564 DRRDIEAIVWEDHEP 578
Lyp1 585 DRREIEAIIWEDDEP 599
Tat2 558 DRKDIDIEIVKQEIA 572
E
Hxt3-Mup1-C-GFP
WT
567 572
acidic patch 2
K567R,K572R
D549R,D551R, E554R,D555R
patch mutant
- N
WT
art4Δ
art2Δ art4Δ

Figure 6

148 **Figure 6: The C-terminus of Mup1 harbors a transplantable, starvation-responsive acidic degron.**
149 **A)** Left: scheme of Mup1 topology with N- and C-terminal ubiquitination sites and acidic patches
150 targeted by Art1-Rsp5 and Art2-Rsp5, respectively, and the C-terminal phosphorylation sites of Mup1
151 that promote its starvation-induced endocytosis. Ubiquitinated lysines (K) shown in green and
152 phosphorylated serines (S) and threonines (T) in red with numbers corresponding to amino acid
153 positions in the Mup1 sequence. Right: Hxt3 as an Art4-Rsp5 dependent cargo during nitrogen
154 starvation. **B)** Live-cell fluorescence microscopy analysis of Mup1-GFP endocytosis in cells expressing
155 *MUP1-GFP* (wild type (WT)) or *MUP1 D549R,D551R,E554R,D555R-GFP*. Cells were treated with 20
156 µg/ml L-methionine (+ Met) for 1.5h or starved (- N) for 6h after 24h exponential growth. **C)** SDS
157 PAGE and Western blot analysis with the indicated antibodies of immunoprecipitated Mup1-GFP from
158 cells expressing *MUP1-GFP* (WT) or *MUP1 D549R,D551R,E554R,D555R -GFP* starved for the
159 indicated times after 24h of exponential growth. Equal amounts of immunoprecipitated Mup1-GFP were
160 loaded to compare the extent of ubiquitination. **D)** Amino acid sequence alignment of the C-terminal
161 acidic patches of Mup1, Can1, Lyp1 and Tat2. The boxes indicate acidic residues (red) and
162 phosphorylation sites (blue), which are required for Art2-dependent starvation-induced endocytosis.
163 Red letters illustrate further acidic residues. **E)** Live-cell fluorescence microscopy analysis of wild type
164 (WT), *art4*Δ and *art2*Δ *art4*Δ cells expressing *HXT3-MUP1-C-GFP* (top panels), *HXT3-MUP1-C*
165 *K567,572R-GFP* (middle panels) or *HXT3-MUP1-C D549R,D551R,E554R,D555R -GFP* (bottom
166 panels). Cells were starved (- N) for 6h after 24h exponential growth. Scale bars = 5 µm. See also Fig.
167 S6.
168
169

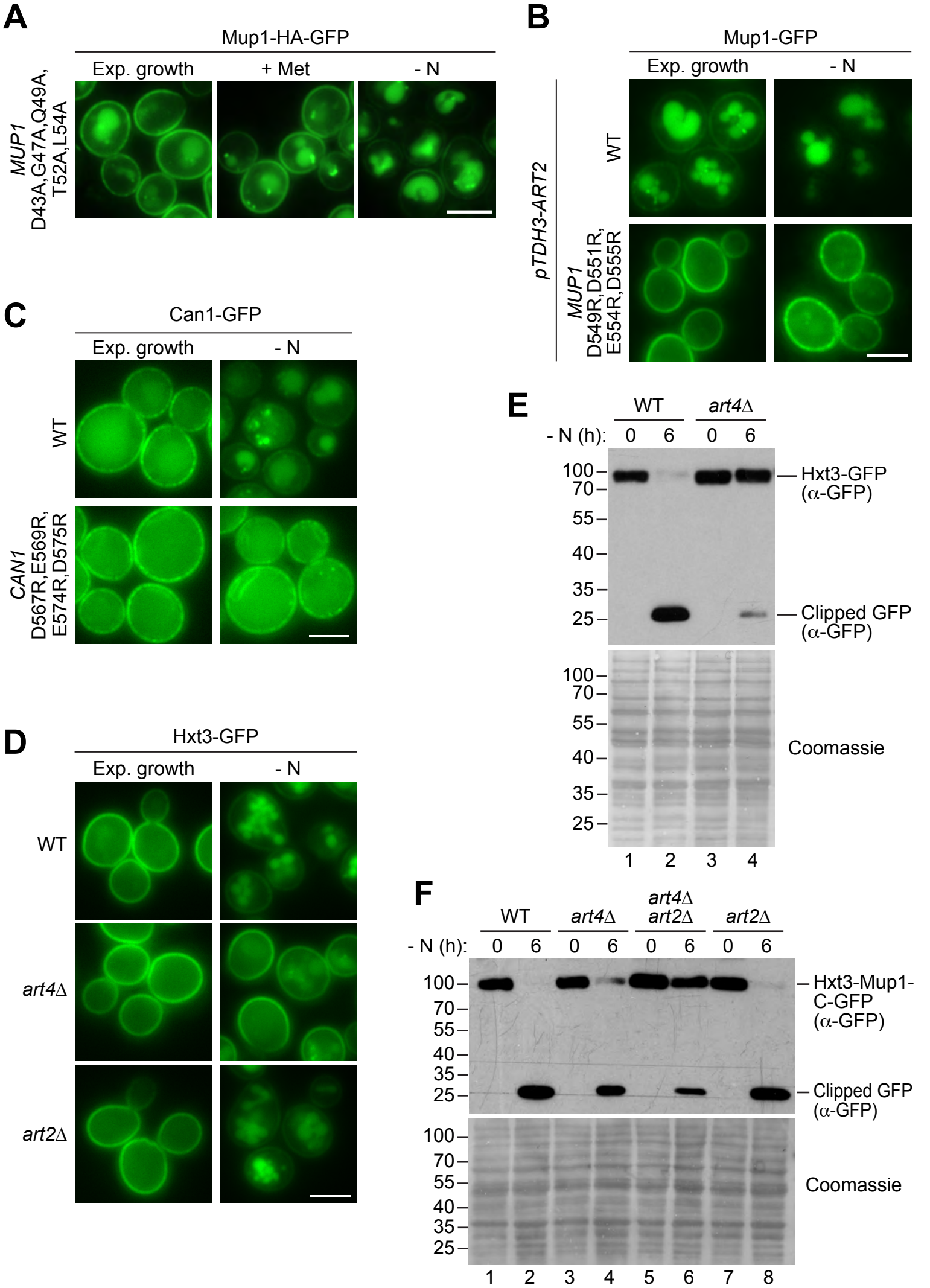

Figure S6 - related to Fig. 6

170 **Figure S6: Related to Fig. 6**

171 **A)-D)** Live-cell fluorescence microscopy analysis of the indicated strains treated with 20 µg/ml L-
172 methionine (+ Met) for 1.5h or starved (- N) for 6h after 24h exponential growth. **E)** SDS PAGE and
173 Western blot analysis with the indicated antibodies of whole cell protein extracts from wild type (WT)
174 and *art4*Δ cells expressing *HXT3-GFP*. Cells were starved (- N) for 6h after 24h exponential growth.
175 Coomassie staining of the membrane serves as loading control. **F)** Wild type (WT), *art4*Δ, *art2*Δ *art4*Δ
176 and *art2*Δ cells expressing *HXT3-MUP1-C-GFP* were treated as in E). Scale bars = 5 µm.

177

178

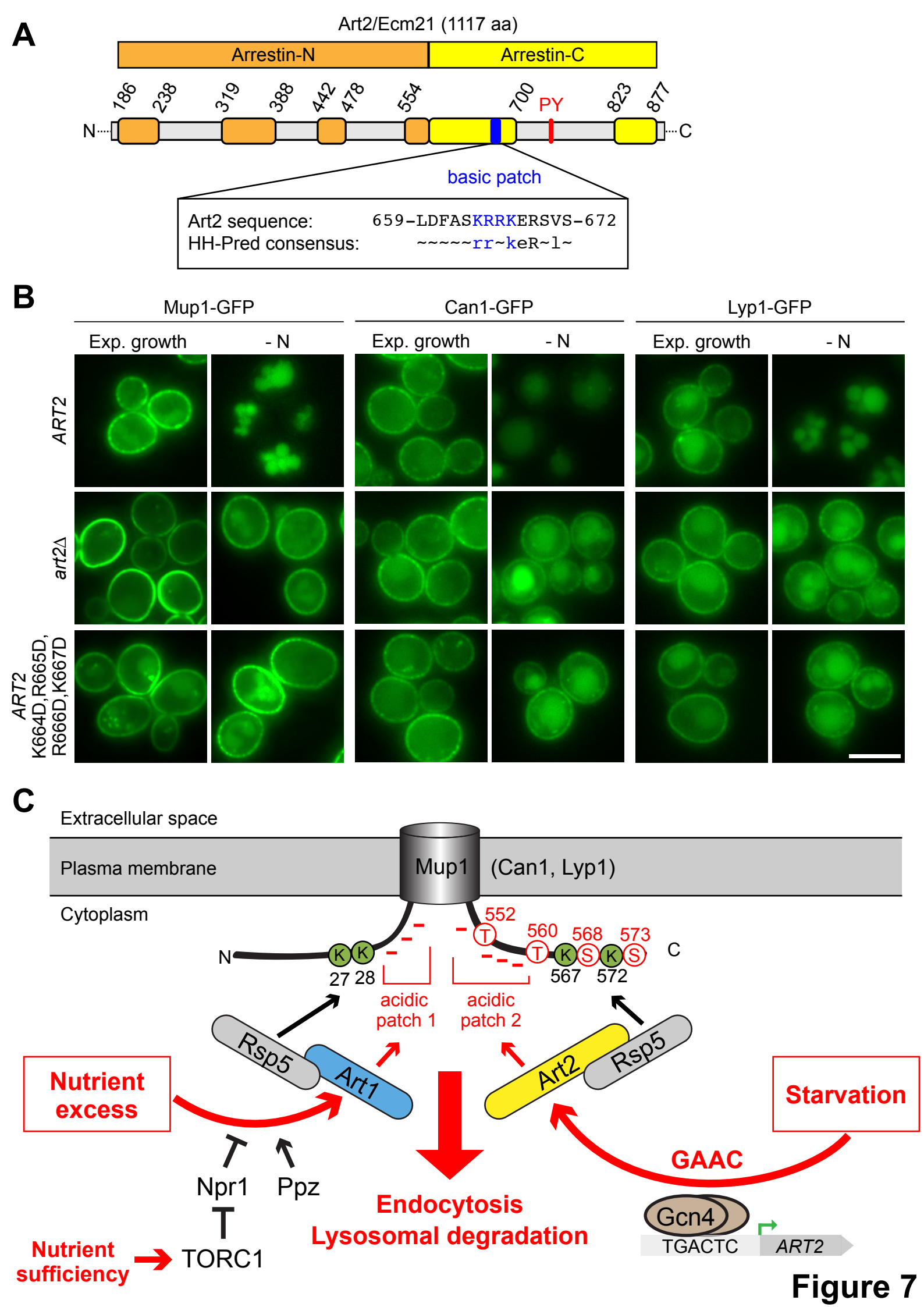
A
Art2/Ecm21 (1117 aa)
Arrestin-N
Arrestin-C
186
238
319
388
442
478
554
700
PY
823
877
N
C
basic patch
Art2 sequence: 659-LDFASKRRKERSVS-672
HH-Pred consensus: ~~~~~rr~keR~l~
B
Mup1-GFP
Can1-GFP
Lyp1-GFP
Exp. growth
- N
ART2
art2Δ
ART2 K664D,R665D, R666D,K667D
C
Extracellular space
Plasma membrane
Mup1
(Can1, Lyp1)
Cytoplasm
552
560
568
573
N
C
27 28
567
572
acidic patch 1
acidic patch 2
Rsp5
Art1
Art2
Rsp5
Nutrient excess
Starvation
GAAC
Npr1
Ppz
Endocytosis
Lysosomal degradation
Gcn4
TGACTC
ART2
Nutrient sufficiency
TORC1

Figure 7

179 **Figure 7: A basic patch of Art2 promotes the starvation-induced endocytosis of Mup1, Can1 and**
180 **Lyp1.**
181 **A)** Scheme of Art2 topology with arrestin-N domain in orange, arrestin-C domain in yellow and tails
182 and interspersed extended loops (Baile et al., 2019) in light grey. The basic amino acid residues shown
183 in blue mediate the starvation-induced endocytosis of Mup1, Can1 and Lyp1 (numbers correspond to
184 amino acid positions in the Art2 sequence). Below is aligned the HHpred consensus sequence for
185 Art2/Ecm21 derived from three HHblits iterations (Zimmermann et al., 2018), suggesting conservation
186 of the basic patch in the Art2 protein family. **B)** Live-cell fluorescence microscopy analysis of *art2*Δ
187 cells expressing *MUP1-GFP*, *CAN1-GFP* or *LYP1-GFP* and pRS416-*ART2-WT*, empty vector or
188 *pRS416-ART2 K664D,R665D,R666D,K667D.* Cells were starved (- N) for 6h after 24h exponential
189 growth. **C)** Scheme for the regulation of the substrate- and starvation-induced endocytosis of Mup1.
190 During substrate excess TORC1 inhibits the Npr1 kinase which otherwise would phosphorylate and
191 inhibit Art1. Art1-Rsp5 becomes dephosphorylated and subsequently binds the acidic patch 1 at the N-
192 terminal tail of Mup1, leading to the ubiquitination of K27 and K28 and degradation of Mup1 (left).
193 During amino acid and nitrogen starvation the general amino acid control (GAAC) pathway upregulates
194 the ubiquitin ligase adaptor Art2 via the transcriptional regulator Gcn4. The ensuing Art2-Rsp5 complex
195 binds with its basic patch to the acidic patch 2 of Mup1 leading to the ubiquitination of K567 and K572
196 and degradation of Mup1 (right). At the same time, starvation causes TORC1 inhibition and activation
197 of Npr1 and inhibits Art1-dependent ubiquitination. Ubiquitinated lysines (K) shown in green and
198 phosphorylated serines (S) and threonines (T) in red with numbers corresponding to amino acid
199 positions in the Mup1 sequence. Scale bars = 5 µm. See also Fig. S7.
200
201

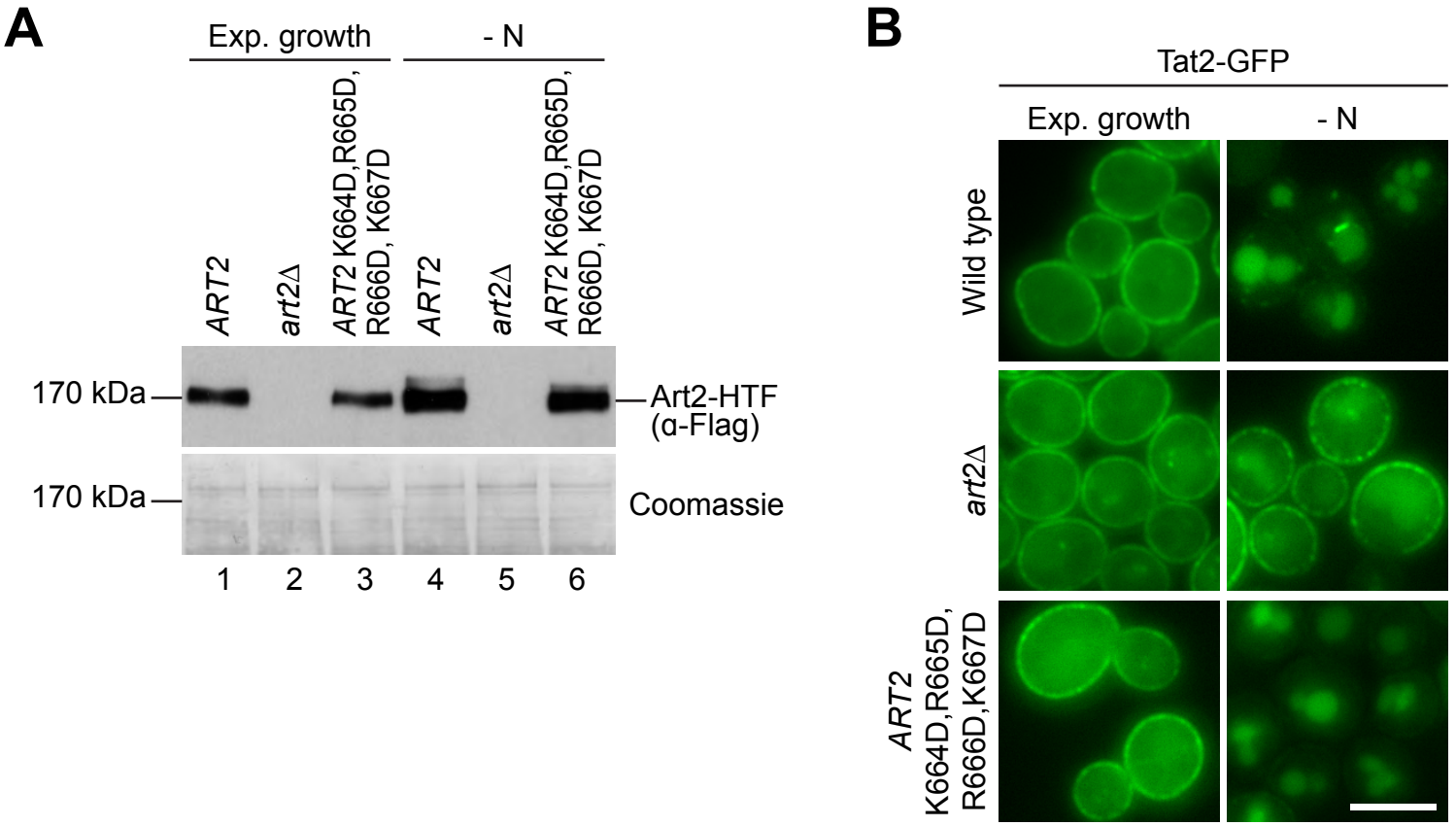

Figure S7 - related to Fig. 7

202 **Figure S7: Related to Fig. 7**

203 **A)** SDS PAGE and Western blot analysis with the indicated antibodies of whole cell protein extracts
204 from *art2*Δ cells expressing pRS416-*ART2-HTF*, empty vector or pRS416-*ART2*
205 *K664D,R665D,R666D,K667D-HTF*. Cells were starved (- N) for 3h after 24h exponential growth. **B)**
206 Live-cell fluorescence microscopy analysis of *art2*Δ cells expressing *TAT2-GFP* and *pRS416-ART2*,
207 empty vector or *pRS416-ART2 K664D,R665D,R666D,K667D*. Cells were starved (- N) for 6h after 24h
208 exponential growth. Scale bars = 5 µm.

209

Table S1: **Fluorescence microscopy-based screen for substrates of starvation-induced endocytosis**

Color code:
Signal at PM decreased during starvation
Signal at PM increased during starvation
Signal at PM unchanged during starvation

Standard name	Systematic name	Fluorescence at PM during exp. growth	- N (fluorescence at PM compared to exp. growth)	+ Met (fluorescenceat PM compared to - Met)	SGD annotated Function
MUP1	YGR055W	**Yes**	**Decreased**	**Decreased**	High affinity methionine permease
CAN1	YEL063C	**Yes**	**Decreased**	**Unchanged**	Arginine permease
TAT2	YOL020W	**Yes**	**Decreased**	**Unchanged**	Broad-specificity amino-acid permease - inductible by most neutral amino acids
LYP1	YNL268W	**Yes**	**Decreased**	**Unchanged**	Lysine permease
HXT1	YHR094C	**Yes**	**Decreased**	**Unchanged**	Low-affinity hexose facilitator
HXT2	YMR011W	**Yes**	**Decreased**	**Unchanged**	Hexose facilitator of moderately low affinity for glucose
HXT3	YDR345C	**Yes**	**Decreased**	**Unchanged**	Low-affinity hexose facilitator
ITR1	YDR497C	**Yes**	**Decreased**	**Unchanged**	Inositol permease
FUR4	YBR021W	**Yes**	**Decreased**	**Unchanged**	Uracil permease
HNM1	YGL077C	**Yes**	**Decreased**	**Unchanged**	Choline permease
PMP1	YCR024C-A	**Yes**	**Decreased**	**Unchanged**	Regulatory subunit for the plasma membrane H(+)-ATPase Pma1p
PDR5	YOR153W	**Yes**	**Decreased**	**Unchanged**	`Full-size` ABC transporter involved in multidrug resistance
ENB1	YOL158C	**Yes**	**Decreased**	**Unchanged**	Transporter of the siderophore enterobactin
CTR1	YPR124W	**Yes**	**Decreased**	**Unchanged**	Plasma membrane copper transport protein
GAP1	YKR039W	**Not detected**	**Increased**	**Not detected**	General amino acid permease
MEP2	YNL142W	**Not detected**	**Increased**	**Not detected**	High affinity ammonium permease - proposed role also as ammonium sensor involved in pseudohyphal growth
DIP5	YPL265W	**Yes**	**Unchanged, but vacuolar signal increased**	**Unchanged**	Glutamate and aspartate permease
ATO3	YDR384C	**Yes**	**Unchanged, but vacuolar signal increased**	**Unchanged**	Putative ammonium transporter
FTR1	YER145C	**Yes**	**Unchanged, but vacuolar signal increased**	**Unchanged**	High affinity iron transporter
RSN1	YMR266W	**Yes**	**Unchanged, but vacuolar signal increased**	**Unchanged**	Membrane protein of unknown function, by similarity : Acts as an osmosensitive calcium-permeable cation cha
PUN1	YLR414C	**Yes**	**Unchanged, but vacuolar signal increased**	**Unchanged**	Plasma membrane protein with a role in cell wall integrity
GNP1	YDR508C	**Yes**	**Unchanged, but vacuolar signal increased**	Not analyzed	High-affinity glutamine permease
YOR1	YGR281W	**Yes**	**Unchanged, but vacuolar signal increased**	Not analyzed	`Full-size` ABC transporter involved in tolerance to toxic organic anions
SNQ2	YDR011W	**Yes**	**Unchanged**	**Unchanged**	`Full-size` ABC transporter involved in multidrug resistance
VHT1	YGR065C	**Yes**	**Unchanged**	**Unchanged**	Biotin (vitamin H) permease
BAP2	YBR068C	**Yes**	**Unchanged**	Not analyzed	High-affinity leucine permease
TAT1	YBR069C	**Yes**	**Unchanged**	Not analyzed	Amino acid transporter for valine, leucine, isoleucine, and tyrosine
HXT5	YHR096C	**Yes**	**Unchanged**	Not analyzed	Hxt family protein with intrinsic hexose transport activity
HXT7	YDR342C	**Yes**	**Unchanged**	Not analyzed	High-affinity hexose facilitator
FET3	YMR058W	**Yes**	**Unchanged**	Not analyzed	Ferro-O2-oxidoreductase
ATR1	YML116W	**Yes**	**Unchanged**	Not analyzed	Putative substrate-H+ antiporter conferring resistance to aminotriazole, and acting as a boron export protein.
AQR1	YNL065W	**Yes**	**Unchanged**	Not analyzed	Plasma membrane transporter of the major facilitator superfamily
YDR090C	YDR090C	**Yes**	**Unchanged**	Not analyzed	Protein similar to the human lysosomal CTNS cystine transporter mediating H+-driven cystine export from lyso
QDR2	YIL121W	**Yes**	**Unchanged**	Not analyzed	Putative substrate-H+ antiporter - confers resistance to quinidine
HOL1	YNR055C	**Yes**	**Unchanged**	Not analyzed	Putative substrate-H+ antiporter - unknown biological function
PDR12	YPL058C	**Yes**	**Unchanged**	Not analyzed	`Full-size` ABC transporter of the plasma membrane acting as a weak organic acids extrusion pump
PMA1	YGL008C	**Yes**	**Unchanged**	Not analyzed	Plasma membrane H+ pump
YRO2	YBR054W	**Yes**	**Unchanged**	Not analyzed	7TMD-Protein of unknown function with similarity to archaeal rhodopsins
MID2	YLR332W	**Yes**	**Unchanged**	Not analyzed	O-glycosylated plasma membrane protein
PSR1	YLL010C	**Yes**	**Unchanged**	Not analyzed	Plasma membrane associated protein phosphatase
SFK1	YKL051W	**Yes**	**Unchanged**	Not analyzed	Plasma membrane protein that may act to generate normal levels of PI4P
SLG1	YOR008C	**Yes**	**Unchanged**	Not analyzed	Sensor-transducer of the stress-activated PKC1-MPK1 kinase pathway
YDR034W-B	YDR034W-B	**Yes**	**Unchanged**	Not analyzed	Predicted tail-anchored plasma membrane protein
YDR210W	YDR210W	**Yes**	**Unchanged**	Not analyzed	Predicted tail-anchored plasma membrane protein with a CYSTM module
YBR016W	YBR016W	**Yes**	**Unchanged**	Not analyzed	Tail-anchored plasma membrane protein with a conserved CYSTM module
AXL2	YIL140W	**Yes**	**Unchanged**	Not analyzed	Integral plasma membrane protein required for axial budding
SKG1	YKR100C	**Yes**	**Unchanged**	Not analyzed	Transmembrane protein with a role in cell wall polymer composition
NCE102	YPR149W	**Yes**	**Unchanged**	Not analyzed	Protein of unknown function
PMP2	YEL017C-A	**Yes**	**Unchanged**	Not analyzed	Proteolipid associated with plasma membrane H(+)-ATPase (Pma1p)
YOL019W	YOL019W	**Yes**	**Unchanged**	Not analyzed	Protein of unknown function,
TPO4	YOR273C	**Yes**	**Unchanged**	Not analyzed	Proposed vacuolar polyamine transporter

Table S2: **Flow cytometry and fluorescence microscopy-based screen for genes specifically involved in starvation-induced endocytosis**

Color code:	- N phenotype	Description
Starvation-induced endocytosis and vacuolar sorting of Mup1-pHluorin	1	fluorescence at the plasma membrane
Methionine- and starvation-induced endocytosis and vacuolar sorting of Mup1-pHluorin	2	fluorescence in small cytoplasmic objects
Methionin-induced endocytosis not tested	3	fluorescence in class E like objects
	4	fluorescence inside vacuoles

Systematic name	Standard name	- N (% cells with Mup1-pH signal)	- N phenotype	+ Met (% cells with Mup1-pH signal)
YIL087C	AIM19	79	1	12
YIL158W	AIM20	77	1	18
YHR126C	ANS1	100	1	1
YHL019C	APM2	100	1	2
YHR018C	ARG4	100	1	55
YHL047C	ARN2	100	1	10
YBL101C	ART2	88	1	1
YIL146C	ATG32	98	1	25
YML081C-A	ATP18	84	1	7
YIL015W	BAR1	77	1	6
YER155C	BEM2	61	1	2
YML042W	CAT2	58	1	10
YMR038C	CCS1	55	1	23
YIL035C	CKA1	66	1	5
YFR046C	CNN1	100	1	3
YHR191C	CTF8	46	1	20
YLR422W	DCK1	66	1	3
YOR030W	DFG16	100	1	3
YOR005C	DNL4	100	1	2
YKL213C	DOA1	100	1	20
YHL043W	ECM34	100	1	14
YHR110W	ERP5	100	1	2
YPR062W	FCY1	100	1	4
YIL065C	FIS1	87	1	19
YIL098C	FMC1	72	1	8
YJL161W	FMP33	61	1	9
YKL220C	FRE2	75	1	15
YCL058C	FYV5	74	1	25
YBR020W	GAL1	80	1	5
YER027C	GAL83	51	1	2
YDR283C	GCN2	46	1	27
YFR009W	GCN20	53	1	10
YKR026C	GCN3	100	1	10
YGR252W	GCN5	61	1	27
YAL031C	GIP4	48	1	n.a.
YIL053W	GPP1	74	1	13
YDL035C	GPR1	65	1	10
YIL041W	GVP36	100	1	9
YJL165C	HAL5	71	1	1
YNL281W	HCH1	100	1	3
YIL020C	HIS6	49	1	21
YIL170W	HXT12	58	1	7
YNL215W	IES2	60	1	14
YKR019C	IRS4	73	1	20
YNL265C	IST1	54	1	30
YJL162C	JJJ2	100	1	1
YCL005W	LDB16	45	1	0
YLL007C	LMO1	82	1	1
YNL100W	MIC27	71	1	5
YJL186W	MNN5	100	1	1
YHL036W	MUP3	100	1	16
YLR194C	NCW2	100	1	0
YDR176W	NGG1	59	1	0
YNL183C	NPR1	46	1	0
YBR129C	OPY1	48	1	0
YHL013C	OTU2	47	1	0
YOL115W	PAP2	83	1	8
YDR466W	PKH3	66	1	0
YIL122W	POG1	71	1	0
YKR013W	PRY2	100	1	4
YNL180C	RHO5	100	1	11
YHL027W	RIM101	100	1	1
YFL033C	RIM15	74	1	10
YNL294C	RIM21	100	1	2
YMR063W	RIM9	68	1	1
YKL006W	RPL14A	100	1	2
YHR200W	RPN10	100	1	10
YDL081C	RPP1A	76	1	16
YHR031C	RRM3	100	1	1
YHL034C	SBP1	58	1	9
YJL145W	SFH5	47	1	0
YBR130C	SHE3	78	1	0
YDL047W	SIT4	73	1	20
YMR216C	SKY1	51	1	4
YNR023W	SNF12	87	1	13
YIL016W	SNL1	91	1	2
YGL127C	SOH1	62	1	19

YOL148C	**SPT20**	52	**1**	n.a.
YHR041C	**SRB2**	78	**1**	11
YLR389C	**STE23**	70	**1**	5
YIL039W	**TED1**	100	**1**	100
YGR033C	**TIM21**	100	**1**	3
YNL299W	**TRF5**	100	**1**	1
YKL211C	**TRP3**	57	**1**	10
YBR166C	**TYR1**	69	**1**	1
YFR010W	**UBP6**	59	**1**	31
YIL017C	**VID28**	82	**1**	5
YHL035C	**VMR1**	100	**1**	22
YOR043W	**WHI2**	100	**1**	3
YBR063C	**YBR063C**	56	**1**	14
YDL034W	**YDL034W**	69	**1**	27
YER137C	**YER137C**	94	**1**	20
YGR117C	**YGR117C**	58	**1**	9
YHL041W	**YHL041W**	73	**1**	20
YHR182W	**YHR182W**	100	**1**	1
YIL029C	**YIL029C**	89	**1**	13
YIL077C	**YIL077C**	75	**1**	25
YJL144W	**YJL144W**	73	**1**	14
YKR005C	**YKR005C**	100	**1**	2
YNL013C	**YNL013C**	89	**1**	0
YNL057W	**YNL057W**	85	**1**	20
YNL108C	**YNL108C**	88	**1**	1
YNL338W	**YNL338W**	100	**1**	0
YOR364W	**YOR364W**	70	**1**	97
YJL139C	**YUR1**	67	**1**	24
YDR456W	**ARS608**	45	**2**	99
YGR260W	**TNA1**	70	**2**	91
YOR106W	**VAM3**	69	**2**	88
YDL077C	**VAM6**	61	**2**	80
YKR001C	**VPS1**	100	**2**	90
YJL154C	**VPS35**	49	**2**	n.a.
YGL095C	**VPS45**	68	**2**	n.a.
YKR035W-A	**DID2**	100	**3**	100
YKL002W	**DID4**	96	**3**	92
YDR069C	**DOA4**	100	**3**	11
YKR035C	**OPI8**	100	**3**	100
YPL002C	**SNF8**	100	**3**	100
YMR077C	**VPS20**	92	**3**	100
YCL008C	**VPS23**	100	**3**	100
YKL041W	**VPS24**	97	**3**	94
YJR102C	**VPS25**	98	**3**	99
YNR006W	**VPS27**	70	**3**	80
YPL065W	**VPS28**	100	**3**	100
YPL084W	**VPS31**	100	**3**	100
YLR417W	**VPS36**	83	**3**	100
YPR173C	**VPS4**	100	**3**	100
YNR005C	**YNR005C**	57	**3**	100
YPL154C	**PEP4**	100	**4**	85

Table S3: **Gene ontology term analysis of 128 genes required for starvation-induced endocytosis of Mup1-pHluorin**

Starvation-induced endocytosis and vacuolar sorting of Mup1-pHluorin
Methionine- and starvation-induced endocytosis and vacuolar sorting of Mup1-pHluorin

color code:
starvation-specific gene
general endocytic trafficking
not discriminated

	GO-TERM MACROMOLECULAR COMPLEX	enrichment over genome	CLUSTER_FREQUENCY	GENOME_FREQUENCY	ANNOTATED_GENES
GO:0000814	ESCRT II complex	53,60	2.50%	0.05%	SNF8, VPS25, VPS36
GO:0000815	ESCRT III complex	35,73	3.33%	0.09%	DID2, DID4, VPS20, VPS24
GO:0000813	ESCRT I complex	26,80	1.67%	0.06%	STP22, VPS28
GO:0031499	TRAMP complex	17,87	1.67%	0.09%	PAP2, TRF5
GO:0022626	cytosolic ribosome	13,40	1.67%	0.12%	GCN2, GCN20
GO:0005671	Ada2/Gcn5/Ada3 transcription activator complex	10,72	1.67%	0.16%	GCN5, NGG1
GO:0046695	SLIK (SAGA-like) complex	9,46	2.50%	0.26%	GCN5, NGG1, SPT20
GO:0000124	SAGA complex	8,04	2.50%	0.31%	GCN5, NGG1, SPT20
GO:0070847	core mediator complex	5,36	1.67%	0.31%	SOH1, SRB2
GO:0000502	proteasome complex	4,02	2.50%	0.62%	DOA4, RPN10, UBP6
GO:0031201	SNARE complex	3,97	1.67%	0.42%	VAM3, VPS45
GO:0016592	mediator complex	3,97	1.67%	0.42%	SOH1, SRB2
GO:0000775	chromosome, centromeric region	1,37	1.67%	1.21%	CNN1, GCN5
GO:0022625	cytosolic large ribosomal subunit	1,13	1.67%	1.48%	RPL14A, RPP1A
GO:0010494	cytoplasmic stress granule	1,12	1.67%	1.49%	SBP1, SKY1
GO:0005840	ribosome	0,44	1.67%	3.76%	RPL14A, RPP1A

Table S3: **Gene ontology term analysis of 128 genes required for starvation-induced endocytosis of Mup1-pHluorin**

color code:
starvation-specific gene
general endocytic trafficking
not discriminated

	GO-TERM PROCESS	CLUSTER_FREQUENCY	GENOME_FREQUENCY	enrichment over genome	starvation-specific genes	ANNOTATED_GENES
GO:0007034	vacuolar transport	15.00%	2.83%	**5,31**	**2 of 18**	APM2, BRO1, DID2, DID4, IST1, PEP4, SNF8, STP22, VAM3, VPS1, VPS20, VPS24, VPS25, VPS27, VPS28, VPS36, VPS4, VPS45
GO:0007568	aging	5.00%	1.06%	**4,73**	**6 of 6**	DNL4, GCN5, GPR1, NGG1, RIM15, SIT4
GO:0016192	vesicle-mediated transport	14.17%	3.37%	**4,20**	**4 of 17**	APM2, BRO1, DID2, DID4, DOA4, ECM34, ERP5, SNF8, STP22, VAM3, VAM6, VPS20, VPS24, VPS25, VPS27, VPS4, VPS45
GO:0007165	signal transduction	18.33%	5.68%	**3,23**	**20 of 22**	ATG32, BAR1, BEM2, DCK1, FYV5, GAL83, GCN2, GPR1, HAL5, IRS4, LMO1, NPR1, PKH3, POG1, RHO5, RIM15, SIT4, SKY1, SPT20, VAM6, WHI2, YHR182W
GO:0051604	protein maturation	4.17%	1.48%	**2,82**	**4 of 5**	DFG16, PEP4, RIM21, STE23, YMR038C
GO:0061024	membrane organization	6.67%	2.56%	**2,60**	**3 of 8**	BRO1, DID4, DOA4, MIC27, SFH5, VPS20, VPS24, VPS4
GO:0006605	protein targeting	9.17%	3.88%	**2,36**	**1 of 11**	DID2, PEP4, SNF8, STP22, TIM21, VPS1, VPS25, VPS27, VPS28, VPS36, VPS45
GO:0000003	reproduction	5.00%	2.25%	**2,22**	**6 of 6**	BAR1, CKA1, FYV5, POG1, SHE3, STE23
GO:0071554	cell wall organization or biogenesis	10.00%	4.64%	**2,15**	**12 of 12**	BAR1, ECM21, ECM34, FYV5, IRS4, MNN5, NCW2, PKH3, RIM101, RIM21, SIT4, YUR1
GO:0006810	transport	17.50%	8.18%	**2,14**	**6 of 21**	APM2, BRO1, DID2, DID4, ECM21, ERP5, IST1, SNF8, STP22, TIM21, VAM3, VAM6, VPS20, VPS24, VPS25, VPS27, VPS28 , VPS35, VPS36, VPS4, VPS45
GO:0009056	catabolic process	18.33%	8.71%	**2,10**	**15 of 22**	ATG32, BAR1, DCK1, DOA1, FIS1, FMC1, GAL1, GCN2, IRS4, LMO1, PEP4, RIM15, RPL14A, STE23, STP22, VAM3, VAM6, VID28, VPS27, VPS36, VPS4, WHI2
GO:0007005	mitochondrion organization	8.33%	4.44%	**1,88**	**10 of 10**	ATG32, ATP18, DCK1, FIS1, FMC1, LMO1, MIC27, RRM3, TIM21, WHI2
GO:0051301	cell division	5.83%	3.28%	**1,78**	**6 of 7**	CNN1, DNL4, PAP2, POG1, SIT4, TRF5, VPS1
GO:0007049	cell cycle	9.17%	5.58%	**1,64**	**10 of 11**	AIM20, CNN1, CTF8, DNL4, FYV5, PAP2, POG1, SIT4, TRF5, VPS1, WHI2
GO:0030154	cell differentiation	5.00%	3.08%	**1,63**	**6 of 6**	CKA1, RIM101, RIM21, RIM9, SHE3, VID28
GO:0042592	homeostatic process	5.00%	3.35%	**1,49**	**6 of 6**	ARN2, DOA1, DOA4, FRE2, GPR1, RRM3
GO:0007010	cytoskeleton organization	5.83%	4.38%	**1,33**	**6 of 7**	BEM2, GVP36, LMO1, RHO5, SIT4, VPS1, WHI2
GO:0006457	protein folding	2.50%	1.88%	**1,33**	**3 of 3**	HCH1, JJJ2, SNL1
GO:0065003	protein-containing complex assembly	8.33%	6.34%	**1,32**	**6 of 10**	ATP18, CNN1, DID2, FMC1, GAL83, RPN10, SRB2, VAM6, VPS1, VPS45
GO:0006950	response to stress	5.00%	3.94%	**1,27**	**5 of 6**	GCN2, PKH3, RIM101, SBP1, SPT20, YJL144W
GO:0006629	lipid metabolic process	6.67%	5.31%	**1,26**	**6 of 8**	CAT2, IRS4, LDB16, NPR1, OPY1, SFH5, TED1, VPS4
GO:0048646	anatomical structure formation involved in morphogenesis	3.33%	2.69%	**1,24**	**4 of 4**	RIM101, RIM21, RIM9, VID28
GO:0007059	chromosome segregation	3.33%	3.42%	**0,98**	**3 of 4**	CNN1, CTF8, GIP4, SOH1
GO:0006520	cellular amino acid metabolic process	3.33%	3.45%	**0,97**	**3 of 4**	ARG4, HIS6, TRP3, TYR1
GO:0055085	transmembrane transport	6.67%	7.08%	**0,94**	**7 of 8**	ARN2, ATP18, MUP3, NPR1, TIM21, TNA1, VMR1, YIL170W
GO:0009058	biosynthetic process	12.50%	13.65%	**0,92**	**14 of 15**	ARG4, ATP18, DNL4, FCY1, GPP1, HIS6, LDB16, MNN5, NGG1, NPR1, OPY1, TRP3, TYR1, VID28, YUR1
GO:0005975	carbohydrate metabolic process	3.33%	3.85%	**0,87**	**4 of 4**	GAL1, GPP1, MNN5, VID28
GO:0034641	cellular nitrogen compound metabolic process	7.50%	8.91%	**0,84**	**9 of 9**	BAR1, CAT2, FCY1, HIS6, NGG1, PAP2, STE23, TRF5, TRP3
GO:0051276	chromosome organization	3.33%	4.63%	**0,72**	**4 of 4**	CNN1, CTF8, RRM3, SOH1
GO:0006351	transcription, DNA-templated	4.17%	6.13%	**0,68**	**5 of 5**	GAL1, IRS4, RIM15, RRM3, SOH1
GO:0006259	DNA metabolic process	2.50%	3.71%	**0,67**	**3 of 3**	CTF8, DNL4, RRM3
GO:0006412	translation	2.50%	4.43%	**0,56**	**3 of 3**	GCN2, GCN3, RPL14A
GO:0044281	small molecule metabolic process	2.50%	4.57%	**0,55**	**3 of 3**	GAL1, GPP1, VID28

Table S3: **Gene ontology term analysis of 128 genes required for starvation-induced endocytosis of Mup1-pHluorin**

color code:
starvation-specific gene
general endocytic trafficking
not discriminated

	GO-TERM COMPONENT	CLUSTER_FREQUENCY	GENOME_FREQUENCY	enrichment over genome	starvation-specific genes	ANNOTATED_GENES
GO:0005768	endosome	16.67%	2.88%	**5,79**	**6 of 20**	APM2, ARN2, BRO1, DID2, DID4, DOA1, DOA4, ECM34, IST1, SNF8, STP22, VPS1, VPS20, VPS24, VPS25, VPS27, VPS28, VPS35, VPS36, VPS4
GO:0005773	vacuole	18.33%	8.02%	**2,29**	**13 of 22**	AIM20, ANS1, ARN2, ATG32, FRE2, MIC27, MUP3, NCW2, PEP4, PRY2, RHO5, SFH5, TNA1, VAM3, VAM6, VID28, VMR1, VPS1, VPS20, VPS27, VPS35, VPS45
GO:0005886	plasma membrane	15.83%	8.75%	**1,81**	**18 of 19**	ANS1, ARN2, BEM2, DCK1, DFG16, FRE2, FYV5, GPR1, HAL5, IRS4, LMO1, NCW2, NPR1, OPY1, RHO5, RIM21, RIM9, SFH5, STP22
GO:0005777	peroxisome	2.50%	1.43%	**1,75**	**2 of 3**	CAT2, FIS1, VPS1
GO:0005622	intracellular	5.00%	2.94%	**1,70**	**6 of 6**	APM2, ATP18, BEM2, IRS4, RHO5, SFH5
GO:0005618	cell wall	3.33%	2.21%	**1,51**	**4 of 4**	ANS1, BAR1, FYV5, NCW2
GO:0005576	extracellular region	2.50%	1.79%	**1,40**	**3 of 3**	BAR1, FYV5, PRY2
GO:0005829	cytosol	21.67%	16.46%	**1,32**	**16 of 26**	ARG4, BRO1, CKA1, DOA4, ECM21, ECM34, FYV5, GAL1, GCN3, GCN5, GVP36, HCH1, NPR1, PAP2, RPN10, SFH5, SNF12, STP22, VPS1, VPS20, VPS24, VPS25, VPS28, VPS35, VPS45, YMR038C
GO:0005794	Golgi apparatus	5.83%	4.76%	**1,23**	**6 of 7**	APM2, ERP5, GVP36, MNN5, NPR1, VPS45, YUR1
GO:0005737	cytoplasm	48.33%	39.60%	**1,22**	**43 of 58**	ERP5, FCY1, GAL1, GAL83, GCN2, GIP4, GPP1, GVP36, HAL5, HCH1, HIS6, IRS4, IST1, JJJ2, LMO1, NPR1, OPY1, OTU2, RHO5, RIM101, RIM15, RPL14A, RPP1A, SBP1, SFH5, SHE3, SIT4, SKY1, SNF8, STP22, TRP3, TYR1, VID28, VPS1, VPS20, VPS24, VPS25, VPS28, VPS36, VPS4, VPS45, YGR117C, YHR182W, YJL144W, YMR038C, YNL108C
GO:0031410	cytoplasmic vesicle	2.50%	2.07%	**1,21**	**3 of 3**	APM2, ERP5, RHO5
GO:0005739	mitochondrion	22.50%	18.92%	**1,19**	**24 of 27**	AIM19, ATG32, ATP18, BEM2, CAT2, DCK1, DOA1, DOA4, FIS1, FMC1, FMP33, IRS4, LDB16, LMO1, MIC27, OPY1, PEP4, RHO5, SNL1, STE23, TIM21, TNA1, VMR1, VPS1, YIL077C, YKR005C, YMR038C
GO:0043226	organelle	8.33%	7.20%	**1,16**	**8 of 10**	APM2, ERP5, IRS4, LDB16, RHO5, SFH5, SHE3, SNL1, TED1, VAM6
GO:0005634	nucleus	34.17%	36.27%	**0,94**	**39 of 41**	AIM20, APM2, CKA1, CNN1, CTF8, DNL4, DOA1, FCY1, GAL83, GCN5, GPP1, HAL5, HCH1, HIS6, IES2, JJJ2, NGG1, NPR1, PAP2, POG1, RHO5, RIM101, RIM15, RPN10, RRM3, SBP1, SFH5, SIT4, SKY1, SNF12, SNL1, SOH1, SPT20, SRB2, TRF5, UBP6, VID28, VPS4, WHI2, YMR038C, YNL108C
GO:0005783	endoplasmic reticulum	9.17%	10.29%	**0,89**	**7 of 11**	ERP5, PEP4, PRY2, RIM21, SFH5, SHE3, SNL1, TED1, VPS20, VPS4, YUR1
GO:0005730	nucleolus	2.50%	5.39%	**0,46**	**3 of 3**	PAP2, SBP1, TRF5

Table S4: **Yeast strains, plasmids and primer**

Identifier	Source	Yeast strain
SEY6210	Robinson et al., 1988	SEY6210 *MATα leu2-3,112 ura3-52 his3-Δ200 trp1-Δ901 suc2-Δ9 lys2-801 GAL*
SEY6210.1	Robinson et al., 1988	SEY6210.1 *MATa leu2-3,112 ura3-52 his3-Δ200 trp1-Δ901 suc2-Δ9 lys2-801 GAL*
DTY557	Gift from the Emr lab	SEY6210 *rsp5Δ:HIS3 pRS415-6xHIS-TEV-3xFLAG-RSP5*
DTY558	Gift from the Emr lab	SEY6210 *rsp5Δ:HIS3 pRS415-6xHIS-TEV-3xFLAG-RSP5-WW1**
DTY559	Gift from the Emr lab	SEY6210 *rsp5Δ:HIS3 pRS415-6xHIS-TEV-3xFLAG-RSP5-WW2**
DTY560	Gift from the Emr lab	SEY6210 *rsp5Δ:HIS3 pRS415-6xHIS-TEV-3xFLAG-RSP5-WW3**
ISY001	This study	SEY6210 *art4Δ::HIS3 HXT3-GFP::TRP1*
ISY013	This study	SEY6210 *art2Δ::HIS3 HXT3-GFP::TRP1*
ISY018	This study	SEY6210 *MUP1 D549,551,555R,E554R-GFP::HIS3*
ISY025	This study	SEY6210 *HXT3-MUP1-C AA545-574 D549,551,555R,E554R-GFP::TRP1*
ISY026	This study	SEY6210.1 *art4Δ::HIS3 HXT3-MUP1-C AA545-574 D549,551,555R,E554R-GFP::TRP1*
ISY027	This study	SEY6210 *art2Δ::HIS3 art4Δ::HIS3 HXT3-MUP1-C AA545-574 D549,551,555R,E554R-GFP::TRP1*
ISY028	This study	SEY6210 *art2Δ::HIS3 HXT3-MUP1-C AA545-574 D549,551,555R,E554R-GFP::TRP1*
ISY029	This study	SEY6210 *HXT3-MUP1-C AA545-574-GFP::TRP1*
ISY030	This study	SEY6210.1 *art4Δ::HIS3 HXT3-MUP1-C AA545-574-GFP::TRP1*
ISY031	This study	SEY6210 *art2Δ::HIS3 art4Δ::HIS3 HXT3-MUP1-C AA545-574-GFP::TRP1*
ISY032	This study	SEY6210 *art2Δ::HIS3 HXT3-MUP1-C AA545-574-GFP::TRP1*
ISY033	This study	SEY6210 *CAN1 D567,575R,E569,574R-GFP::HIS3*
ISY042	This study	SEY6210 *HXT3-MUP1-C AA545-574 K567,572R-GFP::TRP1*
ISY053	This study	SEY6210.1 *art4Δ::HIS3 HXT3-MUP1-C AA545-574 K567,572R-GFP::TRP1*
ISY054	This study	SEY6210 *art2Δ::HIS3 art4Δ::HIS3 HXT3-MUP1-C AA545-574 K567,572R-GFP::TRP1*
ISY055	This study	SEY6210 *art2Δ::HIS3 HXT3-MUP1-C AA545-574 K567,572R-GFP::TRP1*
JZY1	This study	SEY6210.1 *gcn1Δ::HIS3*
JZY2	This study	SEY6210.1 *gcn3Δ::HIS3*
JZY3	This study	SEY6210.1 *gcn5Δ::HIS3*
OSY250	This study	SEY6210.1 *gcn4Δ::HIS3*
OSY354	This study	SEY6210.1 *gcn2Δ::HIS3*
OSY888	This study	SEY6210.1 *art2Δ::TRP1, gcn4Δ::HIS3*
TSY3	This study	SEY6210.1 *art2Δ::HIS3 MUP1-GFP::TRP1*
TSY4	This study	SEY6210 *art2Δ::HIS3*
VIY011	This study	SEY6210.1 *art1Δ::HIS3*
VIY012	This study	SEY6210.1 *art2Δ::TRP1*
VIY030	This study	SEY6210 *ART2-6xHIS-TEV-3xFLAG::HIS3*
VIY031	This study	SEY6210 *ART1-6xHIS-TEV-3xFLAG::HIS3*
VIY036	This study	SEY6210 *CAN1-GFP::HIS3*
VIY042	This study	SEY6210 *HXT3-GFP::TRP1*
VIY054	This study	SEY6210 *MUP1-GFP::TRP1*
VIY059	This study	SEY6210 *MUP1 S568,573A-GFP::TRP1*
VIY062	This study	SEY6210.1 *art2Δ::TRP1 CAN1-GFP::HIS3*
VIY063	This study	SEY6210.1 *art2Δ::TRP1 HXT2-GFP::HIS3*
VIY064	This study	SEY6210.1 *art2Δ::TRP1 TAT2-GFP::HIS3*
VIY065	This study	SEY6210.1 *art2Δ::TRP1 HXT1-GFP::HIS3*
VIY068	This study	SEY6210.1 *art2Δ::TRP1 LYP1-GFP::HIS3*
VIY073	This study	SEY6210 *MUP1 K567,572R-GFP::TRP1*
VIY076	This study	SEY6210 *MUP1 T552,560A-GFP::TRP1*
VIY079	This study	SEY6210.1 *art1Δ::HIS3 MUP1-GFP::TRP1*
VIY082	This study	SEY6210 *MUP1 K27,28R-GFP::TRP1*
VIY092	This study	SEY6210.1 *art2Δ::TRP1 MUP1-GFP::HIS3*
VIY093	This study	SEY6210 *MUP1 K27,28,567,572R-GFP::TRP1*
VIY107	This study	SEY6210.1 *art1Δ::HIS3 art2Δ::TRP1*
VIY200	This study	SEY6210 *MUP1-HA-TEV-GFP K1R::TRP1*
VIY242	This study	SEY6210 *MUP1 S568,573A-HA-TEV-GFP K1R::TRP1*
VIY255	This study	SEY6210 *MUP1 T552,560A-HA-TEV-GFP K1R::TRP1*
VIY263	This study	SEY6210 *MUP1 G78N-HA-TEV-GFP K1R::TRP1*
VIY291	This study	SEY6210.1 *ART2-6xHIS-TEV-3xFLAG::HIS3 gcn4Δ::HIS3*
VIY295	This study	SEY6210 *MUP1 D43A,G47A,Q49A,T52A,L54A-HA-TEV-GFP K1R::TRP1*
VIY335	This study	SEY6210 *MUP1 T6,25,26,34A,S9,22,23,24,31,33,42A,K16,27,28R-HA-TEV-GFP K1R::TRP1*
YSM24	This study	SEY6210 *MUP1-GFP::HIS3*

Identifier	Source	Plasmid
empty centromer vector HIS	Sikorski & Hieter, 1989	pRS413
empty centromer vector LEU	Sikorski & Hieter, 1989	pRS415
empty centromer vector URA	Sikorski & Hieter, 1989	pRS416
p180	Hinnebusch et al., 1985	YCp5O *-GCN4*
p227	Mueller et al., 1987	YCp5O *-GCN4*^{C}
pCHL571	Lin et al., 2008	pRS416 *-CAN1-GFP*
pCHL642	Lin et al., 2008	pRS416 *-MUP1-GFP*
pIS001	This study	pRS416 *-ART2-6xHIS-TEV-3xFLAG*
pIS003	This study	pRS416 *-ART2 P748,749A,Y750A-6xHIS-TEV-3xFLAG*
pIS004	This study	pRS416 *-ART2 K664,667D,R665,666D-6xHIS-TEV-3xFLAG*
pJZ001	This study	pRS415 *-ART2-6xHIS-TEV-3xFLAG*
pJZ002	This study	pRS415 *-pART2*-ART2-6xHIS-TEV-3xFLAG*
pLZ78	Gift from the Emr lab	pRS416 *-MUP1-pHluorin*
pMM02	Schmidt et al., 2017	pRS415 *-MUP1-GFP*
pSR21	MacGurn et al., 2011	pRS416 *-FUR4-GFP*
pVI009	This study	pRS415 *-ART1*
pVI013	This study	pRS416 *-pTDH3-ART2-6xHIS-TEV-3xFLAG*

Table S4: **Yeast strains, plasmids and primer**

Used for strain	Primer name	Primer for gene knock out / knock in
ISY001, ISY013, VIY042	HXT3-LT-F	GCATTGATGCATGATGACCAGCCATTCTACAAGAAAATGTTCGGCAAGAAATACCGGATCCCCGGGTTAATTAA
ISY001, ISY013, VIY042	HXT3-LT-R	CCAATGTCTTTTATTAACTGTATCAGAGAATTATATATATAAAGTCATAAATCGAATTCGAGCTCGTTTAAAC
ISY001, ISY026, ISY027, ISY030, ISY031, ISY053, ISY054	Art4d-F	ATCAACGCGATTTCATCACACCATTCGCTTCTCTTCCTCCATAAGTAATACGGATCCCCGGGTTAATTAA
ISY001, ISY026, ISY027, ISY030, ISY031, ISY053, ISY054	Art4d-R	TATTGCTCATATCTTTTTGTCGAAATTTCGAAGACAAAAAATAAAGCAGTGAATTCGAGCTCGTTTAAAC
ISY013, ISY027, ISY028, ISY031, ISY032, ISY054, ISY055, VIY012, VIY062, VIY063, VIY064, VIY065, VIY068, VIY092, VIY107	Art2d-F	TCTTTTAAATAGAGAAGAACAAGCAAGATTTTTCCCTACCCCTATTGGGCCGGATCCCCGGGTTAATTAA
ISY013, ISY027, ISY028, ISY031, ISY032, ISY054, ISY055, VIY012, VIY062, VIY063, VIY064, VIY065, VIY068, VIY092, VIY107	Art2d-R	CCTAATTAAATAGCATGTAGTCAACAAAAAGGGAGTAAAACATGCAGTGGGAATTCGAGCTCGTTTAAAC
ISY018	Mup1 DE/R F	GGCAGAGTCAGAACACAAAGAAGGGGCGTTATTGAAACGAATATAATCGAAC
ISY018	Mup1 DE/R R	CCTTCTTTGTGTTCTGACTCTGCCAATAGTGTCATCATAAACTTTGG
ISY018	Mup1-1533-F	GGTGGTGTTTACTACGTTGTTTGG
ISY018	188-Mup1-R	TTTTGATTTCGCGCAATAGTAGG
ISY025, ISY026, ISY027, ISY028	Hxt3-Mup1(DE/R)_SHORT_F	CATTGATGCATGATGACCAGCCATTCTACAAGAAAATGTTCGGCAAGAAAGACACTATTGGCAGAGTCAGAACACAAAGAAGGG
ISY025, ISY026, ISY027, ISY028, ISY029, ISY030, ISY031, ISY032, ISY042, ISY053, ISY054, ISY055	Hxt3-1223-F	TACGCTTCTGTTGGTGTCACCAG
ISY025, ISY026, ISY027, ISY028, ISY029, ISY030, ISY031, ISY032, ISY042, ISY053, ISY054, ISY055	GFP-OE-F	CCATTACCTGTCCACACAATCTGCC
ISY025, ISY026, ISY027, ISY028, ISY029, ISY030, ISY031, ISY032, ISY042, ISY053, ISY054, ISY055	GFP-OE-R	GGCAGATTGTGTGGACAGGTAATGG
ISY025, ISY026, ISY027, ISY028, ISY029, ISY030, ISY031, ISY032, ISY042, ISY053, ISY054, ISY055	236 Hxt3 R	TGTTCGGCTCTCGCCGATGGTATG
ISY029, ISY030, ISY031, ISY032, ISY042, ISY053, ISY054, ISY055	Hxt3-Mup1 1732 F	GCATTGATGCATGATGACCAGCCATTCTACAAGAAAATGTTCGGCAAGAAAGACACTATTGGCGATGTCGATACACAAGAAG
ISY033	Can1-D,E567R-F	ATTAGAGCAATTGTATGGAGACGTCATGAACCAAAGACTTTTTGG
ISY033	Can1-D,E567R-R	ACGTCTCCATACAATTGCTCTAATGCGTCTTCTATCGGAATCGATGTCG
ISY033	1099-CAN1-F	GAGAACTCTGGTACAAAGGTTTTGCCAC
ISY033	204-CAN1-R	GGTCTGAAGGAGTTTCAAATGCTTCTAC
JZY001	GCN1 -50 KO F	GATCATTAAGACAAACAAAGCTCTGACTGACACCAATAACTCCTACAGTGCGGATCCCCGGGTTAATTAA
JZY001	GCN1 +53 KO R	GAGAATAATATATCAAATACAAAAAGTAACGAGGTTACCACATTGAATTTTCTGAATTCGAGCTCGTTTAAAC
JZY002	GCN3 -50 KO F	GATAGAAAGAATTTTAAAAGTCCTACGTATACCAGAAATCGAGAGGAAGGCGGATCCCCGGGTTAATTAA
JZY002	GCN3 +60 KO R	CTCTTGCGCTTTTTCTCCTTTTCTATTAAGTCATTGCGTGCATATATTATGTGATTTTTTGAATTCGAGCTCGTTTAAAC
JZY003	GCN5 -50 KO F	GTGAGCCGCCCAAAAGTCTTCAGTTAACTCAGGTTCGTATTCTACATTACGGATCCCCGGGTTAATTAA
JZY003	GCN5 +50 KO R	GTACTAAACATTTATTTCTTCTTCGAAAGGAATAGTAGCGGAAAAGCTTCTTCTACGCAGAATTCGAGCTCGTTTAAAC
OSY250	GCN4_KO_F	CAATTTGTCTGCTCAAGAAAATAAATTAAATACAAATAAACGGATCCCCGGGTTAATTAA
OSY250	GCN4_KO_R	TGACGAAAAGAAAGATTCCACTACAGCGTCATCTAGCTCCGAATTCGAGCTCGTTTAAAC
OSY354	GCN2_KO_F	TCAATAATTTTCCGTTCCCCTTAACACATACTATGTATAACGGATCCCCGGGTTAATTAA
OSY354	GCN2_KO_R	CCAACTCTCTTTGAACAATTTCATCTATCCTTCGCTGCTCATCTGGAATTCGAGCTCGTTTAAAC
VIY011, VIY079, VIY107	Art1d-F	TGATTTTTACTCCTACTTAGTATACATTTCACTAAACAATACGTTTTACCCGGATCCCCGGGTTAATTAA
VIY011, VIY079, VIY107	Art1d-R	AGGTATCTAAGATAAAAATATATGGTAAATACCTTTAACGAATATTATAAGAATTCGAGCTCGTTTAAAC
VIY030	Art2-tag-F	GAGCCTCCGCGTTATGACGAAATAGTGCCTTTGATGAGTGATGAAGAACGGATCCCCGGGTTAATTAA
VIY030	Art2-tag-R	TATATATATAATTATCGTAGAATAATTCAAAAAAAAATAAAAAACGAAAAAATGAATTCGAGCTCGTTTAAAC
VIY031	Art1-tag-F	ATCAGAATACAAAACTTTTCCGATTTTCTAGATTCCAATAGAATAACCCAGCGGATCCCCGGGTTAATTAA
VIY031	Art1-tag-R	TATCTAAGATAAAAATATATGGTAAATACCTTTAACGAATATTATAAAATGAATTCGAGCTCGTTTAAAC
VIY036, VIY062	Can1-LT-F	AAGATCATGAACCAAAGACTTTTTGGGACAAATTTTGGAATGTTGTAGCACGGATCCCCGGGTTAATTAA
VIY036, VIY062	Can1-LT-R	TGTTGTGGTGAATCATCGATAAAAATAAATATACTGAGATTATAGTAAGCGAATTCGAGCTCGTTTAAAC
VIY054, VIY059, VIY076, VIY079, VIY082, VIY092, VIY242, VIY255, VIY263, YSM24	Mup1-LT-R	GAAACGGAATAGCATCTTAAACTATTAAATGGCAGAAATTATAATGAGGTGAATTCGAGCTCGTTTAAAC
VIY054, VIY076, VIY079, VIY092, VIY255, VIY263, YSM24	Mup1-LT-F	TTGAAACGAATATAATCGAACATTACAAAAGTGAACAAGAAAAATCGCTGCGGATCCCCGGGTTAATTAA
VIY059, VIY242	S568-573A-F	CAAGAAGACGGCGTTATTGAAACGAATATAATCGAACATTACAAAGCTGAACAAGAAAAAGCGCTGCGGATCCCCGGGTTAATTAA
VIY063	HXT2-LT-F	TGGAAATCTGGTAGCTGGATCTCAAAAGAAAAAAGAGTTTCCGAGGAATACCGGATCCCCGGGTTAATTAA
VIY063	HXT2-LT-R	CCAGACGTATGTAGGAACTTTTTAACGTCGAGTCCGTAAGATTTGATCAGGAATTCGAGCTCGTTTAAAC
VIY064	Tat2-LT-R	AGAGAAAAAAAAAATATTCTACAAAAATAAATTGAACTTGTTTCTTCGGTAGAATTCGAGCTCGTTTAAAC
VIY064	Tat2NG-F	TGTACCTAGATTCCCGTCCATGGTACGTGAGACAGTTCCATTTCTGGTGTCGGATCCCCGGGTTAATTAA
VIY065	HXT1-LT-F	TAATGCATGATGACCAACCATTTTACAAGAGTTTGTTTAGCAGGAAATACCGGATCCCCGGGTTAATTAA
VIY065	HXT1-LT-R	TTTCTTGTTCCTTGGTGAAGGTCAAGAACTAGCAAAGAAAAGAACATCTGGAATTCGAGCTCGTTTAAAC
VIY068	Lyp1-LT-F	AAGACGACGAGCCTAAGAATTTATGGGAGAAATTCTGGGCTGCTGTTGCACGGATCCCCGGGTTAATTAA
VIY068	Lyp1-LT-R	TCTATTTTTTTATTTTTTTCTATTTTGAAGGCATGCAAGAGGTTCTGTGAGAATTCGAGCTCGTTTAAAC
VIY073, VIY093	K567-572R-F	CAAGAAGACGGCGTTATTGAAACGAATATAATCGAACATTACAGAAGTGAACAAGAAAGATCGCTGCGGATCCCCGGGTTAATTAA
VIY076, VIY255	T560A-F	CAAGAAGACGGCGTTATTGAAGCGAATATAATCG
VIY076, VIY255	T552A-R	TTCAATAACGCCGTCTTCTTGTGCATCGACATCGCCAATAG
VIY082	K27,28R-F	GAACTATCAATTTTCTTCTTCTACTACAAGAAGGGAAGTAAGTAACTCGAC
VIY263	G78N-F	TGTAATAGAATGCTTGGTACCAATGTTTTCGCCGTTTCCTCGACC
VIY263	G78N-R	GGTCGAGGAAACGGCGAAAACATTGGTACCAAGCATTCTATTACA
VIY295	NpatchF	TCCGCTTTTGAGGCAGCCCAGGCATTTGCTGCAGAAGCGGACCAAGGTGAAAAGCAG
VIY295	NpatchR	TGCCTGGGCTGCCTCAAAAGCGGAGGCACCGTTGTCAGC
VIY335	Nmod0F	GCTGCTGCTGCTGCAAGAAGGGAAGTAGCTAACGCGGCAGTGGATGCTGACAACGGTGCCGCCGATTTTGAGGCAGGCCAG
VIY335	Nmod0R	CCTTCTTGCAGCAGCAGCAGCAAATTGATAGTTCTCCCTGTTGAAGACATTCAACTGTGCCAGAAACGCTCTTCCTTCCGAC
Used for plasmid	**Primer name**	**Primer for plasmid cloning**
pIS001	XhoI -pART2-F	AAAAACTCGAGATATCATTTTCGCAAGCACAGACTCCACGG
pIS001	NotI -Tart2-R	AAAAAGCGGCCGCAACCTAACCTAATTAAATAGCATGTAGTC
pIS003	Art2(PY748/A)-2192-F	GAAGTTCCCCAAATACGAAGATTTGGATAAAAGAACCGCAAAGATAATAGCAGCTGCCGGTATCGATGCATACACGAGC
pIS003	Art2-PY/A-748-F	GATAATAGCAGCTGCCGGTATCGATGCATACACG
pIS003	Art2-PY/A-748-R	GCATCGATACCGGCAGCTGCTATTATCTTTGCG
pIS003	Art2 +236 R	GGTGTCAATTCGGCAAGAGGTGTTC
pIS003, pIS004	M13+	GTAAAACGACGGCCAGTGAGC
pIS003, pIS004	M13+R	GGAAACAGCTATGACCATGATTACG
pIS004	Art2-KR 664 D-F	GATGACGATGACGAAAGAAGTGTATCATTATTTGAAATCAGAACTAAGG
pIS004	Art2-KR 664 D-R	TACACTTCTTTCGTCATCGTCATCGGAGGCGAAATCTAAATAATACGGATTATAAGGGTC
pJZ1, pJZ2	pGcn4mut Art2-HTF AF	GATATCGAATTCCTGCAGCCCGGGGCGTTCAAATTACATTCAAATCACCAAGTGT
pJZ1, pJZ2	pGcn4mut Art2-HTF CR	ACCCGGGGATCCGTTCTTCATCACTCATCAAAGGCACTATTTC
pJZ1, pJZ2	pGcn4mut Art2-HTF DF	GAGTGATGAAGAACGGATCCCCGGGTTAATTAACAG
pJZ1, pJZ2	pGcn4mut Art2-HTF ER	GGTGGCGGCCGCTCTAGAACTAGTGGTTGCCGTCATTTATTATGCTATTTCATATTTC
pJZ2	pGcn4mut Art2-HTF AR	AGAACCCTTGGAAGATCAGAGATTGGAAAAATTAAGACCAATG
pJZ2	pGcn4mut Art2-HTF BF	CCAATCTCTGATCTTCCAAGGGTTCTCCACTTTCC
pJZ2	pGcn4mut Art2-HTF BR	TCTCTATTTAAAACCTTTCCGATGGACCTTCAAAAATATAAAC
pJZ2	pGcn4mut Art2-HTF CF	TCCATCGGAAAGGTTTTAAATAGAGAAGAACAAGCAAGATTTTTC
pJZ2	pGnc4mut Art2-HTF DR	TAAAAAACGAAAAAATTCACTTGTCATCGTCATCCTTGTAATC
pJZ2	pGcn4mut Art2-HTF EF	CGATGACAAGTGAATTTTTTCGTTTTTTATTTTTTTTTTGAATTATTCTACG
pVI009	XhoI-pART1-F	AAAAACTCGAGGGATAAAGCTAAGTTCCATGTATG
pVI009	NotI-Tart1-R	AAAAAGCGGCCGCAATGCCTGTATGTAGTTATCTGTG
pVI013	SfiI-Art2-F	AAAAGGCCCGTACGGCCATGCCGTTTATAACATCAAGACCGG
pVI013	SfiI-flag-R	AAAAGGCCCTTGTGGCCTCACTTGTCATCGTCATCCTTG